THE
PHYSICAL REVIEW
A journal of experimental and theoretical physics established by E. L. Nichols in 1893

SECOND SERIES, VOL. 65, NOS. 3 AND 4 FEBRUARY 1 AND 15, 1944

Cascade Showers and Nuclear Disintegrations at 10,000 Feet

WAYNE E. HAZEN
University of California, Berkeley, California
(Received October 11, 1943)

A large cloud chamber containing eight lead plates was operated without counter control at 10,000 feet. In 8500 photographs, 1090 cascade showers and 58 nuclear disintegrations were observed. The differential energy spectrum for the shower-producing rays, which was obtained from the relative frequency of occurrence for showers of a given size, is proportional to $E^{-1.7}$ for $E=2\times10^8$ ev and to $E^{-3.0}$ for $E=10^9$ ev. The shower-producing rays with $E>2\times10^8$ ev constituted 6.5 percent of the radiation observed in the cloud chamber; one-third of the shower-producing rays were photons. Approximately one-third of the observed nuclear disintegrations contained particles that penetrated at least 0.7 cm of lead and four contained particles that penetrated at least 2.8 cm of lead. Most of the disintegration particles were protons or mesotrons. The initiating particles were neutrons and protons, with the former predominant for the lower energy disintegrations. There appears to be no sharp line of distinction between low energy and high energy disintegrations. No correlation was observed between the disintegrations and the cascade showers.

VARIOUS types of cloud-chamber experiments have been performed in order to analyze the cosmic radiation at altitudes of ten to fifteen thousand feet.[1] In the present experiment the details of the interaction of cosmic rays with lead were studied at an altitude of 10,000 ft. A large cylindrical cloud chamber (30 by 30 cm) was operated at Tioga Pass, Yosemite National Park, without counter control. The chamber contained eight lead plates each consisting of a 0.6-cm lead plate and two reflecting steel sheets plated with chromium. The equivalent lead thickness, calculated on the basis of densities, was 0.7 cm, and since the steel constituted such a small fraction of the absorber, it is assumed in all subsequent calculations that the plates were simply 0.7-cm lead sheets. Since there was sufficient illumination to obtain images of individual drops, diffuse tracks could be photographed, and these are included in the statistics in some cases. The chamber was filled with air and the saturated vapor from a 1 : 3 liquid mixture of water and ethyl alcohol to a total pressure of ~70 cm when compressed and ~60 cm when expanded. Other details of the apparatus have been given previously.[2]

The lead plates made possible the classification of the ionizing particles in two groups: particles of electronic mass, and particles of many times electronic mass (mesotrons and protons). Furthermore, the details of the interaction of each type of particle with lead could be observed. Essentially all of the photons initiated cascade showers in the lead and thus could be detected,

[1] Several of these experiments will be mentioned later in the paper.

[2] W. E. Hazen, Phys. Rev. **64**, 7 (1943).

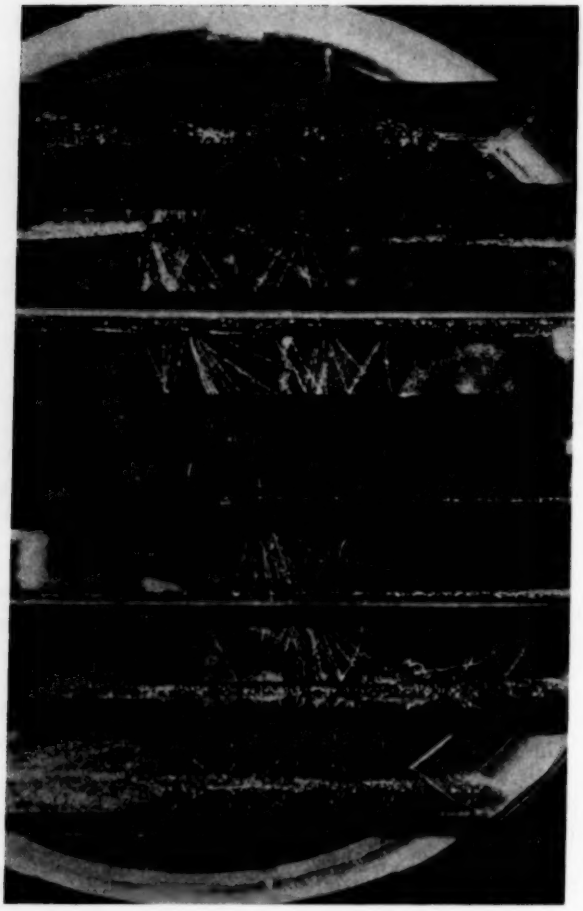

FIG. 1. Three time-associated showers were photographed in this expansion. The initiating particles are probably part of an air shower. There are 30 particles in the largest shower at its maximum, which occurs under the sixth lead plate (4.2 cm of lead). The energy of the particle that initiated this shower was 1.5×10^9 ev and the predicted position of the maximum is 4.5 cm of lead. Reflected images of the tracks can be seen in the plate surfaces, most clearly in the top and bottom plates.

whereas only a small fraction of the non-ionizing particles interacted with the lead. The analysis of the data pertaining to the production of collision electrons by the heavier particles has already been given.[2]

CASCADE SHOWERS

If an electron or photon has an energy greater than 10^8 ev, it is very unlikely to pass through a series of 0.7-cm lead plates without producing an observable cascade shower. In the cases where the initiation of the shower is observed, it is possible to distinguish between electrons and photons as the originating rays; where the maximum of the shower is observed, the energy of the originating ray can be estimated.

In the 8500 useful photographs, 1090 cascade showers with maxima of four or more particles were observed; 731 were classified as giving rise to sharp tracks, the rest as giving rise to diffuse tracks. Examples of the photographs are reproduced in Fig. 1. In the same series of photographs, 8678 sharp tracks from penetrating particles were observed. A size-frequency block diagram for the showers is given in Fig. 2. The relative number of four-particle showers is too low because many showers of this size originated in one plate and stopped in the next plate. This situation makes the chance of observation less than that for the larger showers, which nearly always passed through several plates.

The energy values shown along the scale of abscissae were obtained from the number of particles at the shower maximum by the use of Eq. (2.104) of Rossi and Greisen.[3] The number of particles at the shower maximum is not appreciably different for showers initiated by electrons and those initiated by photons of the same energy. When plotted with logarithmic scales the data are only reasonably well represented by a straight line (wth a slope of -2.4); see Fig. 3. If a simple power law is used to describe portions of the differential energy spectrum, the exponent

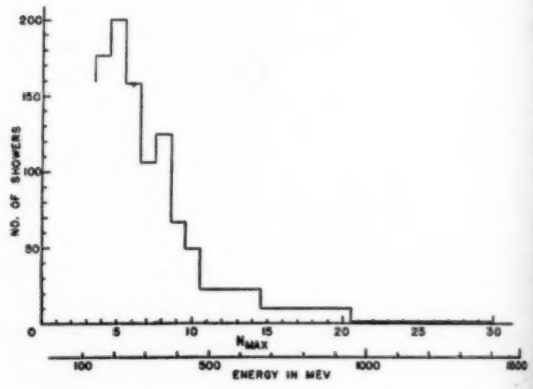

FIG. 2. Frequency of occurrence of cascade showers in lead as a function of the size of the shower. The size of the shower is expressed in terms of the number of particles at the maximum of the shower. The energy scale is obtained from shower theory [Eq. (2.104) of Rossi and Greisen, reference 3].

[3] B. Rossi and K. Greisen, Rev. Mod. Phys. **13**, 240 (1941).

varies from -1.7 for the lowest energies (2×10^8 ev) to -3.0 for the highest energies (10^9 ev).

The intensity of the shower-producing particles relative to the penetrating particles was obtained by considering sharp tracks only (the uncertainty in the equivalence of the total times of observation is thereby reduced). Since the total number of sharp tracks caused by showers with maxima greater than four particles was 605, while in the same series of photographs there were 8678 sharp penetrating tracks, the relative number of high energy electrons and photons ($E>2\times10^8$) is seven percent at 10,000 ft. From the cases where it was believed that the beginning of the shower was observed, the ratio of photons to electrons was found to be 1 : 2.5.

Auger[4] has compared the absorption of cosmic rays in lead and in aluminum, at about the same altitude as in the present experiment. Since Auger used a counter telescope with the absorber placed between the counters, the number of photons that would have been recorded is negligible. He obtained a ratio of 8 : 54 or 15 percent for the number of shower-producing particles with $E>10^8$ ev compared with the number of penetrating particles. If the spectrum from the present data is extrapolated to an energy of 10^8 ev, the value for the relative number of shower-producing rays (photons and electrons) with $E>10^8$ would not be much greater than 15 percent, even if the largest reasonable slope for the lower end of the spectrum is used in the extrapolation. A comparison of the results from the two experiments would thus lead one to the conclusion that the number of photons is negligible; however, the experimental uncertainties are fairly large in both cases and the result of the comparison cannot be considered as in conflict with the above-mentioned value of 1 : 2.5 for the ratio of photons to electrons. Most of the shower-producing rays originate as electrons,[5] and hence one would expect to observe more electrons than photons in a region where the rays are still being produced.

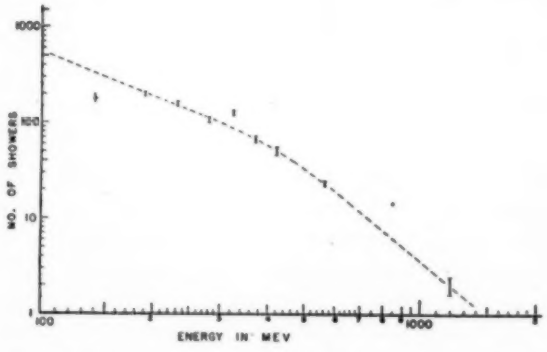

FIG. 3. The energy spectrum for photons and electrons (shower-producing rays). The ordinates represent the number of rays in an energy band of width 45 Mev. The experimental point with the smallest abscissa, which is represented by +, is relatively too low because showers of this size seldom penetrate more than one lead plate and therefore are less likely to be observed than larger showers; the other experimental observations are represented by lines whose lengths indicate the probable errors.

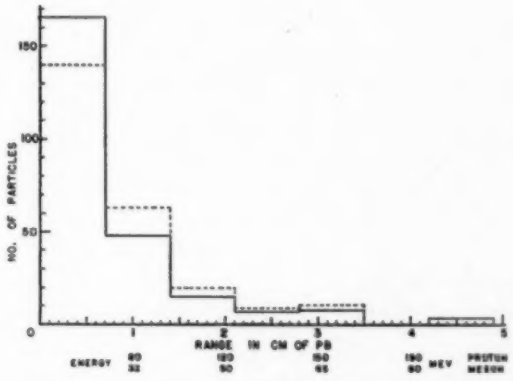

FIG. 4. The observed number of star particles as a function of their range in lead. The auxiliary scales of abscissae give the energies for protons and mesotrons. The dotted lines indicate the results of the correction for the finite size of the lead plates.

STAR SHOWERS OR NUCLEAR DISINTEGRATION

A few stars have been observed in the course of many cloud-chamber experiments and in one recent investigation 156 stars were observed.[6] In the present experiments a total of 58 stars consisting of two or more particles has been found in the photographs. The large area and close spacing of the lead plates resulted in a reasonably large chance that a particle would find several lead plates in its path if its range was several centimeters of lead. The interaction of a particle with the lead plates provides information concerning the nature of the particle.

Thirty-one of the stars consisted entirely of

[4] P. V. Auger, Phys. Rev. **61**, 684 (1942).

[5] K. Greisen, Phys. Rev. **63**, 323 (1943).

[6] W. M. Powell, Phys. Rev. **61**, 670 (1942).

the particles with range less than one lead plate (0.7 cm) and greater than 2.5 cm of air. Included in these thirty-one stars are the two which originated in the gas rather than in one of the lead plates. The rest of the stars contained particles with range of one or more lead plates, in addition to particles with range less than one lead plate. The average number of observed particles per star in the former group was 3.3, and in the latter group 5.5.

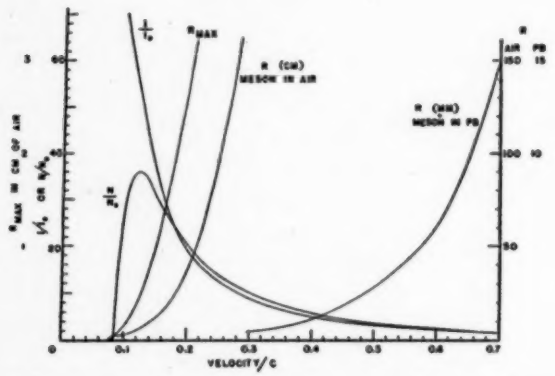

FIG. 5. Curves for δ-ray frequency, ionization, maximum range of δ-rays, and residual range of mesotrons or protons as a function of the velocity of the primary particle. N/N_0 and I/I_0 are, respectively, the frequency of δ-ray production and the ionization, both of them relative to the value of these quantities for a primary particle with velocity $\simeq c$. R_{max} is the maximum possible range for a δ-ray. R is the residual range of the primary particle. For an α-particle, N/N_0 and I/I_0 are four times as large as indicated, R_{max} is unchanged, and R is the same as for a proton.

A block diagram showing the observed frequency-range distribution for particles originating in nuclear disintegrations is given in Fig. 4. The relative numbers of short-range particles are too high since the solid angle subtended by a plate decreases as we proceed away from the origin of the star; the dotted lines of Fig. 4 indicate the results of the corrections for this effect. The original range distribution of the star particles is distorted by their passage through the lead plate in which they originated. The observed distribution is approximately the same as the original distribution for particles of range greater than one lead plate, but the observed distribution gives no idea of the original distribution for particles with range less than one lead plate. The *total* number of particles in the latter group can be estimated from the fact that 2/58 of the stars originated in the air between plates whereas the stopping power of the air relative to the plates in g/cm² was only 2/5800. We therefore conclude that there were roughly 100 stars (containing only short-range particles) that were not observed for each one that was observed; Powell[6] calculated a value of 50 for one-cm lead plates, which would reduce to 35 for 0.7-cm lead plates, in contrast to the value of 100 found in the present experiment. However, his calculation was made by dividing the lead thickness by the average range of the star particles; if Powell's data are analyzed in terms of stopping power of the gas relative to that of the lead, we again obtain a value of 100 for the number of unobserved stars per observed star. The discrepancy is attributable partly to experimental uncertainty and partly to the assumption that the frequency of star production is proportional to the nuclear mass. Thus we conclude that the true range distribution of star particles includes 35 to 100 times the observed number for particles with range less than one centimeter of lead; most of these unobserved short-range particles have ranges much less than one millimeter of lead.

In many cases the nature of the particles can be inferred from their ionization, change in ionization, scattering, or production of δ-rays. The first three methods have been discussed many times, but quantitative information for the latter method has not been found in the literature. Since low energy transfers predominate, the interaction due to spin is negligible and the collision probability for heavy particles[7] with electrons is proportional to

$$(1/\beta^2)(1-\beta^2 E/E_{max})dE/E^2, \qquad (1)$$

where E is the energy of the ejected electron, β the velocity of the primary particle in units of c, and E_{max} is the maximum energy that can be transferred to the electron. For the type of collisions considered here, E_{max} is given by Eq. (1.5a) of Rossi and Greisen[3] with sufficient accuracy,

$$E_{max}=2m_0c^2\beta^2/(1-\beta^2), \qquad (2)$$

where m_0c^2 is the rest energy of the electron. The expression for the number of δ-rays per unit path with energy between E_{min} and E_{max} found by

[7] H. J. Bhabha, Proc. Roy. Soc. **164**, 257 (1938).

integrating (1) and expressing E_{max} in terms of β from Eq. (2) is

$$N=\frac{\text{const.}}{\beta^2}\left[\frac{2m_0c^2}{E_{min}}-\frac{1-\beta^2}{\beta^2}-(1-\beta^2)\ln\frac{2m_0c^2\cdot\beta^2}{E_{min}(1-\beta^2)}\right]. \quad (3)$$

In the present experiment δ-rays with ranges as short as one mm could be observed, and this fact leads to a value of 7 kev for E_{min}.[8] If we define N_0 as the value of N for $\beta\simeq 1$, then N/N_0 represents the frequency of occurrence of δ-rays relative to the minimum frequency of occurrence (primary particle with $\beta\simeq 1$). A plot of N/N_0 as a function of β is given in Fig. 5. The ionization, the maximum possible range for a δ-ray, and the residual range of the primary are also plotted in Fig. 5. The value for N_0 obtained by Hornbeck and Howell[9] is 0.011 per cm of air at 76 cm and 15°C for $E_{min}=12$ kev. For $E_{min}=7$ kev the value for N_0 would be $0.011\times 12/7$ or 0.019 per cm, since we see from Eq. (3) that N_0 (the value of N for $\beta\simeq 1$) varies inversely with E_{min}.

Of the 166 tracks of particles with range less than 0.7 cm of lead, 70 showed ionization corresponding to singly-charged particles with velocity greater than 0.75 c; such particles could be either electrons or mesotrons. The remaining 96 short-range particles ionized at least several times more strongly and therefore could not be electrons. Three of these particles were probably α-particles because of the large number of δ-rays occurring along their paths. Each of them had four or more δ-rays with range at least one mm in a track length of $\sim$2.5 cm. Thus N/N_0 is $\sim$85, which is a highly unlikely value for a proton or mesotron (Fig. 5). The rest of the particles were probably not α-particles since an α-particle with range $<$0.5 cm of lead would produce at least one δ-ray per cm. Shapiro[10] has found that 90 percent of the star particles registered by photographic emulsions are protons, and the remainder probably are α-particles. Since such particles lie near the short-range group under discussion, there is good agreement with the present results in respect to the small number of α-particles.

Among the particles with range greater than 0.7 cm of lead, there were twelve that might have been electrons, as judged from scattering and ionization; three of these twelve also multiplied and this indicates that the three were probably electrons. However, the identity of the twelve is not certain even in the case of the latter group of three. Three of the long-range particles might be interpreted as α-particles, but they might also be protons. The remaining 65 long-range particles were either protons or mesotrons. It is difficult to estimate how many of these long-range star particles are mesotrons rather than protons. Nielsen and Powell[11] photographed the tracks of slow particles at 14,000 ft. with a technique that left virtually no uncertainty in the identification of mesotrons. They found that only about one percent of the heavy tracks observed at high altitudes was due to mesotrons. However, this does not necessarily indicate that most of the star particles are not

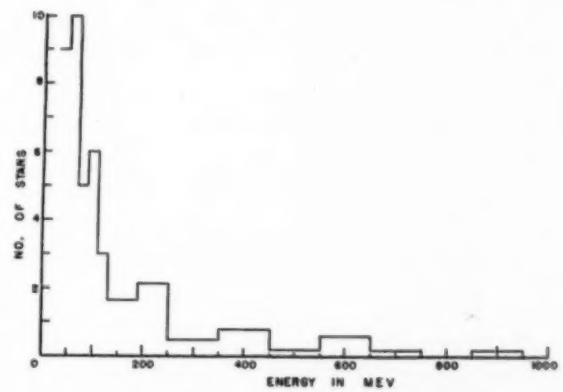

FIG. 6. Frequency of occurrence of stars in an energy band of width 20 Mev as a function of the total observed energy. The energy, which is calculated on the assumption that all the particles are protons, would be approximately one-half as great if the particles are mesotrons.

mesotrons. In the first place, the range of a slow proton is ten times that of a mesotron moving with the same velocity, and hence the observations of Nielsen and Powell indicate that the relative frequency of formation might be ten percent. In the second place, a large fraction of the slow particles occurs singly; that is, such

[8] G. Fr. von Droste, Zeits. f. Physik **84**, 17 (1933).
[9] G. Hornbeck and I. Howell, Proc. Am. Phil. Soc. **84**, 33 (1941).
[10] M. M. Shapiro, Phys. Rev. **61**, 115 (1942).
[11] C. E. Nielsen and W. M. Powell, Phys. Rev. **63**, 384 (1943).

particles did not originate as part of what we have termed a star shower (although the distinction may be based on energy alone). It is difficult to estimate the number of single slow particles from the present series of photographs because contamination α-particles traversed the full distance between the plates even when the path was inclined 45 degrees from the vertical. A lower limit, which may be several times too small, is 400 single particles that certainly were not α-particles. Anderson and Neddermeyer[12] observed on Pikes Peak about twenty times as many single heavily-ionizing particles as stars. Consequently, it is quite likely that Nielsen and Powell observed very few star particles, and their results do not necessarily indicate that most of the star particles are not mesotrons. Anderson and Neddermeyer[12] identified two particles in one star (Fig. 10, reference 12) as probably protons; one particle in each of two stars (Figs. 12 and 13) is definitely a mesotron; and four other particles in one star (Fig. 12) are either mesotrons or electrons. Crussard and Leprince-Ringuet[13] photographed a star (Fig. 3, reference 13) containing two particles that are certainly protons. There are two other cases that have been reported in which the multiple production of identifiable heavy particles has been observed.[14,15] The particles have been identified as mesotrons in both cases. In several other reports penetrating particles produced in multiples have been interpreted as mesotrons without any real justification for such an interpretation.

Only one of the thirty-one stars containing merely short-range particles was observed to have been caused by an ionizing ray, but in several cases such a ray could not have been observed. A time-coincident cascade shower accompanied one of the stars; in this case a non-ionizing ray gave rise to the star. Eight of the stars containing long-range particles were initiated by ionizing rays and thirteen by non-ionizing rays. In two photographs time-coincident cascade showers were also present. In one of these cases the star was initiated by a penetrating ionizing particle, which also appeared to initiate the shower through the medium of a knock-on electron; in the other case the nature of the ray that initiated the star could not be ascertained.

Twenty of the stars consisting of short-range particles contained only particles that were projected downward whereas the other eleven contained both upward and downward projected particles, the number of upward and downward projected particles being about equal in the latter case. On the other hand, only six of the stars containing long-range particles included upward projected particles, and the total number of such particles was only eight.

The energies of the particles can be estimated from their range limits in lead[3] (see Fig. 4). The most energetic particles had energies greater than 100 Mev if they were mesotrons or 200 Mev, if they were protons. A block diagram of the frequency *versus* total energy actually observed in the star is given in Fig. 6. The energies were calculated by assuming that all the star particles were protons. Examples of the photographs of stars are reproduced in Fig. 7.

In the above analysis, heavily-ionizing particles that occurred singly and originated in the lead plates have been omitted because, in the first place, it was impossible in many cases to distinguish between α-particles from radioactive sources and heavily-ionizing particles ejected by cosmic rays, and, in the second place, it is not known that the single particles result from the same type of event.

SINGLE HEAVILY-IONIZING PARTICLES

As mentioned in the preceding section, there were observed at least 400 heavily-ionizing particles that were projected from the lead plates and that could not have been contamination α-particles. Most of these particles evidently were projected from lead nuclei by neutrons, i.e., the incident ray was non-ionizing and the event was not associated with a cascade shower. Eight of the heavily-ionizing particles were projected from the lead by penetrating particles, which lost only a portion of their energies in the process and then continued through the remaining lead plates.

[12] C. D. Anderson and S. H. Neddermeyer, Phys. Rev. **50**, 263 (1936).
[13] J. Crussard and L. Leprince-Ringuet, J. de phys. et rad. **8**, 213 (1937).
[14] G. Herzog and W. H. Bostick, Phys. Rev. **59**, 122 (1941).
[15] D. J. Hughes, Phys. Rev. **60**, 414 (1941).

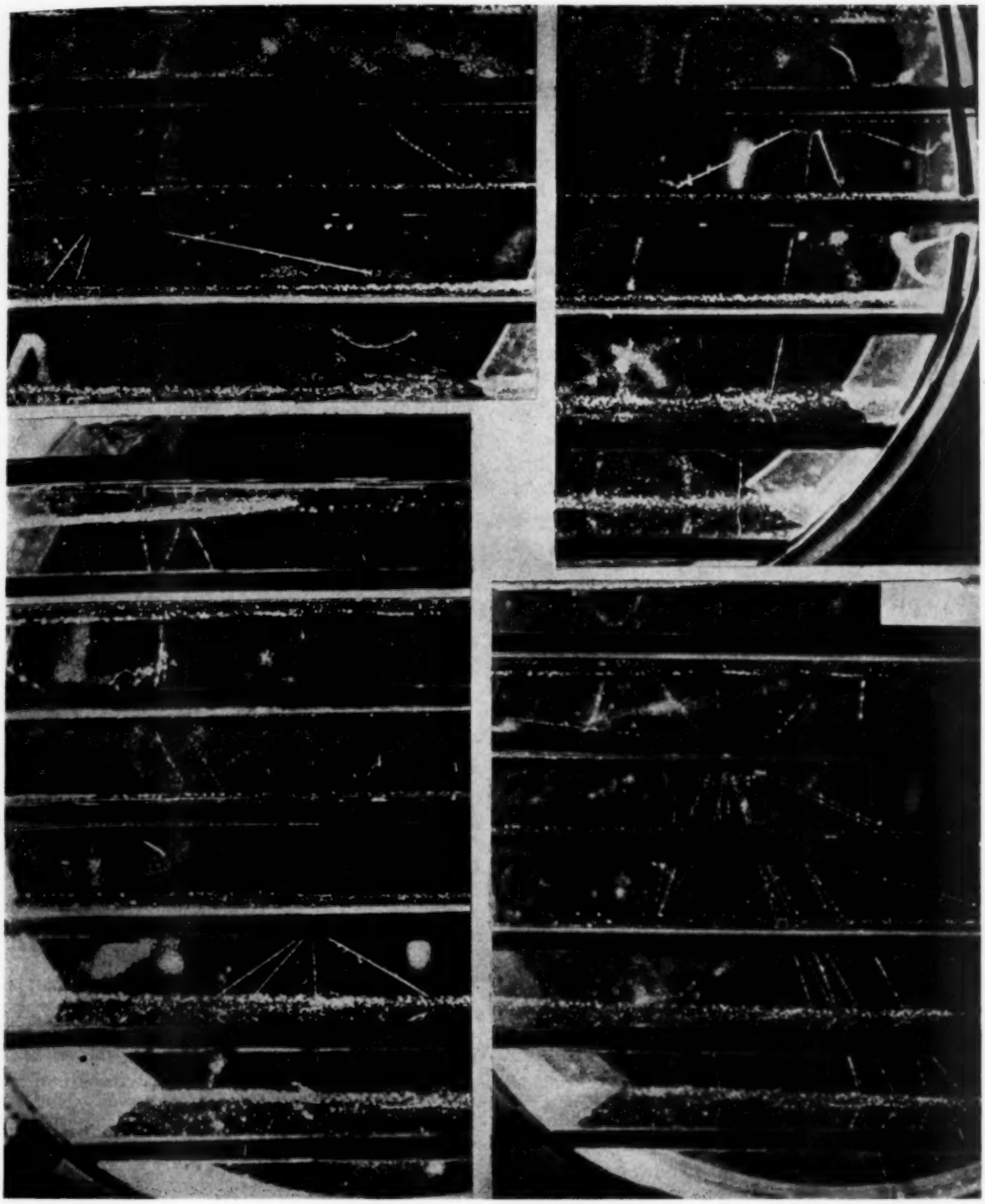

FIG. 7. Examples of nuclear disintegrations or star showers. *Upper left:* the most frequent type of star. The particles have short range and heavy ionization. *Upper right:* a star containing long- and short-range particles, probably initiated by a neutron. *Lower left:* a similar star initiated by a charged penetrating ray. *Lower right:* a star containing several long-range particles. The track doubling in one section results from a residual clearing field. The right long-range particle produces secondaries, but it is probably not an electron.

In some cases heavily-ionizing particles, which originated outside the chamber or in the glass cylinder, passed nearly horizontally through the chamber, and twenty or more centimeters of track length could be observed. In several cases eight or ten δ-rays occurred, a number that corresponds to about twenty-five times the number for $\beta \simeq 1$. These particles could not have been mesotrons since the range of such a mesotron would be only twenty centimeters (Fig. 5). They might be protons or α-particles.

A number of penetrating particles were observed that terminated their ranges in the lead plates but originated outside the chamber. In the last 4000 of the pictures, 5 inches of paraffin were placed above a portion of the chamber in order to determine whether the particles were protons projected from hydrogenous material by neutrons, as suggested by Powell.[6] A more detailed analysis of the photographs will be required before any conclusion can be drawn.

CONCLUSIONS CONCERNING NUCLEAR DISINTEGRATIONS

(1) The initiating particles are very seldom, if ever, electrons or photons. If they were electrons or photons with sufficient energy to produce the observed disintegrations, they would produce cascade showers in the lead plates above the star origin or they would be accompanied by other electrons or photons. In previous cloud-chamber experiments that seem to indicate a correlation between stars and cascade showers the cloud chamber was tripped by counters, in some cases with counter arrangements that selected multiple events only. For example, Anderson and Neddermeyer[12] observed cascade showers in more than one-third of their photographs taken at Pikes Peak. Hence their observation of 30 cases of time-coincident showers in 113 photographs with heavily-ionizing particles does not indicate association between the two types of events. The other published results also indicate no more association between cascade showers and stars or heavily-ionizing particles than would be expected of independent events. In the present work expansions were not counter controlled, and hence there was much less distortion in the relative frequencies of occurrence of the various events. Since eight percent of the photographs showed cascade showers of four or more particles, one would expect four or five of the 58 photographs of nuclear disintegrations to contain cascade showers; the observed number was three. Powell[6] also noted little if any association between showers and stars. On the other hand, Auger[16] observed a real correlation between heavily-ionizing particles and extensive (Auger) showers. However, this does not necessarily indicate production of penetrating rays by the soft component since it is known that penetrating rays are also present in Auger showers.

(2) The stars are probably produced by neutrons and protons. Since the non-ionizing rays that initiate stars are not photons, we are left with neutrons as the reasonable alternative choice. The ionizing rays that initiate showers are neither electrons nor α-particles, but in this case there are two further alternatives: protons or mesotrons. However, the frequency of occurrence of stars increases several times more rapidly than the intensity of the penetrating particles as we go to higher altitudes from sea level.[12] Since most of the penetrating particles are mesotrons, it would be possible for the relative number of protons to increase several times in going from sea level to 14,000 feet, whereas the relative number of mesotrons could not. Hence it seems most likely that the star-initiating ionizing particles are protons.

(3) There may be no sharp line of distinction between low energy stars with particles projected in all directions and high energy stars with long-range particles projected in the general direction of the incident particle. Rather there appears to be a gradual change from one type to the other with increasing energy of the initiating particle. Examples of all types of intermediate cases were photographed (Fig. 7). The single heavily-ionizing particles originating in the lead plates are perhaps merely the limiting case for low energies.

(4) The initiating particles are predominately neutrons for the lower energy stars and about equally divided between ionizing and non-ionizing particles (protons and neutrons) for the higher energy stars. Nearly all of the single

[16] P. Auger, R. Maze, P. Ehrenfest, and A. Freon, J. de phys. et rad. **10**, 39 (1939).

heavily-ionizing particles were produced by neutrons.

(5) The star particles are mostly mesotrons and protons. In the present work very few electrons or α-particles were observed in the high energy stars and less than half of the short-range particles could have been electrons. Examples have been quoted from other papers that gave proof of the presence of both mesotrons and protons.

Two other conclusions, which are related to reported results from other investigations, should be mentioned. (1) It seems rather presumptuous to assume that an observation of the multiple production of long-range particles with either counters or a cloud chamber is necessarily an observation of the production of mesotrons, in cases where there is no evidence that the particles are not protons. (2) Detailed analyses of stars observed in photographic emulsions that make use of conservation of momentum or of energy are likely to be meaningless with present techniques since particles with minimum ionization occur in a few of the stars and are not observed in photographic emulsions.

The observed characteristics of stars are satisfactorily described in terms of the semiquantitative theory of nuclear collisions as discussed by Heitler.[17] He not only suggests that all of the transferred energy of the incident particle might be dissipated in "heating" the entire nucleus, with subsequent emission of many particles, but he also suggests the possibility that the particles near the edge of the nucleus receive the energy and escape before sharing their energy with the rest of the nucleus. Heitler's estimates give 2×10^7 ev for the maximum energy of the emitted particles in the former process, when the energy of the incident particle is 2×10^9 ev. In the present as well as in previous work energies at least five or ten times larger than 2×10^7 ev have been observed for star particles. This result might indicate that the initiating particles had energies $\sim10^{11}$ ev or else that the latter of the processes suggested by Heitler was occurring.

There appears to be a gradual transition from the low energy uncollimated type of star produced mostly by neutrons to the high energy collimated type initiated by neutrons and protons. It may be that stars of the latter type constitute examples of the production of mesotrons by protons such as is indicated by the experiments of Schein, Jesse, and Wollan.[18] If this is so, it seems likely that protons are also produced in the same events.

Hamilton, Heitler, and Peng[19] have suggested a cascade process for the mutiple production of mesotrons. None of the present photographs gives evidence for such a process.

The author welcomes this opportunity to express again his gratitude to Superintendent Frank A. Kittredge and other members of the staff of Yosemite National Park for their helpfulness.

[17] W. Heitler, Phys. Rev. **54**, 873 (1938).

[18] M. Schein, W. P. Jesse, and E. O. Wollan, Phys. Rev. **59**, 615 (1941).

[19] J. Hamilton, W. Heitler, and H. W. Peng, Phys. Rev. **64**, 78 (1943).

On the Term Values of X-Ray Spectra

TSI-MING HU
Department of Physics, National University of Chekiang, Meitan, Kweichow, China
(Received October 8, 1943)

It is shown in this paper that the term values of the K, L, and M levels of x-ray spectra can be given by the empirical formula

$$\nu(n,j)=\frac{1}{n^2}[Z-\sigma_0-\varphi(Z)]^2+\frac{1}{n^4}\alpha^2(Z-\sigma_2)^4\left(\frac{n}{j+\frac{1}{2}}-\frac{3}{4}\right)+\cdots-2\,\Sigma_i\,Z_i\frac{Z-S_i}{n_i^2},$$

where σ_0 and σ_2 are constants for a given level and

$$\varphi(Z)=-0.098-1.80\times10^{-3}Z+1.40\times10^{-4}Z^2$$

for the K and L levels and equal to zero for the M level. The values of the screening constants best suited to the above formula are also given in the paper.

SINCE Moseley's discovery of x-ray spectra, many attempts have been made to calculate the term values of different levels. So far as the author knows, the most satisfactory formula is the one given by Pauling.[1] The formula is

$$\nu(n,j)=\frac{1}{n^2}(Z-\sigma_0)^2+\frac{1}{n^4}\alpha^2(Z-\sigma_2)^4\left(\frac{n}{j+\frac{1}{2}}-\frac{3}{4}\right)+\cdots-2\sum_i Z_i\frac{Z-S_i}{n_i^2}. \quad (1)$$

By means of this formula and the S_i values calculated by him, Pauling has shown that the values of σ_0 are nearly constant for a given level (independent of Z). He has also calculated the theoretical values of σ_0 and σ_2 and found that they agree in general with the empirical values. But detailed calculations based upon his formula show that the agreement is still not quite satisfactory. The discrepancy is most prominent in the case of the K level. In order to see what correction must be introduced into (1), the term values of the K, L, and M levels have been calculated by means of this formula with the screening constants given by Pauling. The experimental values chosen for comparison are taken from the *Handbuch der Experimental Physik*.[2] Since all the empirical values were determined by the crystal spectrometer, they have been multiplied by a numerical factor (1–0.002) on account of the fact that the value of the electronic charge is 4.803×10^{-10} e.s.u. instead of 4.774×10^{-10} e.s.u. The value of the fine structure constant used is 1/136.9.[3]

If the term values thus calculated are denoted by ν^c and the experimental values by ν^e, then the deviations $\Delta\nu$ are given by $\nu^c-\nu^e$. Plotting $\Delta\nu$ against Z, we find the points obtained do not lie on smooth curves. But the deviations are certainly systematic in case of K and L levels. The precision of the calculations is limited by the presence of uncertain errors in the values of the size screening constants, especially for electrons in the incomplete shell. To overcome this difficulty the values of the wave numbers (in Rydberg units) for K and L lines have been calculated also and compared with empirical values. In this case, only the screening constants for electrons of a single complete shell enter into the calculations. The values of $\Delta\nu$ thus obtained change continuously with Z and can be joined with smooth curves (see Figs. 1 and 2). The similarity between the two curves naturally suggests that there may be some simple relation between them. Further investigations show that they are connected by the relation $\Delta\nu K_\alpha'=3\Delta\nu L_\beta+0.15Z$.[4] The screening constants used in the calculations are given in Tables I and II.

Encouraged by the simplicity of the relation and the smoothness of the curves, attempts have

[1] L. Pauling and Goudsmit, *The Structure of Line Spectra* (1930), pp. 180–191.
[2] *Handbuch der Experimental Physik*, Vol. 24, Part 2. A. B. Lindh, *Röntgen Spektroskopie* (1930), pp. 124–174, 227–231.
[3] Compton and Allison, *X-Rays in Theory and Experiment*, pp. 697–703.
[4] According to Sommerfeld's nomenclature, the K_α' line corresponds to the transition $K\rightarrow L_{II}$ and the L_β line corresponds to the transition $L_{II}\rightarrow M_{IV}$.

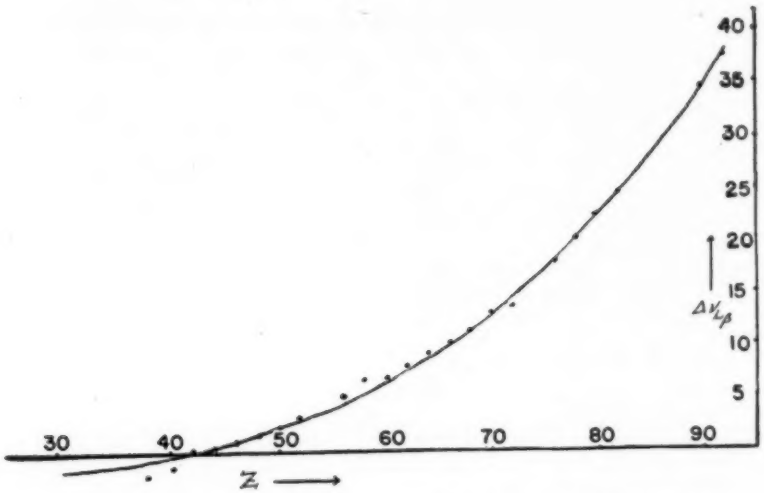

FIG. 1. $\Delta\nu_{K'_\alpha}$ against Z. Equation of the solid curve is given by (3).

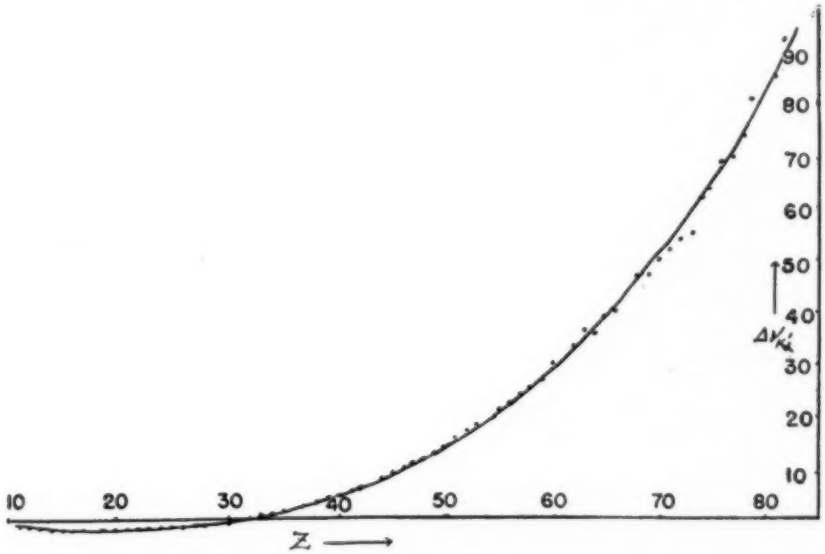

FIG. 2. $\Delta\nu_{L_\beta}$ against Z. Equation of the solid curve is given by (4).

been made first to smooth up the correction curves for different levels by making some alterations of the size screening constants[5] and then to introduce some simple corrections into (1) to bring it in better agreement with experiment. The results of such attempts may be summed up as follows:

(a) The values of different terms may be given by the formula

$$\nu(n,j)=\frac{1}{n^2}[Z-\sigma_0-\varphi(Z)]^2+\frac{1}{n^4}\alpha^2(Z-\sigma_2)^4\left(\frac{n}{j+\frac{1}{2}}-\frac{3}{4}\right)+\cdots-2\sum_i Z_i\frac{Z-S_i}{n_i^2}, \quad (2)$$

where

$$\varphi(Z)=-0.098-1.80\times10^{-3}Z+1.40\times10^{-4}Z$$

[5] The alterations of the values of size screening constants are quite arbitrary; they are given only to illustrate that the seeming irregularities of the values of $\Delta\nu$ for different levels can be eliminated by using suitable size screening constants.

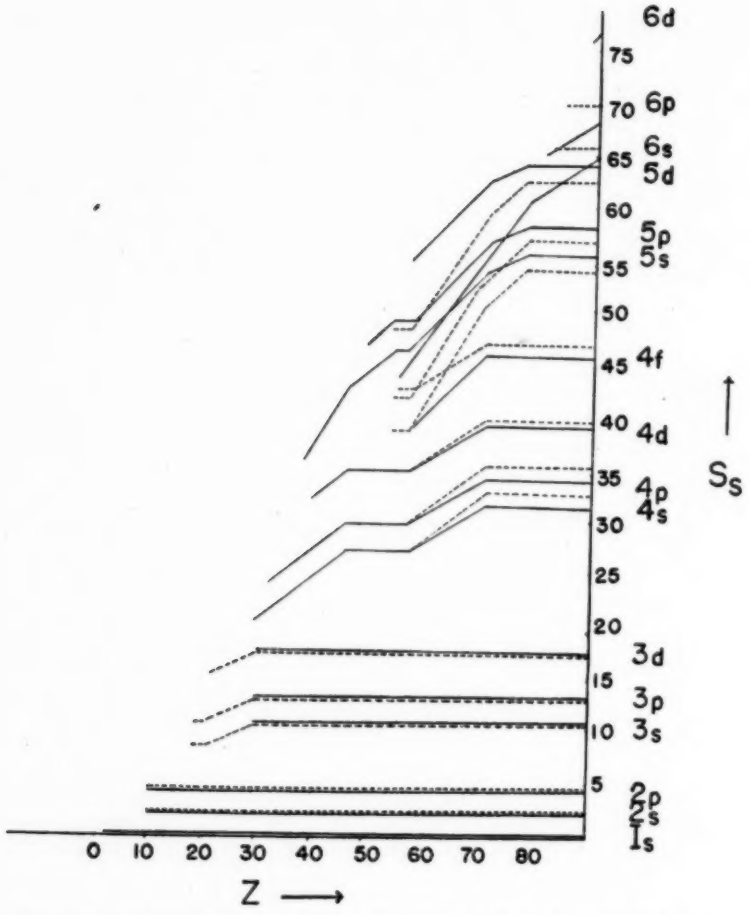

FIG. 3. S against Z. Dotted lines indicate the values given by Pauling.

for the K and L levels and equal to zero for the M level.

(b) The values of σ_0 and σ_2 best suiting the above formula are given in Table III and that of S may be read from Fig. 3.

Assuming the validity of (2) the values of $\Delta\nu K_{\alpha'}$ and $\Delta\nu L_\beta$ can be taken as the difference between the values of the wave numbers given by (1) and (2). We get, therefore,

$$\Delta\nu K_{\alpha'} = (1.5Z+2.2)\varphi(Z)+0.005Z+1.2 \quad (3)$$

and

$$\Delta\nu L_\beta = (0.5Z-3.4)\phi(Z)-0.005Z-1.2. \quad (4)$$

The constant terms in these formulas are introduced by the difference of the values of the size screening constants for L and M shells used in (1) and (2) (see Fig. 3). These relations are represented by the solid curves in Figs. 1 and 2. All the points lie close to these curves. As a further illustration of the validity of (2), the term values

TABLE I. Screening constants.

	$2s$	$2p$	$3s$	$3p$	$3d$
S	2.84	4.52	10.9	13.2	17.7

TABLE II. Screening constants.

	K	L_{II}	M_{IV}
σ_0	0.625[a]	6.80	23.8
σ_2	0.17	3.6	13.3

[a] This value was assigned by considering the structure of the two K electrons and the nucleus to be helium-like.

TABLE III. Values for formula (2).

	K	L_I	$L_{II\,III}$	M_I	$M_{II\,III}$	$M_{IV\,V}$
σ_0	0.625	5.89	6.79	20.0	21.3	23.8
σ_2	0.17	2.2	3.6	7.0	8.6	13.3

TABLE IV. Calculated and observed term values.

Z	ν_K	$\nu_K{}^r$	$\nu_K{}^c$	$\nu_{L_{II}}$	$\nu_{L_{II}}{}^r$	$\nu_{L_{II}}{}^c$	ν_{M_V}	$\nu_{M_V}{}^r$	$\nu_{M_V}{}^c$
30	711.7	710.3	711.2	77.1	76.9	77.8	0.9	0.9	2.0
35	992.6	990.6	990.6	117.7	117.5	117.3	5.2	5.2	5.2
40	1325.7	1323.1	1322.4	170.0	169.7	168.5	13.4	13.4	12.3
45	1709.6	1706.2	1707.5	231.2	230.7	231.3	22.1	22.1	23.6
52	2345.0	2340.3	2340.1	340.3	339.6	340.2	42.4	42.3	42.6
56	2756.4	2750.9	2752.6	414.3	413.5	413.7	57.6	57.5	56.7
60	3214.2	3207.8	3203.1	495.5	494.5	494.7	72.5	72.4	71.8
66	3972.5	3964.6	3972.2	632.2	630.9	630.6	95.8	95.6	94.8
70	—	—	—	735.4	733.9	733.7	112.8	112.6	112.3
74	5113.8	5103.6	5109.9	850.6	848.9	849.2	133.7	133.4	133.4
78	5764.0	5752.5	5763.1	978.7	976.7	977.1	156.4	156.1	157.0
82	6463.0	6450.1	6471.1	1121.9	1119.7	1118.1	183.0	182.6	183.1
90	8073.5	8057.4	8066.8	1451.5	1448.6	1447.3	244.9	244.4	244.0

of K, L, and M levels have been calculated from (2) and given in Table IV together with the empirical values chosen for comparison. From this table it is easily seen that the term values of L_{II} and M_V levels given by (2) are quite close to the empirical values. Since either (1) or (2) can account for the doublet structure of x-ray spectra successfully, it follows naturally that (2) can be applied to calculate the term values of any of the L and M levels with results agreeing with experiment. In the case of the K level the agreement is less satisfactory for heavy elements. Since (2) gives the values of wave numbers for K lines and L levels close to the empirical values, it may be inferred from the combination principle that the term values of the K level given by (2) must be close to the actual values, and the deviations may arise from some systematic errors of experiment. In Table IV ν_K, $\nu_{L_{II}}$, and ν_{M_V} are the experimental term values.

$$\nu_K{}^r=(1-0.002)\nu_K,$$

and similar equation for $\nu_{L_{II}}{}^r$ and $\nu_{M_V}{}^r$. $\nu_{L_{II}}{}^c$, $\nu_{M_V}{}^c$ and $\nu_K{}^c$ are the values calculated from (2).

The above corrections may arise from manifold sources, but the electronic interaction is the most probable one as is usually the case in spectroscopy. It is interesting to note that the correction term $\varphi(Z)$ is the same for the K and L level. Attempts have been made to use the same function for the M level by changing the value of σ_0 and S, but the result is less satisfactory. Evidently, the required correction may be introduced into (1) in other ways. We may, for example, write the correction formula in the form

$$\nu(n,j)=\frac{1}{n^2}[Z-\sigma_0]^2+\frac{\alpha^2}{n^4}[Z-\sigma_2]^4\left(\frac{n}{j+\frac{1}{2}}-\frac{3}{4}\right)+\cdots-2\sum_i Z_i\frac{Z-S_i}{n_i{}^2}-\Delta\nu(n,Z),$$

where $\Delta\nu(n,Z)$ may be taken as the difference between (1) and (2) or expressed in any other form. But whatever may be the form of the correction term, two facts are certain. Firstly, $\Delta\nu(1,Z)$ and $\Delta\nu(2,Z)$ are connected by the relation

$$\Delta\nu(1,Z)=4\Delta\nu(2,Z)+aZ+b.$$

The values of a and b are affected by the screening constants. They can be made to vanish if suitable screening constants are used. Secondly, the corrections for the M level are small and masked by the errors in the values of the screening constants.

In conclusion the author wishes to express his sincere thanks to Professor K. C. Wang. This work was assigned by him and has been done under his direction.

The Angular Distribution of Alphas from $Li^7(p, \alpha)\alpha$

C. D. SWARTZ,* H. H. ROSSI, B. JENNINGS,† AND D. R. INGLIS
Johns Hopkins University, Baltimore, Maryland

(Received November 12, 1943)

The tracks formed in photographic emulsions by alphas from the reaction $Li^7(p, \alpha)\alpha$ at various angles from the beam were observed at bombarding energies E between 400 and 900 kev. The angular distribution proportional to $1+A(E)\cos^2\theta$, as found by Young, Ellett, and Plain at lower voltages, was also observed here, and a maximum of $A(E)$ was found at 675 kev.

ONE of the simplest reactions yielding disintegration products whose angular distribution is of some theoretical interest is:

$$Li^7+H^1=He^4+He^4+17 \text{ Mev.} \quad (1)$$

The alphas from this reaction have a range of about 8 cm in standard air. This reaction has been studied by several observers,[1] and especially carefully by Young, Ellett, and Plain,[2] who employed proton energies up to 400 kev and showed that in this energy range the intensity as a function of angle $I(\theta)$ was very well represented by

$$I(\theta)\sim 1+A(E)\cos^2(\theta). \quad (2)$$

Here θ is the angle between the incident proton and the observed alpha in the center-of-mass coordinate system, and $A(E)$ is a factor depending only on the energy E of the proton. Their values of $A(E)$ are represented by the small circles in Fig. 2. Although the statistical uncertainties were too great to allow a definite conclusion on this point, the curve seemed to level off as it approached their maximum bombarding voltage, 400 kev, which suggested the existence of a maximum nearby.

Critchfield and Teller,[3] in a theoretical discussion of this reaction, correlated this apparent maximum with a resonance at about 400 kev indicated by the yield curve[4] together with a theoretical treatment of the penetration factor. They showed that both of these observations could be explained by simple assumptions involving only a broad S and a narrow P state of the compound nucleus Be^8.

The protons with energies up to 900 kev were provided by the pressure insulated Van de Graaff generator[5] in the Johns Hopkins University Physics Department. The target chamber assembly is shown diagrammatically in Fig. 1. The beam entered the chamber through a slit 2 mm high by 6 mm wide. The inclination of the target block made the target spot about 5 by 6 mm. The thin lithium targets used were made by evaporating metallic lithium onto a hexagonal target block made of copper, which could be turned to present any one of its faces to the beam or to the furnace. The evaporation was done in vacuum with a simple lithium stove as shown. The metallic lithium had to be packed very tightly into the cavity of the furnace to insure a steady and slow evaporation. With small pieces of lithium merely dropped into the stove, much more power was needed, and the pieces disintegrated in an explosive fashion. A rough check by means of the 440-kev gamma-ray resonance indicated that the target thickness was usually equivalent to about 20 to 60 kev.

The bombarding voltage was measured by magnetic deflection of the proton beam. The deflecting field was held constant and voltage was indicated by the angular displacement of the target chamber necessary to put the proton spot on the entrance slit. The deflection was calibrated by the 440-kev gamma-resonance[6] of Li and

* Now at S. A. M. Laboratories, Columbia University, New York, New York.

† Now at the Western Electric Company, Baltimore, Maryland.

[1] F. Kirchner, Physik. Zeits. **34**, 785 (1933); J. Giarratana and C. G. Brennecke, Phys. Rev. **49**, 35 (1936); H. Neuert, Ann. d. Physik **36**, 437 (1939).

[2] Young, Ellett, and Plain, Phys. Rev. **58**, 498 (1940).

[3] C. L. Critchfield and E. Teller, Phys. Rev. **60**, 10 (1941).

[4] Rumbaugh, Roberts, and Hafstad, Phys. Rev. **54**, 651 (1938); Herb, Parkinson, and Kerst, Phys. Rev. **48**, 118 (1935); Heydenburg, Zahn, and King, Phys. Rev. **49**, 100 (1936).

[5] A description will be published in *The Review of Scientific Instruments*.

[6] Hafstad, Heydenburg, and Tuve, Phys. Rev. **50**, 504 (1936).

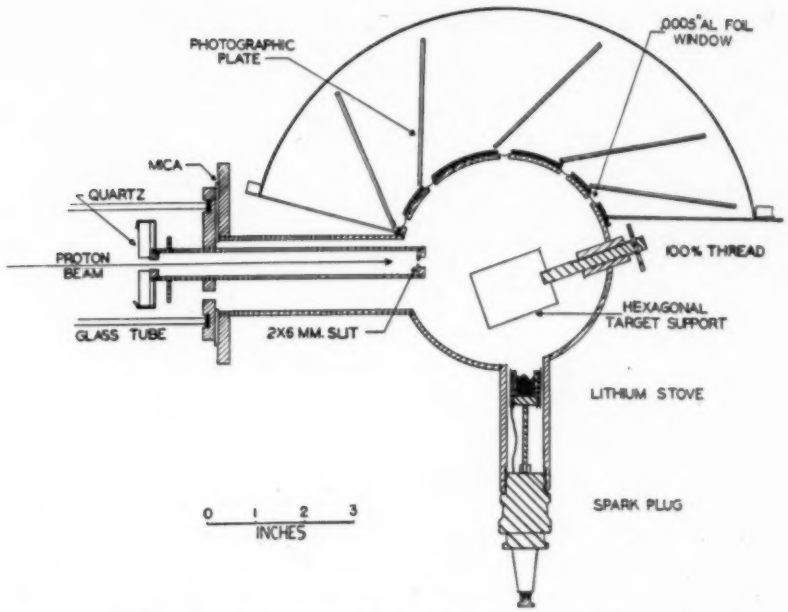

FIG. 1. The angular distribution of alphas from Li^2 $(p, \alpha)\alpha$. Target chamber.

verified by the 334-kev and 660-kev resonances[6,7] of F. Two values of the magnetic field were used to secure convenient deflections over the whole range of energies used. The accuracy of this method of measurement was limited by erratic fluctuations in the position of the undeflected beam position. The uncertainties in voltage arising from voltage fluctuation and inaccurate measurement are expressed by the width of the circles in Fig. 2.

The alphas were detected simultaneously at five different angles by means of photographic plates placed opposite each of the five thin aluminum windows as shown in Fig. 1. Since the range of these alphas in air is about 8 cm and the air equivalent of the 0.0005″ aluminum foil is about 2.5 cm, there is a residual range in the emulsion quite sufficient to produce a track of satisfactory length.

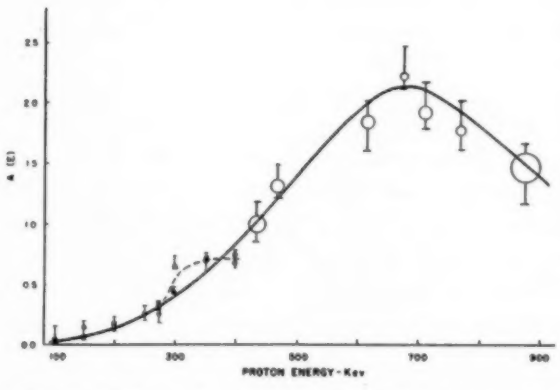

FIG. 2. $A(E)$ as a function of bombarding energy. Small circles and broken curve: data and curve of Young, Ellett, and Plain.

The angle of incidence was made 45° as a mean between normal incidence, in which the track would appear as just one point, and grazing incidence, in which the track would be lost in the surface fog. The plateholder was designed to fit around the target chamber with an aperture opposite each thin-foil window. The apertures were closed by a shutter to allow removal of the plateholder for loading. The plates used were Eastman fine grain Alpha Particle Plates 1″ by 3″. It was found necessary to store the plates in a dry and fairly cool place to avoid fogging which, although still invisible without the microscope, would interfere with the counting of alpha-tracks. After exposure the plates were developed in a specially constructed rack of glass rods, and after drying the exposed parts were protected with a cover glass.

The tracks were counted under a microscope with dark-field illumination and 400-fold mag-

[7] Bennett, Herb, and Parkinson, Phys. Rev. **54**, 398 (1938).

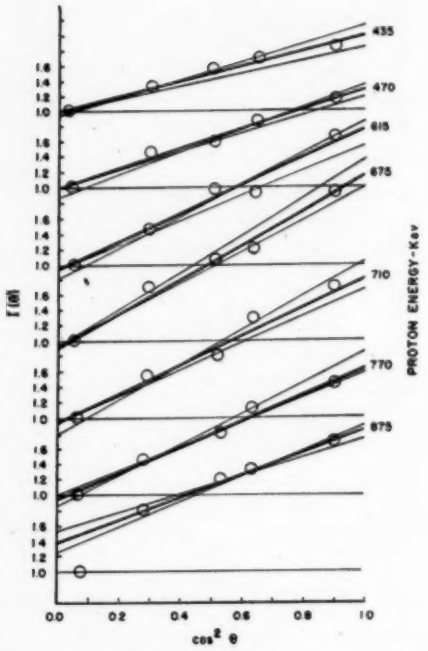

FIG. 3. Angular distribution of alphas from $Li^7(p, \alpha)He^4$ at several bombarding voltages.

nification. The ocular had a diaphragm with a rectangular opening traversed by a cross-hair. The plate was moved by a mechanical stage, and the number of tracks passing the cross-hair in a swath of fixed width was counted as the stage moved through unit distance. About a thousand tracks were counted on each plate.

The photographic method was chosen in preference to electrical counting methods because of its simplicity and because the simultaneous exposure of five plates required less operating time of the generator than the customary electrical counting at only two windows simultaneously. This advantage is, however, partially offset by the tedious task of counting the tracks at leisure.

The data so obtained were transformed[8] to the center-of-mass coordinate system. This introduces modifications up to almost 20 percent in spite of the great energy liberated.

[8] Haxby, Allen, and Williams, Phys. Rev. **55**, 140 (1939).

Figure 3 shows the intensity $I(\theta)$ plotted against $\cos^2\theta$. The results are shown for several different bombarding energies. In most cases it was not possible to draw a straight line through all five of the circles (whose radii equal the standard deviation) which represent the data. In some cases the best straight line passes rather far outside of some of the circles, and there is only a small probability that, at the same time, Eq. (2) applies and no experimental error has occurred other than statistical fluctuations. There is a tendency for one or two of the circles to fall below a straight line through the other four or three, but there is no apparent regularity in these deviations. We prefer to attribute them to experimental error (such as non-uniformity of plates or of development which might possibly persist in spite of precautions), rather than to deviations from (2). In particular, the lowest circle in the set at the highest voltage falls seriously below the line determined by the other four, and we have arbitrarily ignored it. In all cases, the slopes in Fig. 3 were determined by personal judgment. Through each set appear three lines to represent what we consider the most probable and the two extreme admissible slopes.

Figure 2 shows $A(E)$ as a function of bombarding energy E. The circles represent values of A (the slopes of the lines in Fig. 3) which were regarded as the most probable. The length of the vertical lines represents the estimated range of admissible slopes. It can be seen that the curve passes through a moderately sharp maximum and then comes down rather rapidly as predicted.[3] However, the maximum occurs not around 400 kev, but at about 675 kev (which corresponds to about 590 kev in the center-of-mass coordinate system). Our data are not sufficiently detailed to confirm or reject the inflection at 400 kev suggested by the data of Young, Ellett, and Plain, and indicated by the dotted line in Fig. 2.

We are very grateful to Professor J. A. Bearden for his advice and direction during the early part of this work.

The Angular Distribution of Alphas from $F^{19}(p, \alpha)O^{16}$

H. H. Rossi and C. D. Swartz*
Johns Hopkins University, Baltimore, Maryland
(Received November 12, 1943)

The angular distribution of alphas from the reaction $F^{19}(p, \alpha)O^{16}$ has been investigated at bombarding voltages between 500 and 900 kev. The distribution was found to depend markedly on bombarding energy, contrary to the result found by McLean, Ellett, and Jacobs at lower voltages.

THE angular distribution of alphas from the reaction[1,2]

$$F^{19}+H^1=O^{16}+He^4+7.95 \text{ Mev} \qquad (1)$$

has been studied by McLean, Ellet, and Jacobs[3] in the energy range 330 to 435 kev. The variation with voltage observed in this range was so slight that they interpreted it as hardly significant in view of the statistical error. Gerjuoy[4] has shown theoretically that these results could arise from three overlapping levels of Ne^{20} with $J=0$, 1, and 2. These states would lead to no powers higher than the third when the intensity is expanded in powers of $\cos\theta$.

We have investigated the reaction (1) in the energy range 500 to 900 kev. This was done in conjunction with the experiments reported in the preceding paper, and the apparatus and the methods employed were essentially the same. The targets used were slabs of fluorite (CaF_2) about $\frac{1}{32}''$ thick mounted on the copper target support. Attempts to use a thin target of NiF_2, made by electrolizing HF with a nickel electrode, were unsuccessful with proton currents through the defining slit of the order of one microampere available.

The use of a thick target seemed justified at first by the combination of two circumstances: the very rapid rise of the total yield with voltage and the slow variation of the distribution which was anticipated by extrapolation from the earlier experiments.[3] Our results show that this anticipation was false, however, and the rapid variation of yield is not by itself sufficient to justify substitution of thick for thin targets, except for the sake of a rough indication of trends. A thin-target result may, of course, be obtained from sufficiently complete thick-target data by differentiation with respect to voltage. But our thick-target data are not complete enough to allow this to be done accurately.

Between 500 and 900 kev the yield curve[2] of this reaction is not a steadily and rapidly increasing function, but has two pronounced maxima. Therefore, for certain values of the bombarding energy V_b the production of alphas will be less abundant at the surface of the target than at some distance below it, where the protons have a lower energy V. The number of collisions of energy between V and $V+dV$ will be proportional to the thickness of the layer in which the corresponding deceleration takes place. This distance is equal to dV divided by V', the slope of the energy-range curve at energy V. This must be multiplied by $y(V)$, the yield at V and $q(V)$, the charge decelerated from $V+dV$ to V, to get a measure of the number of alphas produced between $V+dV$ and V. In the experiment the bombarding voltage varied during an exposure, and a record was made of the incident charge as a function of V_b. By integrating over all charges incident at values of V_b greater than V, one obtains the total charge $q(V)$. Thus the number of alphas arising from collisions of energy between V and $V+dV$ during an entire exposure is proportional to dV multiplied by

$$I(V)=q(V)y(V)/V'. \qquad (2)$$

The results of three exposures at the lower ranges of bombarding voltages are shown in Fig. 1. The relative numbers of alphas produced by collisions of various energies are indicated by the

* Now at S. A. M. Laboratories, Columbia University, New York, New York.
[1] W. E. Burcham and C. L. Smith, Proc. Roy. Soc. **A168**, 176 (1938).
[2] Streib, Fowler, and Lauritsen, Phys. Rev. **59**, 253 (1941).
[3] McLean, Ellett, and Jacobs, Phys. Rev. **58**, 500 (1940).
[4] E. Gerjuoy, Phys. Rev. **58**, 503 (1940).

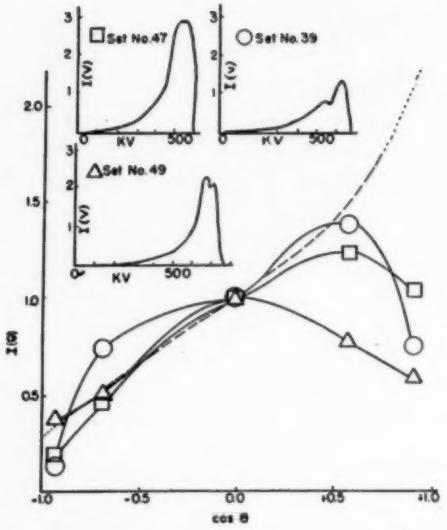

FIG. 1. Angular distribution of alphas from $F^{19}(p, \alpha)O^{16}$ at low bombarding voltages. The broken line represents the data of McLean, Ellett, and Jacobs between 330 and 435 kev. The inserts give in arbitrary units the relative number of α's as a function of voltage for each set.

functions $I(V)$ shown in the inserts to the figure. In order to verify that the striking variation of the angular distribution with voltage was not due to some erratic experimental error, three exposures were made at the higher voltage range with two different fluorite crystals as target. The results are in satisfactory agreement, as shown in Fig. 2. The insert in this figure gives $I(V)$ for one of the exposures, the other two having quite similar curves of $I(V)$.

The "points" are plotted as circles, squares, and triangles (the dimensions of these figures are approximately equal to the standard deviation). We were unable to check the data of McLean, Ellett, and Jacobs. Every attempt to secure data at voltages below 500 kev produced very heavy general fogging of the region of the plates exposed to the alphas. The cause of this fogging appears to have been some soft radiation from the target, since it could penetrate the 0.0005″ aluminum window but not the $\frac{1}{16}$″ brass wall of the target chamber. It should be pointed out, however, that the data of McLean, Ellett, and Jacobs do not extend beyond $\cos\theta = 0.70$, so it is possible that even at their voltages the curve turns downward beyond that point.

Particular pains were used to check possible sources of error. Evidence that the photographic method of determining relative intensities is not at fault is furnished by the consistency of the three sets of data at higher voltages, and also by the good internal consistency of the data on the angular distribution of alphas from the $Li^7(p, \alpha)\alpha$ reaction.[5] The possibility of extraneous alphas produced by contaminations in the target material must be considered. In the arrangement used, an alpha can enter the emulsion only after traversing 0.0005″ of aluminum and about 1 cm of air. Since the air equivalent of aluminum is about 1800, this means that only alphas whose range in air is at least 3.3 cm can enter the emulsion at all.

We consider that a range of at least 2-cm air equivalent in the emulsion is necessary in order to assure recognition of a track, so this particular apparatus will detect only alphas at least 5.5-cm range in air. Fluorine alphas, whose range is about 6 cm in air, are already difficult to count. Lithium and fluorine are the only light elements taking part in a (p, α) reaction which produce alphas of over 5-cm range. Precautions were taken to eliminate lithium contamination and, in addition, any large proportion of the long range lithium alphas would have been quite noticeable in examining the plates. The only other reaction

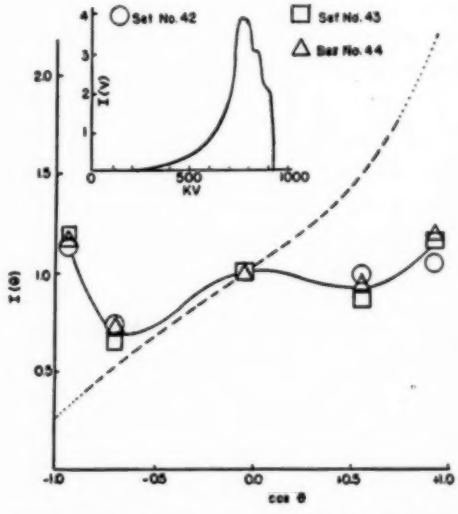

FIG. 2. Angular distribution of alphas from $F^{19}(p, \alpha)O^{16}$ at high bombarding voltages. The broken line represents the data of McLean, Ellett, and Jacobs between 330 and 435 kev. The insert gives in arbitrary units the relative number of alphas as a function of voltage for one set; the other two are quite similar.

[5] Swartz, Rossi, Jennings, and Inglis, Phys. Rev. 65, 80 (1944).

offering any reason for suspicion is $B^9(p, \alpha)Be^8$. Although these alphas have a range of only 4.4 cm in air, the cross section for this reaction is larger than that for fluorine by a factor of the order of 1000. Enough long range stragglers might possibly occur to produce an appreciable effect if a large amount of boron were present.

A rough spectroscopic test revealed no boron. The great strength of a boron line on a comparison spectrum made us believe that the proportion of boron in the fluorite was almost certainly less than one part in a thousand, and probably not more than one part in ten thousand, but we have no definite basis for stating an upper limit.

The fact that the targets from two separate pieces of fluorite (one of which was definitely pink, the other white) which would not be assumed to contain equal boron contamination, gave results identical within experimental error, seems to indicate that the distribution observed is indeed due to fluorine alphas only.

We are very grateful to Professors D. R. Inglis and J. A. Bearden for direction and advice, and to Mr. Burridge Jennings, who constructed almost all the apparatus used.

PHYSICAL REVIEW VOLUME 65, NUMBERS 3 AND 4 FEBRUARY 1 AND 15, 1944

Interpretation of the Angular Distribution of Alphas from $Li^7(p;\alpha)\alpha$

E. EISNER*
Johns Hopkins University, Baltimore, Maryland
(Received November 12, 1943)

Proton penetration factors for $Li^7(p;\alpha)\alpha$ are calculated under several assumptions of nuclear potential. The status of the Critchfield-Teller theory is briefly discussed in the light of these calculations and the angular distribution found by Jennings, Swartz, and Rossi. Measurements at higher energies are called for.

A DETAILED knowledge of $Li^7(p;\alpha)\alpha$, one of the most widely studied of nuclear reactions, is quite important for nuclear theory. Since it is one of the simplest reactions, calculations based on various detailed assumptions of nuclear forces can be carried through and checked against observation. Although experiments do not give directly the energy levels of light nuclei, it is convenient to divide the calculations into two stages, *viz.*, the calculation of energy levels based on detailed assumptions of nuclear structure, and the calculation of excitation and angular distribution functions, based on these levels, but not involving very detailed assumptions of nuclear model. Hence a check of the second part of the calculation with experimental results can be used to infer the actual energy levels.

Critchfield and Teller[1] have treated the theory of the angular distribution and excitation functions in the $Li^7(p;\alpha)\alpha$ reaction by means of the usual perturbation theory formulation. More recently Swartz, Rossi, Jennings, and Inglis[2] have extended the range of angular distribution measurement past 400 kev to about 900 kev. They found that the results could be fitted by a factor of the form $1+A(E)\cos^2\theta$ over the entire range of bombarding energies thus far measured. The maximum value of $A(E)$ was found to occur at 675 kev rather than near 400 kev as anticipated on the basis of Young, Ellett, and Plain's data.[3] The later experiments were not sufficiently good in the neighborhood of 400 kev to exclude the possibility of a secondary peak there, though they made this seem unlikely. A secondary peak there would be incompatible with the assumptions of Critchfield and Teller.

Most of the energy dependence of the matrix

* Now at the National Bureau of Standards, Washington, D. C.

[1] C. L. Critchfield and E. Teller, Phys. Rev. **60**, 10 (1941).

[2] C. D. Swartz, H. H. Rossi, B. Jennings, and D. R. Inglis, Phys. Rev. **65**, 80 (1944).

[3] V. J. Young, A. Ellett, and G. Plain, Phys. Rev. **58**, 498 (1940).

elements involved in the perturbation calculation is due to the Coulomb repulsion of the bombarding proton. Since only P protons are involved in this reaction,[4] it seems legitimate to factor the matrix elements into the so-called penetration factor for P protons impinging on Li^7, which contains most of the energy dependence, and the "internal yield" factor, which is relatively constant. Critchfield and Teller[1] pointed out that the maximum in $A(E)$ would be expected to occur at lower bombarding energy than the maximum in the internal yield at right angles, as deduced in reference 1 from the data of Rumbaugh, Roberts, and Hafstad[5] and others. Actually the opposite was found, and the discrepancy is now accentuated in the light of the more recent data, by the shift of the maximum of $A(E)$ to a higher energy than anticipated.

Since the internal yield is equal to the measured yield divided by the calculated penetration factor, or Y/P, it seems reasonable to examine the calculation of the penetration factor for stability of the result under reasonable changes in the details of the model used. The dispersion formula will be most accurate if the unperturbed wave functions used cause rapid convergence of the perturbation calculation. A proper choice will make the matrix elements $V(r; n, p)$ occurring in the second-order terms as small as possible. Now

$$V(r; n, p) = \int \psi_{Cr} V_{AP} \psi_{An} \psi_{Pp} d\tau,$$

where ψ_{Cr} is the wave function of the compound nucleus as calculated from the Hamiltonian of Be^8, except that it reduces rapidly to zero at about $r = r_0$. ψ_{An} is the wave function of the Li^7 nucleus as calculated from its Hamiltonian, H_A. ψ_{Pp} is the wave function of the incident proton, calculated with the Hamiltonian $T_{AP} + U_P$. The Hamiltonian for the complete system may be written $H = H_A + T_{AP} + U_P + V_{AP}$ and V_{AP} is the perturbation potential.

The choice of U_P which minimizes $V(r; n, p)$ is not the average potential of a proton in the Li^7 field, which is attractive at small distance, but rather a repulsive potential. This has a reasonable interpretation, *viz.*, that the proton does not exist as such inside the nucleus, and hence its wave function should die out there.[6] Since H is fixed, $U_P + V_{AP}$ is not subject to choice. If U_P is chosen as a large repulsive potential, V_{AP} must be chosen large to compensate. There is thus an optimum U_P which makes $V(r; n, p)$ smallest. For this U_P, ψ_{Pp} is small inside $r = r_0$. Since ψ_{Cr} reduces to zero rapidly at about $r \geqq r_0$, the important contribution comes from the region about r_0, and hence the dependence of $V(r; n, p)$ on bombarding energy is closely the same as that of $(|\psi_{Pp}|)_{r=r_0}$ since the other factors are independent of bombarding energy.

By use of Yost, Wheeler, and Breit's[7] tables of Coulomb wave functions, values of the relative penetration factor $P \sim (F_1^2/\rho^3)_{r=r_0}$ were calculated for several different values of r_0 and for several different choices of U_P.

(A) With U_P a constant repulsive potential U_0 for $r < r_0$, and a Coulomb potential for $r > r_0$ (cut off to zero at large distance for convenience of calculation), the result was not significantly dependent on the choice of U_0 for the several trial values 785, 1500, 3000, and 15,000 kev.

(B) Calculations were also made by using for U_P a Coulomb potential down to $r = 0$, again cut off at large distance.

(C) Penetration factors arising from Kapur and Peierls'[8] treatment of the dispersion formula, i.e., $1/\rho G_1^2$ in the notation of reference 7, were also calculated for the case of U_P a Coulomb potential down to $r = 0$. As Breit pointed out,[9] $1/\rho G_1^2$ is almost the same as F_1^2/ρ^3 as long as $\phi_1 \theta_1 \geqq 1$, which is true in this region of bombarding energies.

With $r_0 \geqq 4 \times 10^{-13}$ cm, a maximum was obtained in all cases, below $A(E)$ max., independent of the details of the nuclear model used. For r_0 in this neighborhood the values for the right angle yield[5] Y would have to be badly in error to make the maximum of Y/P occur at higher energy than the maximum of $A(E)$. As r_0 is assumed larger, differences appear in the shape

[4] E. D. Courant, Phys. Rev. **63**, 219A (1943).
[5] L. H. Rumbaugh, R. B. Roberts, and L. R. Hafstad, Phys. Rev. **54**, 657 (1938).
[6] H. A. Bethe, Rev. Mod. Phys. **9**, 91 (1937).
[7] F. L. Yost, J. A. Wheeler, and G. Breit, Terr. Mag. **40**, 443 (1935).
[8] P. L. Kapur and R. Peierls, Proc. Roy. Soc. **166**, 277 (1938).
[9] G. Breit, Phy. Rev. **58**, 506 (1940).

TABLE I. Internal yield at right angles, calculated from the observed data for various nuclear radii by several methods of approximation. Values listed are log Y/P plus a constant selected to make yield and penetration factor match at $E=225$ kev.

Bombarding energy (kev)	895	711	565	449	357	225
Energy (K.E. in center of mass system)	783	622	494	393	312	197
Calculation (A)						
I	0.40	0.38	0.38	0.37	0.34	0
II	0.38	0.36	0.36	0.36	0.34	0
III	0.32	0.33	0.34	0.35	0.33	0
IV	0.29	0.32	0.34	0.34	0.33	0
Calculation (B)						
I	0.35	0.35	0.36	0.36	0.33	0
II	0.33	0.34	0.35	0.35	0.33	0
III	0.30	0.32	0.34	0.34	0.32	0
IV	0.28	0.31	0.33	0.34	0.32	0
Calculation (C)						
I	0.50	0.48	0.45	0.43	0.36	0
II	0.47	0.45	0.43	0.40	0.36	0
III	0.38	0.38	0.38	0.37	0.33	0
IV	0.34	0.35	0.36	0.36	0.33	0

I. $r_0=6.17\times10^{-13}$ cm III. $r_0=3.80\times10^{-13}$ cm
II. $r_0=5.50\times10^{-13}$ cm IV. $r_0=3.09\times10^{-13}$ cm

of Y/P depending on the type of calculation used. (See Table I.)

Calculation (B) apparently still shows a maximum in the same region as before, but in (A) and (C) the maximum, if it exists, is moved out of the range of energies thus far used. One may take these results to indicate either that r_0 must be in the neighborhood of 4×10^{-13} cm, as is customarily assumed, or that this perturbation calculation is not particularly trustworthy, as Breit[9] has remarked.

A closer examination also reveals that the first choice above is not necessarily at odds with the Critchfield-Teller theory. It[1] leads to the result:

$$\sigma\sim\left[1+\frac{2(\epsilon-\epsilon_0)\beta\cos\delta\cos\xi+2\beta^2}{1+\epsilon^2}\right]+\cos^2\theta\left[\frac{6\beta\cos\delta\cos\xi(\epsilon_0-\epsilon)}{1+\epsilon^2}\right],$$

where

$$\epsilon_0=-\tan\delta+(u/2)\cos 2\xi$$

and $u=\beta/\cos\delta\cos\xi$, and also

$$A(E)=\frac{6\beta\cos\delta\cos\xi(\epsilon_0-\epsilon)}{1+\epsilon^2+2(\epsilon-\epsilon_0)\beta\cos\delta\cos\xi+2\beta^2}$$

with $A(\epsilon_0)=0$. Here ξ is the angle denoting admixture of triplet and $\beta\exp(i\delta)$ is a complex number depending on the wave function of the compound nucleus, *viz.*,

$$\beta\exp(i\delta)\equiv 10^{\frac{1}{2}}\alpha_2\Gamma_0/2\alpha_0\Gamma_2.$$

From this result it follows that $A(E)$ max. $=A(\epsilon_m)=-3\beta^2/(\beta^2+u\epsilon_m)$ and σ max. $=\sigma(\epsilon_n)\sim1+\beta^2/u\epsilon_n$, where ϵ_m is the position of $A(E)$ max. and ϵ_n is the position of σ max., and

$$\epsilon\equiv(E-E_2)/\tfrac{1}{2}\Gamma_2.$$

For $u>0$, $\epsilon_m=\epsilon_0-(1+2\beta^2+\epsilon_0^2)^{\frac{1}{2}}<0$ and $\epsilon_n=(\epsilon_0-u)+[(\epsilon_0-u)^2+1]^{\frac{1}{2}}>0$,

leading to $\epsilon_n>\epsilon_m$, contrary to observation.

On the other hand, the sign of u is merely a question of the phase of the triplet admixture in the wave function of the compound nucleus, and for $u<0$, $\epsilon_m=\epsilon_0+[1+2\beta^2+\epsilon_0^2]^{\frac{1}{2}}>0$ and $\epsilon_n=(\epsilon_0-u)-[(\epsilon_0-u)^2+1]^{\frac{1}{2}}<0$. In this case $\epsilon_m>\epsilon_n$ as observed. Also

$$\epsilon_m-\epsilon_0=(1+2\beta^2+\epsilon_0^2)^{\frac{1}{2}}>0$$

and hence ϵ_0 is below ϵ_m. Therefore the observed zero in $A(E)$ in the neighborhood of zero bombarding energy occurs at ϵ_0. There is little difficulty in finding sets of consistent values for ξ, β, δ, and E_2 fitting the observed separations $\epsilon_m-\epsilon_0$ and $\epsilon_m-\epsilon_n$. Their direct calculation, however, hardly seems feasible, since detailed considerations of nuclear model are involved. It does seem reasonable to assume, however, that $X_2=X_2^{(3)}\sin\xi+X_2^{(1)}\cos\xi$, the combination of incident triplet and singlet states with $J=2$ which corresponds most strongly to the compound state involved in the alpha-decay, will not be more triplet than singlet, so that $|\xi|<45°$ and $\cos 2\xi>0$.

Measurements at higher energies are needed. The present expectation is that $A(E)$ goes to zero asymptotically at higher energy. Negative $A(E)$, at least below the region where higher levels of Be^{8*} become involved, would force a revision of the theory.

I gratefully acknowledge the constant encouragement given and the kind interest shown in this work by Dr. D. R. Inglis, under whose direction it was done.

Differential Equations for the Probability Distribution of Events*

ARTHUR E. RUARK
University of North Carolina, Chapel Hill, North Carolina

(Received November 29, 1943)

The differential equations governing the probability distribution of events distributed over a multidimensional domain are derived. They are a generalization of the equations governing the probability distribution in a time series. Let $f_r(x, y)dxdy$ be the chance that an event will occur in the domain $dxdy$ when r events have already occurred in the domain $(0, x; 0, y)$. The equations which are derived then govern the set of functions $W_n(x, y)$, where W_n is the chance that n events occur in the domain $(0, x; 0, y)$. The problem of solving them reduces to the solution of a sequence of first-order ordinary equations, but these are exact, so the solution is merely a matter of quadratures. The general solution is written, and a few simple illustrations are given.

I. INTRODUCTION

IN spite of the frequent use of differential equations in special problems of probability theory, it appears that there is a need for explicit statement of the general equations which govern the probability of having n events in a given domain described in terms of variables x, y, etc. The purpose of this paper is to derive these equations, and to give their solutions for some important cases. The problems in which such probabilities are encountered are exceedingly diversified and numerous. They range from astronomy to zoology, from studies of the distribution of stars and nebulae to problems concerning the distribution of bacteria in culture dishes. The general features of such problems can be well understood from a simple example. Suppose we have a piece of cloth, of length x and width y; and let $f(x, y)dxdy$ be the chance that a flaw occurs in the element $dxdy$. Then the chance that there are n flaws in the area xy may be called $W_n(x, y)$ and we desire a set of differential equations from which we can find the functions W_0, W_1, etc.

In 1910 Professor Bateman[1] solved a problem of this type involving a time series. Considering the emission of alpha-particles from a radioactive source of constant strength, he assumed that the chance an alpha-particle will be produced in time dt is fdt, where f is a constant, namely, the average number emitted per second. Bateman showed that the chance of getting n particles in time t is

$$W_n=(ft)^n e^{-ft}/n! \qquad (1)$$

In 1935 Ruark and Devol[2] formulated the differential equations for a more general case. Suppose we know $f_r(t)dt$, the probability that an event will occur in dt when r have already occurred in time t. Then the chance $W_n(t)$ that n events will occur in the time interval $(0, t)$ is governed by the equation:

$$dW_n/dt=f_{n-1}W_{n-1}-f_nW_n; \quad n=1, 2, \cdots. \qquad (2)$$

When n is 0, we omit the first term on the right.

The fact that the chance of the occurrence of an event now depends on the number which have preceded it represents a considerable increase in scope. It is easily possible to go further, dealing with the situation in which f depends on the *detailed arrangement* of the previous events in time. Dependence of f on the occurrence of still other types of events can also be included, leading to systems of coupled equations describing the chance of each type; but problems which require these refinements have not yet come to the writer's attention.

It has become customary to speak of the events as "random" when f is a constant, and we shall adhere to this nomenclature.

II. EQUATIONS FOR PROBABILITIES WHICH DEPEND ON SEVERAL VARIABLES

For brevity's sake, we shall deal with two variables since the generalization to more than two is simple.

* Presented before the Southeastern Section, American Physical Society, April, 1943.

[1] H. Bateman, Phil. Mag. **20**, 698 (1910).

[2] A. E. Ruark and L. Devol, Phys. Rev. **49**, 355 (1936).

1. Rectangular Coordinates

Referring to the above illustration of the piece of cloth, let $f_n dxdy$ be the chance that an event occurs in the element $dxdy$ when n have occurred in the rectangle whose opposite corners have the coordinates 0, 0 and x, y. We seek the value of $W_n(x+dx, y)$. Holding y constant, we can get n events in the rectangle of base $x+dx$ and height y, in two ways convenient for our purpose. Writing the sum of their probabilities, we have:

$$W_n(x, y)+(\partial W_n/\partial x)dx$$

$$=W_{n-1}\left(\int_0^y f_{n-1}dy\right)dx+W_n\left[1-\left(\int_0^y f_n dy\right)dx\right].$$

A similar equation holds for $\partial W_n/\partial y$. Following a suggestion of Professor John W. Lasley, we shall let $\int f\partial y$ denote an integral in which x is held constant. Writing

$$\int_0^y f_n\partial y=X_n, \quad \int_0^x f_n\partial x=Y_n, \tag{3}$$

we finally have

$$\partial W_0/\partial x=-X_0W_0; \quad \partial W_0/\partial y=-Y_0W_0;$$

$$\left.\begin{aligned}\partial W_n/\partial x&=X_{n-1}W_{n-1}-X_nW_n\\ \partial W_n/\partial y&=Y_{n-1}W_{n-1}-Y_nW_n\end{aligned}\right\} \quad n=1, 2, \text{etc.} \tag{4}$$

The boundary conditions are: $W_0=1$ and all other W's are zero when $x=0$ and $y=0$; all W's are zero when $x=\infty$ and y is finite, etc. The notation in (3) is chosen for the sake of generalization to more dimensions. In three dimensions, for example,

$$X_n=\int_0^x\int_0^y f_n\partial y\partial z.$$

2. Cylindrical Coordinates

A second example will help to show how the method should be handled. For good practical reasons we have defined W_n to be the chance of n events in the particular rectangle mentioned. Of course, we could seek for equations governing the chance of having n events in any contour, in terms of *any* coordinates, but usually this quantity would not obey a manageable set of equations; to get tractable results, the contour should in general follow coordinate lines. Let us consider the case of axial symmetry in cylindrical coordinates. The reader may think of the problem of flaws in a length z of a cast metal bar of radius R, whose properties do not depend on the azimuth in a plane cross section. Let $f_n(r, z)2\pi r dr dz$ be the chance of a flaw in the range $drdz$ when n have already occurred in the range r, z. Then, if we let the area πr^2 be a new variable a, and write

$$\int_0^z f_n\partial z=A_n, \quad \int_0^a f_n\partial a=Z_n, \tag{5}$$

we obtain,

$$\left.\begin{aligned}\partial W_n/\partial a&=A_{n-1}W_{n-1}-A_nW_n\\ \partial W_n/\partial z&=Z_{n-1}W_{n-1}-Z_nW_n\end{aligned}\right\} \quad n=1, 2, \text{etc.}, \tag{6}$$

which are of the same form as (4). Here again we omit the first term on the right in case $n=0$.

III. INTEGRALS OF THE EQUATIONS IN RECTANGULAR COORDINATES

The general theory of simultaneous linear partial equations is old, but I have been unable to find a reference to this particular set. Equations (3) and (4) have some interesting properties connected with the special character of the coefficients which are not obvious at first sight. They can always be integrated as follows:

1. Calculation of W_0

We have

$$\partial \log W_0/\partial x=-X_0, \text{ etc.},$$

so that

$$W_0=\exp(-S_0), \tag{7}$$

where

$$dS_0=X_0dx+Y_0dy. \tag{8}$$

Here dS_0 is a complete differential because of (3), and we obtain S_0 by integrating it from the point (0, 0) to the point (x, y).

2. Calculation of W_n

We have

$$\partial W_1/\partial x+\partial W_0/\partial x=-X_1W_1,$$

with a similar relation involving Y_1W_1. Thus X_1W_1 and Y_1W_1 are components of a gradient

and it follows from the equations for W_2 that the same is true of X_2W_2, Y_2W_2; and so on. Therefore,

$$\partial(X_nW_n)/\partial y=\partial(Y_nW_n)/\partial x,$$

and noting that

$$\partial X_n/\partial y=\partial Y_n/\partial x,$$

we get

$$X_n\partial W_n/\partial y=Y_n\partial W_n/\partial x. \tag{9}$$

By Lagrange's method it follows that

$$W_n=F_n(S_n), \tag{10}$$

where $S_n=c$ is a solution of the auxiliary equation, $dx/Y_n=dy/X_n$. Thus we have a practical method for finding how the variables x, y are contained in W_n, for X_ndx+Y_ndy is always a perfect differential dS_n.

After getting the S's we need only to note that $\exp(S_n)$ is an integrating factor for Eqs. (4). Multiplying each one by this factor, making use of (9), and adding, we get

$$d(\exp(S_n)W_n)=\exp(S_n)W_{n-1}dS_{n-1}$$

and remembering the boundary conditions,

$$W_n=\exp(-S_n)\int_{0,0}^{x,y}\exp(S_n)W_{n-1}dS_{n-1};$$

$$n=1, 2, \text{etc.}, \tag{11}$$

which can be generalized to any number of dimensions. For the case of one dimension, with constant values of the f's, these are the equations governing the disintegrations in a radioactive series, for which Bateman[1] gave the explicit solution. There is no difficulty about writing out the explicit result of (11) when the f_n's are all constants, but the results are lengthy, so we omit them.

3. The Case of Independent Events

In this case f does not depend on n. We can write, X, Y, S in place of X_n, Y_n, S_n. All the W's are functions of S and can be found as follows: Substituting (10) in (4), we get

$$F_n'\partial S/\partial x=X(F_{n-1}-F_n),$$

but $X=\partial S/\partial x$, so F_n obeys an equation of the Bateman form. The complete solution of the problem is

$$W_n=S^ne^{-S}/n! \tag{12}$$

This result can be restated in an instructive form. If S is considered as a new independent variable, the distribution is random in terms of S. On a given surface $S=c$, each W is constant. The surfaces $S=c$ may be thought of as one set of coordinate surfaces in a curvilinear system, the other sets being chosen in any convenient fashion.

4. Random Events

When f is constant, we have $S=fxy$. From general considerations we see that in this case the value of W_n associated with any area A is

$$W_n=(fA)^ne^{-fA}/n! \tag{13}$$

We refrain from further applications, simply noting that most of the useful theorems and formulas which have been developed in studies of fluctuations in one dimension can easily be generalized with the aid of the results presented here.

I wish to thank Dr. Nathan Rosen for reading this paper.

PHYSICAL REVIEW VOLUME 65, NUMBERS 3 AND 4 FEBRUARY 1 AND 15, 1944

On the Currents Carried by Electrons of Uniform Initial Velocity

GEORGE JAFFÉ
Louisiana State University, Baton Rouge, Louisiana
(Received December 8, 1943)

The following problem is treated: Electrons enter the space between two infinite parallel planes with uniform velocity at right angles to the planes. The current is studied for all possible values (positive and negative) of the potential difference between the planes. The complete solution can be obtained if this boundary condition for the current is accepted: The number of electrons entering the discharge space must be *equal to or smaller* than a given number N_0 per cm² per sec., and is for each potential as high as the potential permits. The problem depends on two dimensionless parameters, a reduced plate distance ξ_0 (involving the current) and $\eta_0 = V_0/E_0$, where V_0 is the impressed potential difference and eE_0 the energy of the electrons. For each value of ξ_0 the current is space-charge limited below a critical value of η_0. The limitation, however, is not due to the appearance of a potential minimum low enough to stop the electrons, but is due to the fact that the solution does not exist unless the current is limited. The space-charge limited characteristic is a simple generalization of Child and Langmuir's well-known formula [see Eqs. (28) or (35)]. The deviations from this formula are very considerable if $E_0 \sim V_0$ (see Fig. 2). The behavior of the potential distribution is graphed for some typical cases of positive, zero, and negative potentials V_0. Currents can pass with zero or negative potentials only below critical values of the reduced plate distance.

I. INTRODUCTION

IT has been understood, for almost 30 years, that the well-known space charge equation of Child and Langmuir represents a limiting law which is valid only when the initial velocities of the electrons approach zero. The influence of the initial velocities, first recognized by Schottky, has been studied theoretically in a very complete way under the assumption of a Maxwellian distribution.[1] However, there remains a gap in the theory. The case where all electrons entering the discharge space have a uniform velocity has not been treated in a satisfactory way, not even in the case of parallel planes where the initial velocity is at right angles to the planes.

This latter problem has been treated in an approximate way by Langmuir and Compton,[2] but their solution is subject to the same criticism as the original Child-Langmuir solution, inasmuch as it leads to an infinite space-charge density (and velocity zero) at the point where the potential is minimum. The following analysis will show, furthermore, that one essential assumption in the derivation of Langmuir and Compton is too restricted. The problem itself has practical implications, and it seemed desirable to the author to attempt its complete solution.

It may appear strange that the more complex problem of Maxwellian distribution has been solved in an entirely satisfactory way, whereas the simpler problem of uniform velocity remains open to discussion. However, there is an essential difference between the two cases. If all velocities are represented, e.g., in the Maxwellian distribution, each electron may be considered as subject to an impressed field treated as continuous and created by electrons of other velocities. Then there is no ambiguity as to how any one electron is going to behave in a field so impressed. This supposition has been clearly recognized and formulated by Epstein.[3] If, however, all electrons have the same velocity, they have to travel in a field created by electrons of the same velocity, and it remains an open question whether these electrons are able to create a minimum of potential which is low enough to stop them. It will be seen that this occurs exclusively in a limiting (unstable) case. In general, the minimum will not be low enough to stop electrons which have entered the discharge space. In spite of this fact the current will be space-charge limited (for sufficiently low values of the potential) because the solution of the problem does not exist for any given value of the plate distance unless the current is below a critical value. Thus the space-

[1] W. Schottky, Physik. Zeits. **15**, 526, 624, 656, 872 (1914); Ann. d. Physik **44**, 1011 (1914); Verh. d. D. Phys. Ges. **16**, 490 (1914). P. S. Epstein, Verh. d. D. Phys. Ges. **21**, 85 (1919). T. C. Frey, Phys. Rev. **17**, 441 (1921); **22**, 445 (1923). I. Langmuir, Phys. Rev. **21**, 419 (1923). E. L. E. Wheatcroft, J. I. E. E. **86**, 473 (1940).

[2] I. Langmuir and K. T. Compton, Rev. Mod. Phys. **3**, 191 (1931), see p. 239.

[3] P. S. Epstein, reference 1, see p. 86.

charge limitation is caused, in this case, not by the fact that some of the electrons return to the cathode, but by the fact that only a limited number of them can get into the discharge space.

The analysis of the problem is quite straightforward. The gist of it is the determination of the limits of validity of the solution. If these are known, it is easy to determine the proper form of boundary condition for the current which will have to replace the artificial boundary condition [i.e., $(dE/dx)_0=0$] of Child and Langmuir.

II. THE EQUATIONS AND THEIR SOLUTION

We shall treat here exclusively the case where the electrodes are infinite parallel planes and where all electrons are supposed to enter the space between the two planes with the same velocity v_0 at right angles to the planes. Let x be measured in this normal direction and let the emitter plane, at $x=0$, be kept at the potential $E=0$, and the receiver plane, at $x=d$, at the potential $E=V_0$ (not necessarily positive).

The equations of the problem are given by Poisson's equation

$$d^2E/dx^2=4\pi ne, \tag{1}$$

by the equation of continuity, and by the equation of motion for the individual electron. We write the latter two equations in the integrated form. If n and v represent the number per cm^3 and the velocity of the electrons, respectively, we have

$$evn=i \tag{2}$$

and

$$v=v_0(1+E/E_0)^{\frac{1}{2}}. \tag{3}$$

Here i represents the current density[4] and E_0 the potential which is characteristic of the initial velocity

$$eE_0=mv_0^2/2. \tag{4}$$

Substituting from (2) and (3) into (1) and integrating once, we obtain

$$(dE/dx)^2=(16\pi iE_0/v_0)(1+E/E_0)^{\frac{1}{2}}+C_1. \tag{5}$$

Here we introduce dimensionless variables

$$\eta=E/E_0, \quad \xi=(16\pi i/(v_0E_0))^{\frac{1}{2}}x, \tag{6}$$

and obtain

$$d\eta/d\xi=\pm((1+\eta)^{\frac{1}{2}}+\alpha_1)^{\frac{1}{2}}, \tag{7}$$

where α_1 is a dimensionless constant of integration replacing C_1.

Finally, we set

$$u=(1+\eta)^{\frac{1}{2}} \tag{8}$$

and find, after a second integration,

$$(4/3)(u-2\alpha_1)(u+\alpha_1)^{\frac{1}{2}}=\pm\xi+\alpha_2, \tag{9}$$

with α_2 as second constant of integration.

It follows from (7) that $d\eta/d\xi$, or dE/dx, may be positive or negative. Limiting ourselves at first to the case $V_0>0$, we have to distinguish two possibilities. Either $d\eta/d\xi\geq 0$, and η will increase in a monotonic way, or $d\eta/d\xi<0$ at first, and η will present a minimum.

First Case, Monotonic Increase

Let $\xi=\xi_0$ correspond to the distance d and let

$$u_0=(1+\eta_0)^{\frac{1}{2}}=(1+V_0/E_0)^{\frac{1}{2}}, \tag{10}$$

then the conditions imposed on the potential demand $u=1$ for $\xi=0$, and $u=u_0$ for $\xi=\xi_0$. Hence, from (9) (with the plus sign)

$$(4/3)(1-2\alpha_1)(1+\alpha_1)^{\frac{1}{2}}=\alpha_2 \tag{11}$$

and

$$(4/3)(u_0-2\alpha_1)(u_0+\alpha_1)^{\frac{1}{2}}=\xi_0+\alpha_2. \tag{12}$$

These two equations determine the constants α_1 and α_2 provided i is known. The field distribution then follows from (9) (with the plus sign).

Second Case, Negative Potential Minimum

Let δ be the value of ξ for which the minimum occurs. The value of δ is obtained by integrating (7) from $\xi=0$ to $\xi=\delta$ and bearing in mind that $d\eta/d\xi=-(u+\alpha_1)^{\frac{1}{2}}=0$ for $\xi=\delta$. Thus it is found that

$$\delta=(4/3)(1-2\alpha_1)(1+\alpha_1)^{\frac{1}{2}}. \tag{13}$$

The solution now becomes

$$(4/3)(u-2\alpha_1)(u+\alpha_1)^{\frac{1}{2}}=-\xi+\alpha_3, \quad 0\leq\xi\leq\delta, \tag{14}$$

and

$$(4/3)(u-2\alpha_1)(u+\alpha_1)^{\frac{1}{2}}=\xi+\alpha_4, \quad \xi\geq\delta, \tag{15}$$

where α_3 and α_4 are new constants of integration. They are determined from the boundary conditions for E, and from the condition of continuity

[4] We count, in the usual way, i as positive if an electron current is flowing in the direction of the positive x axis.

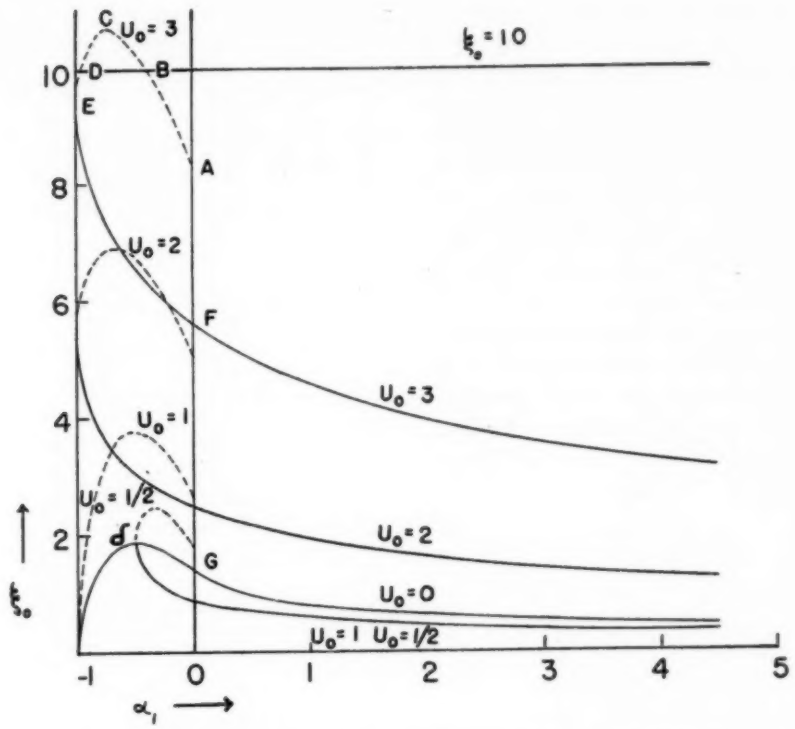

FIG. 1. The curves represent the dependence of the reduced plate distance ξ_0 on the constant α_1 for various values of the external potential ($u_0=(1+\eta_0)^{\frac{1}{2}}=(1+V_0/E_0)^{\frac{1}{2}}=$const.). Solutions of the problem for prescribed values of ξ_0 and η_0 are given by the intersection of the horizontal $\xi_0=$const. with the curve $u_0=$const.

at $\xi=\delta$. We find

$$\alpha_3=\delta, \quad \alpha_4=-\delta, \tag{16}$$

and, for the determination of α_1,

$$(4/3)(u_0-2\alpha_1)(u_0+\alpha_1)^{\frac{1}{2}}=\xi_0-\delta. \tag{17}$$

When the constants are known, the field distribution follows from (14) and (15).

III. THE BOUNDARY CONDITION FOR THE CURRENT

It will be noticed that the Eqs. (11) and (12) in the first case, and Eqs. (13), (16), and (17) in the second case, determine the constants of integration as functions of η_0 and ξ_0. Thus the solution of the problem depends on these two dimensionless parameters only. However, the solution is not complete since ξ_0 involves the knowledge of the current density i. Now i is a constant of integration itself, originating in the integration of the equation of continuity, and has to be determined by a boundary condition.

We shall assume conditions under which a true saturation current exists. Our problem does not correspond to thermionic emission, but rather to the case where electrons of uniform velocity are shot into the discharge space. Therefore, it is not necessary to include the possibility of a Schottky effect. *Preliminarily* we assume that not only the velocity of the electrons is given, but also their number. Let $N_0=n_0v_0$ signify the number of electrons which enter the discharge space per cm² per sec. Then the saturation current will be

$$i=i_0=en_0v_0. \tag{18}$$

With this boundary condition the current will be constant, i.e., independent of the potential V_0, within the limits of validity of our solutions.

It should be noticed that Eq. (9) will give no physical meaning unless the variable u is real. Consequently, from (8), η is subject to the condition $\eta\geq-1$, and the potential minimum cannot become as low as $\eta_{\min}=-1$, and eventually stop the electrons, except in a limiting case. We are going to discuss this limiting case later.

It remains to be seen within what limits our solutions are valid. The practical situation will usually be that η_0 and ξ_0 are given and that the constants α have to be determined. However, the discussion becomes simpler if we assume that, besides η_0, α_1 is given and that, consequently, ξ_0 and the other α's have to be determined. The equations available for the determination of ξ_0 are (11) and (12) in the first case and (13) and (17) in the second case.

It will be seen, from (11), that the constant α_2 in the first case is identical in form with δ in the second case, though it does not have the same physical meaning. Therefore, we can write (12) and (17) in the joint form

$$\xi_0 \pm \delta = (4/3)(u_0 - 2\alpha_1)(u_0 + \alpha_1)^{\frac{1}{2}}, \tag{19}$$

where the plus sign corresponds to the first case. We shall refer to the two cases as "branch I" and "branch II" of the solution.

Because of the last factor in (13), the constant α_1 is subject to the limitation

$$\alpha_1 \geq -1, \text{ for branch I and II.} \tag{20}$$

Furthermore, on branch II, α_1 is limited to negative values as otherwise $d\eta/d\xi$ could not become zero, according to (7). Hence

$$0 \geq \alpha_1 \geq -1, \text{ for branch II.} \tag{21}$$

If α_1 is known, the value of the reduced potential η at the minimum $\eta_{\min}$ is given, from (7), as

$$\eta_{\min} = -(1 - \alpha_1^2). \tag{22}$$

In Fig. 1 the two top curves represent ξ_0 as functions of α_1 for the two values $u_0 = 2$ and $u_0 = 3$ which correspond to the positive values $\eta_0 = 3$ and $\eta_0 = 8$. The curves are calculated from (13) and (19). Branch I is shown by a full line and branch II by a broken line. Branch II has been calculated for the interval (21) only as there is no solution of our problem beyond that interval. A point on branch I represents a possible solution without a potential minimum, a point on branch II a possible solution with a minimum [given by (22)]. A point where the two branches join represents the limiting case where the potential curve starts with a horizontal tangent at the cathode.

It is easy to show that the curves for all values of $u_0 > 1$, i.e., $\eta_0 > 0$, represent the same general character as that exhibited by our two examples: Both branches begin at the value

$$\xi_0 = (4/3)(u_0 + 2)(u_0 - 1)^{\frac{1}{2}} \tag{23}$$

with a vertical tangent. Branch I decreases in a monotonic way and approaches $\xi_0 = 0$ asymptotically. Branch II has a unique maximum at

$$\alpha_1 = -(u_0/(u_0 + 1)), \tag{24}$$

which is given by

$$\xi_{\max} = (4/3)(1 + u_0)^{\frac{1}{2}}, \tag{25}$$

[from substitution of (24) into (19) with the lower sign].

It is the existence of this maximum which is decisive for space-charge limitation. To show this we now return to the usual state of affairs where η_0 and ξ_0 are prescribed. Then the possible solutions will be given by the intersections of the curve $u_0 = \text{const.}$ with the horizontal $\xi_0 = \text{const.}$ Evidently that leads to three possibilities—namely, that there is one solution, that there are two solutions, or that there is no solution at all.

We discuss the last of these possibilities first: it will arise when the given value of ξ_0 is larger than the maximum value (25) corresponding to the given value of u_0. Thus, under our preliminary boundary condition, there will be saturation current for all values of η_0 larger than the critical value η_0^* given by

$$\xi_0 = (4/3)(1 + u_0^*)^{\frac{1}{2}}, \tag{26}$$

and for smaller values there will be no solution. This is a result which cannot be admitted from the physical point of view, and the boundary condition must be modified.

From the definition of the variable ξ [Eq. (6)], it follows that ξ_0 can be lowered by decreasing the value of i involved and that means by decreasing n_0 since v_0 is supposed to be constant. Thus, when the critical value of u_0^* (26) is reached (by decreasing the potential), a solution for lower values of η becomes possible if n_0 is suitably reduced. Therefore, we relax our boundary condition to the following statement: The number of electrons entering the discharge space has to be *equal to or smaller* than the given number $N_0 = n_0 v_0$ per cm² per sec. and is for each potential as high as the potential permits. The last clause has to be added because otherwise the solution

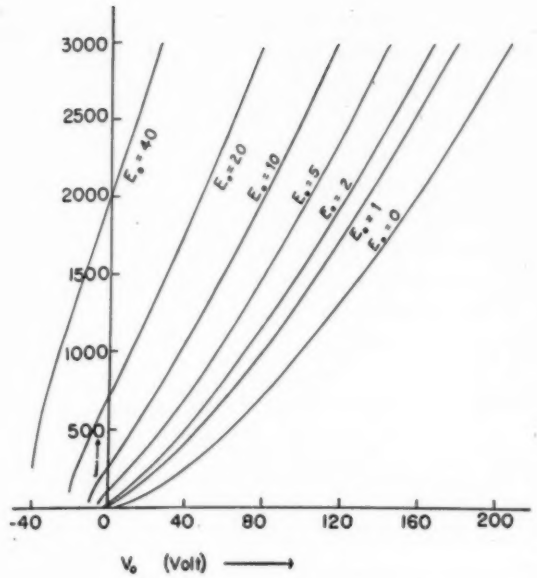

FIG. 2. The curves represent the dependence of the reduced current $j=9\pi id^2/(2e/m)^{\frac{1}{2}}$ on the external potential V_0 (in volts) for different values of the initial velocity ($E_0=e$ volts).

would not be determined. It would be possible to obtain solutions for all values lower than i_0 before the critical η_0^* is reached.

With this boundary condition the current will decrease, from the critical value η_0^* downward in such a way that (26) remains fulfilled since this relation gives the highest value of i which can pass for given values of d and η_0. It should, however, be stressed that the limitation is not due to the appearance of a minimum which makes the electrons (or some of them) return; for the minimum of potential, as given by (22), is less low than $\eta_{\min}=-1$ for all relevant values of α_1 given by (24). Therefore, the space-charge limitation, as stated in the introduction, is due in our case to the fact that, for a given potential, electrons of given velocity can enter the discharge space only in a number limited for each plate distance.

IV. DISCUSSION OF THE SOLUTION

Our Eq. (26) contains the space-charge limited branch of the characteristic. If we bear in mind the definition of u_0 (10) and ξ_0 (6) and introduce the "reduced current density j" by

$$j=9\pi id^2/(2e/m)^{\frac{1}{2}}, \qquad (27)$$

the relation (26) can be written in the form

$$j=V_0^{\frac{1}{2}}[(1+E_0/V_0)^{\frac{1}{2}}+(E_0/V_0)^{\frac{1}{2}}]^3. \qquad (28)$$

This is evidently the generalization of the Child-Langmuir law to the case of electrons with uniform initial velocities, and reduces to it in the limit $E_0/V_0\to 0$. It need hardly be pointed out that our solution does not lead to infinite values of the space-charge density, neither at the cathode nor at the potential minimum. Furthermore, it is automatically limited to the values $i\leq i_0$. As soon as the value $i=i_0$ has been reached by increasing the potential the space-charge limited characteristic, (26) or (28), has to be continued by the horizontal saturation branch.

For small values of E_0/V_0 we obtain

$$j=V_0^{\frac{1}{2}}[1+3(E_0/V_0)^{\frac{1}{2}}+\cdots], \qquad (29)$$

and for large values of E_0/V_0

$$j=8E_0^{\frac{1}{2}}[1+(3/4)(V_0/E_0)+\cdots]. \qquad (30)$$

Thus, for $V_0=0$ the current reduces to the constant value $j_0=8E_0^{\frac{1}{2}}$. However, the characteristic can be continued into the domain of negative V_0's (see Section VI).

In Fig. 2 we have represented the reduced current density j as a function of V_0 (in volts) for various values of E_0 (also in volts). All curves ultimately (for $V_0\to\infty$) approach the curve with $E_0=0$, which is the Child-Langmuir law. It will be seen that, for E_0 comparable with V_0, there are very large deviations from the $\frac{3}{2}$-power law, as was known from the study of Maxwellian distribution.

We now revert to the case where the given values of ξ_0 (with $i=i_0$) and η_0 lead to *two* solutions of the problem. As an example, the horizontal $\xi_0=10$ in our Fig. 1 intersects the curve $u_0=3$ in the two points B and D corresponding to $\alpha_1=-0.39$ and $\alpha_1=-0.975$, respectively. The two solutions which are thus possible may be both on branch II, or one on branch I and the other on branch II; the latter case occurs only if $u_0>1.81$.

The two solutions belong to different values of α_1 and, therefore [according to (9), (14), and (15)], have different potential distributions. It is easy to show that the solution with the smaller negative value has the lower minimum (if both solutions are on branch II) and that it leads to

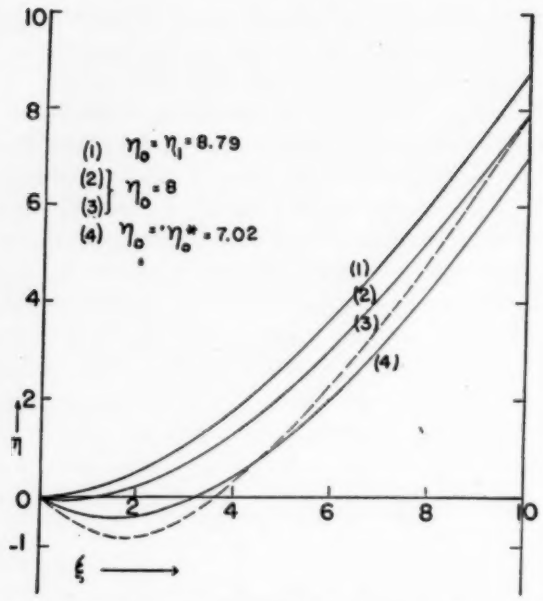

FIG. 3. The curves represent the potential distribution in the case $\xi_0 = 10$ for typical values of the ratio $\eta_0 = V_0/E_0$. At $\eta_0 = \eta_1$ the potential minimum begins to appear and at $\eta_0 = \eta_0^*$ the current becomes space-charge limited. The broken line corresponds to the unstable form of discharge.

lower values of the potential for any value of ξ except $\xi = 0$ and $\xi = \xi_0$. It would require work to change the discharge with the higher potential curve to that with the lower potential curve, and consequently the former discharge is the stable one. Thus we arrive at the result that points to the right of the maximum of branch II, in Fig. 1, represent unstable forms of discharge.

We obtain the following description of the behavior of a discharge for a given value of ξ_0 as the potential is decreased. For very large values of u_0 there will be saturation. The intersection between the curves $\xi_0 = \text{const.}$ and $u_0 = \text{const.}$ will be at large values of α_1, i.e., on branch I, and the potential will be almost linear (see next section). As u_0 is decreased, the intersection remains on branch I until α_1 has reduced to the value -1. This will happen at the value u_1 given by[5]

$$\xi_0 = (4/3)(u_1+2)(u_1-1)^{\frac{1}{2}}. \qquad (31)$$

At this point the potential curve has a horizontal tangent at $\xi = 0$. As the potential is further reduced the intersection will be on branch II, i.e., a maximum begins to make its appearance. The minimum gets lower and δ gets larger (see the curve for δ on Fig. 1) until the point is reached where the horizontal $\xi_0 = \text{const.}$ is tangent to a curve $u_0 = \text{const.}$ This will happen at the critical value of u_0 given by (26). Until this point is reached the current is saturated. If now the potential is further reduced, the representative point will follow downward the line joining the maxima of the various u_0 curves.

We still have to say a few words regarding the limiting case where the potential at the minimum becomes as low as $\eta_{\min} = -1$, i.e., $V_{\min} = -E_0$. This happens exclusively for the value $\alpha_1 = 0$ [see (22)]. The event is, therefore, characterized by points of branch II located on the ordinate $\alpha_1 = 0$. We have just seen that such points represent unstable forms of discharge.

Apart from this fact there are strong reasons which speak against the physical admissibility of this limiting case. For any given value of u_0 the case $\alpha_1 = 0$ (on branch II) occurs for a finite value of ξ_0. Therefore, we must draw the conclusion that the current density i would be finite, as given by this value of ξ_0. Now, the velocity of the electrons naturally becomes zero at a point where $\eta = -1$ [see (3)], and therefore the density n would have to be infinite. We are of the opinion that no solution should be admitted which makes a physically measurable quantity infinite. We, therefore, conclude that the limiting case $\alpha_1 = 0$ (on branch II) should be excluded, even as a possible form of unstable discharge.

V. THE POTENTIAL CURVE

After the constants α have been determined as indicated above, the potential distribution be-

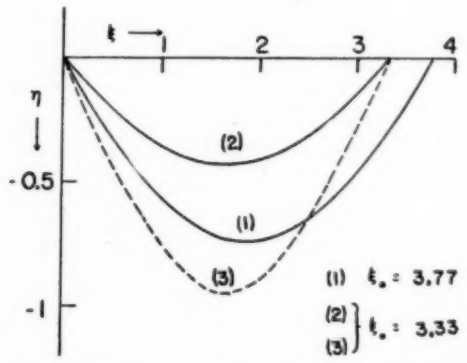

FIG. 4. The curves represent the potential distribution in the case $V_0 = 0$ for two values of the reduced plate distance. The broken line corresponds to the unstable form of discharge.

[5] Equation (31) represents a cubic for u_1 which is easy to solve. It has one real root only.

tween the plates becomes calculable from (9) or (14), (15) for the two branches. We first discuss the case of very high potentials ($\eta_0 \gg 1$).

We obtain the value of α_1 corresponding to this case by developing (19), with the plus sign, and (13) in powers of u_0/α_1. This yields, to a first approximation,

$$\alpha_1^{\frac{1}{2}} = \eta_0/\xi_0. \tag{32}$$

Substituting this value into (9) and (11) we find as limiting law

$$\xi = (\xi_0/\eta_0)\eta. \tag{33}$$

Thus, in the limit $\eta_0 \to \infty$, the potential distribution becomes linear, as has always been assumed and as is evident from the fact that all electrons are swept out of the discharge space with increasing velocity as the potential is increased.

It is not worth while to establish approximate formulae for any other cases as the exact expressions are easy to handle. In Fig. 3 we have graphed some potential curves for the case[6] $\xi_0 = 10$. We have drawn the curves for the value $\eta_0 = \eta_1 = 8.79$ where the minimum begins to appear, for $\eta_0 = 8$, and for the critical value $\eta_0 = \eta_0^* = 7.02$ where the space-charge limitation sets in. For $\eta_0 = 8$ there are two solutions as we have seen above. The unstable form of discharge is given by a broken line.

VI. ZERO POTENTIAL AND NEGATIVE POTENTIALS

In our discussion we have limited ourselves so far to positive values of V_0 though our solutions are valid for all values of $\eta_0 \geq -1$. It is of interest to discuss zero and negative values since the equations developed under the assumption of Maxwellian distribution are not applicable to these cases.[7]

If $V_0 = 0$, or $u_0 = 1$, the branch I of the curve $u_0 = 1$ degenerates into the horizontal axis and the branch II takes the form indicated in Fig. 1. It has its maximum $\xi_{max} = (4/3)2^{\frac{1}{2}} = 3.771$ at $\alpha_1 = -\frac{1}{2}$. Therefore, currents can pass with $V_0 = 0$ only if $\xi_0 \leq 3.771$. For the interval $2.667 \leq \xi_0 \leq 3.771$ there are two solutions, one of them unstable.

[6] The case $\xi_0 = 10$ does not correspond to any practical case of thermionic emission. Much larger values of ξ_0 would have to be chosen (order of 10^3 to 10^4). However, the minima are much more marked with comparatively low values of η_0 and ξ_0.

[7] I. Langmuir, reference 1, see p. 424.

In Fig. 4 we have drawn the potential distribution for $V_0 = 0$ and for two values of ξ_0, namely, the limiting case $\xi_0 = 3.771$, and the intermediate case $\xi_0 = 3.33$. The unstable distribution is given by a broken line.

If, finally, V_0 becomes negative we have again to distinguish two cases, namely, the case of a potential decreasing in a monotonic way: branch I, and the case of a negative potential minimum: branch II. By calculations which are exactly like

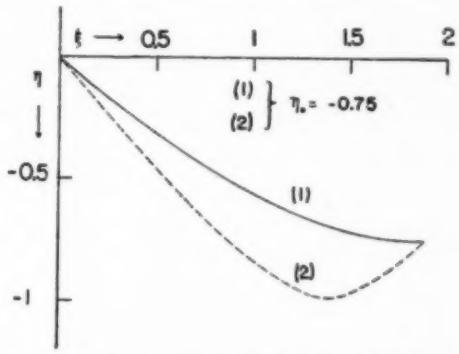

FIG. 5. The curves represent the potential distribution in the case of a negative potential $V_0 = -(3/4)E_0$ for the value $\xi_0 = 1.886$. The broken line corresponds to the unstable form of discharge.

those following Eq. (9), we find for the determination of α_1 on branch I (negative potentials)

$$\delta - \xi_0 = (4/3)(u_0 - 2\alpha_1)(u_0 + \alpha_1)^{\frac{1}{2}}, \tag{34}$$

where δ retains its definition (13).

For branch II our previous formulae remain valid without any change. Thus α_1 can be determined from (19) with the lower sign. Also the maximum, as defined by (24), (25), retains its significance and the current begins to decrease on the space-charge limited curve as soon as the critical value is reached. Therefore, the characteristic (28) remains valid though it has to be written now in the form

$$j = [(E_0 + V_0)^{\frac{1}{2}} + E_0^{\frac{1}{2}}]^3. \tag{35}$$

The reduced current decreases according to this equation down to the value $V_0 = -E_0$ giving $j = E_0^{\frac{3}{2}}$. For still lower values of V_0, no solution exists and no current, therefore, can flow. We have continued the characteristics of Fig. 2 down to their limit. The tangents are vertical at the limits.

As for the limits of validity of the solutions, the argument remains similar as for positive po-

tentials. It follows from (34) and (19) (lower sign) that solutions exist only for

$$\alpha_1 \geq -u_0. \tag{36}$$

Both branches of the curves $u_0=$const. begin with the value $\alpha_1=-u_0$ at the value $\xi_0=\delta$ and with vertical tangent. They form together a loop which contracts around the point G on Fig. 1 ($\alpha_1=0$, $\xi_0=4/3$) as u_0 decreases from $u_0=1$ to $u_0=0$, and for $u_0=0$ there remains only the branch I. In Fig. 1 the curves for $u_0=\frac{1}{2}$ and $u_0=0$ have been added.

It is now easy to discuss the behavior of the solution. Three intervals have to be distinguished:

(a) $0\leq\xi_0\leq 4/3$. The solution starts, with $V_0=0$, on branch II until, with decreasing potentials, the value $\xi_0=\delta$ is reached. Then the solution changes to branch I (no minimum) and ends on the curve $u_0=0$. The current has the saturation value throughout.

(b) $4/3\leq\xi_0\leq 1.886$. The upper limit of this interval is set by the maximum of δ which occurs for $\alpha_1=-0.5$. The solution begins, with $V_0=0$, on branch II, changes to branch I when the δ curve is intersected for the first time, changes back to branch II when the δ curve is met for the second time, and finally becomes space-charge limited.

(c) $1.886\leq\xi_0\leq 3.771$. In this interval the solution is on branch II throughout. The current is saturated at first and becomes space-charge limited as soon as the critical value (26) is reached. All space-charge limited solutions [in cases (b) and (c)] end at the point G of Fig. 1, i.e., at $\xi_0=4/3$ or $j=E_0^{\frac{1}{2}}$.

In Fig. 5 we have represented the potential distribution in the case of a negative potential V_0. We have taken the value $u_0=\frac{1}{2}$ corresponding to $V_0=-(3/4)E_0$, and have chosen ξ_0 on the δ curve; i.e., $\xi_0=(4/3)2^{\frac{1}{2}}=1.886$. Whenever, in the intervals (a) and (b), the limiting case $\xi_0=\delta$ is realized, the solution of branch I coincides with the (stable) solution of branch II. This case, therefore, corresponds to the case $(d\eta/d\xi)_0=0$ for positive potentials, but the horizontal tangent is now at the receiver plate.

The two solutions on branch II correspond to the values $\alpha_1=-\frac{1}{2}$ and $\alpha_1=-0.025$, respectively. Both potential distributions are represented in Fig. 5, the unstable one by a broken line.

PHYSICAL REVIEW VOLUME 65, NUMBERS 3 AND 4 FEBRUARY 1 AND 15, 1944

The Electrical Oscillations of a Prolate Spheroid. Paper II

Prolate Spheroidal Wave Functions

LEIGH PAGE
Sloane Physics Laboratory, Yale University, New Haven, Connecticut

(Received October 4, 1943)

The vector wave equation in prolate spheroidal coordinates ξ, η, ϕ is set up, the variables are separated, and the characteristic values (eigenvalues) and characteristic functions (eigenfunctions) of the resulting ordinary differential equations are obtained in series which converge rapidly in the neighborhood of resonance for spheroids of eccentricity near to unity. The coefficients of the two independent primitives in the linear combinations representing diverging and converging waves at infinity are calculated. The zeros of certain of the characteristic values are investigated.

IN a previous paper[1] both the free oscillations of a perfectly conducting prolate spheroid and the oscillations forced by a plane wave with the electric field parallel to the long axis of the spheroid were discussed. The forced oscillations were treated by an approximate method valid only for very eccentric spheroids. For the exact investigation of these oscillations the complete solutions of the vector wave equation in prolate spheroidal coordinates are needed. The object of the present paper is

[1] L. Page and N. I. Adams, Jr., Phys. Rev. **53**, 819 (1938). This paper will be referred to as I and the present paper as II.

to obtain these solutions in the form of series which converge rapidly in the neighborhood of resonance. In a following paper these solutions will be applied to the problem of the antenna.

1. FIELD EQUATIONS

If the time factor is taken as $e^{-i\omega\tau}$, where τ is the time, the field equations for simple harmonic waves of angular frequency ω in a medium of permittivity κ and permeability μ are

$$\nabla\times\mathbf{E}=i\frac{\omega\mu}{c}\mathbf{H},\quad \nabla\times\mathbf{H}=-i\frac{\omega\kappa}{c}\mathbf{E}, \tag{II-1}$$

in Heaviside-Lorentz symmetrical units, leading to the wave equations

$$\nabla\times\nabla\times\mathbf{E}=\frac{\omega^2\kappa\mu}{c^2}\mathbf{E},\quad \nabla\times\nabla\times\mathbf{H}=\frac{\omega^2\kappa\mu}{c^2}\mathbf{H}. \tag{II-2}$$

In the right-handed orthogonal prolate spheroidal coordinates ξ, η, ϕ defined in I, either of these vector wave equations yields the three scalar equations

$$\frac{\partial}{\partial\eta}\left[\frac{1-\xi^2}{\eta^2-\xi^2}\frac{\partial F_\eta}{\partial\xi}\right]-\frac{\partial}{\partial\eta}\left[\frac{\eta^2-1}{\eta^2-\xi^2}\frac{\partial F_\xi}{\partial\eta}\right]-\frac{1}{(1-\xi^2)(\eta^2-1)}\frac{\partial^2F_\xi}{\partial\phi^2}+\frac{1}{\eta^2-1}\frac{\partial^2F_\phi}{\partial\xi\partial\phi}=\epsilon^2F_\xi, \tag{II-3}$$

$$\frac{1}{1-\xi^2}\frac{\partial^2F_\phi}{\partial\eta\partial\phi}-\frac{1}{(1-\xi^2)(\eta^2-1)}\frac{\partial^2F_\eta}{\partial\phi^2}-\frac{\partial}{\partial\xi}\left[\frac{1-\xi^2}{\eta^2-\xi^2}\frac{\partial F_\eta}{\partial\xi}\right]+\frac{\partial}{\partial\xi}\left[\frac{\eta^2-1}{\eta^2-\xi^2}\frac{\partial F_\xi}{\partial\eta}\right]=\epsilon^2F_\eta, \tag{II-4}$$

$$\frac{\partial}{\partial\xi}\left[\frac{1}{(1-\xi^2)(\eta^2-1)}\frac{\partial F_\xi}{\partial\phi}\right]-\frac{1}{\eta^2-1}\frac{\partial^2F_\phi}{\partial\xi^2}-\frac{1}{1-\xi^2}\frac{\partial^2F_\phi}{\partial\eta^2}+\frac{\partial}{\partial\eta}\left[\frac{1}{(1-\xi^2)(\eta^2-1)}\frac{\partial F_\eta}{\partial\phi}\right]=\epsilon^2\frac{\eta^2-\xi^2}{(1-\xi^2)(\eta^2-1)}F_\phi, \tag{II-5}$$

where

$$F_\xi\equiv\{(\eta^2-\xi^2)(1-\xi^2)\}^{\frac{1}{2}}\begin{Bmatrix}E_\xi\\H_\xi\end{Bmatrix},$$

$$F_\eta\equiv\{(\eta^2-\xi^2)(\eta^2-1)\}^{\frac{1}{2}}\begin{Bmatrix}E_\eta\\H_\eta\end{Bmatrix},$$

$$F_\phi\equiv\{(1-\xi^2)(\eta^2-1)\}^{\frac{1}{2}}\begin{Bmatrix}E_\phi\\H_\phi\end{Bmatrix},$$

and

$$\epsilon\equiv\frac{\omega f}{c}(\kappa\mu)^{\frac{1}{2}}=\frac{2\pi f}{\lambda},$$

f being the semi-interfocal distance, and λ the wave-length.

Evidently the solutions are of the form

$$F_\xi=G_\xi\begin{Bmatrix}\sin m\phi\\\cos m\phi\end{Bmatrix},\quad F_\eta=G_\eta\begin{Bmatrix}\sin m\phi\\\cos m\phi\end{Bmatrix},\quad F_\phi=G_\phi\begin{Bmatrix}\cos m\phi\\-\sin m\phi\end{Bmatrix},$$

where m is a positive integer, and G_ξ, G_η, G_ϕ are functions of ξ and η only, satisfying the equations

$$\frac{\partial}{\partial\eta}\left[\frac{1-\xi^2}{\eta^2-\xi^2}\frac{\partial G_\eta}{\partial\xi}\right]-\frac{\partial}{\partial\eta}\left[\frac{\eta^2-1}{\eta^2-\xi^2}\frac{\partial G_\xi}{\partial\eta}\right]+\frac{m^2}{(1-\xi^2)(\eta^2-1)}G_\xi-\frac{m}{\eta^2-1}\frac{\partial G_\phi}{\partial\xi}=\epsilon^2G_\xi, \tag{II-6}$$

$$-\frac{m}{1-\xi^2}\frac{\partial G_\phi}{\partial\eta}+\frac{m^2}{(1-\xi^2)(\eta^2-1)}G_\eta-\frac{\partial}{\partial\xi}\left[\frac{1-\xi^2}{\eta^2-\xi^2}\frac{\partial G_\eta}{\partial\xi}\right]+\frac{\partial}{\partial\xi}\left[\frac{\eta^2-1}{\eta^2-\xi^2}\frac{\partial G_\xi}{\partial\eta}\right]=\epsilon^2G_\eta, \tag{II-7}$$

$$\frac{\partial}{\partial\xi}\left[\frac{mG_\xi}{(1-\xi^2)(\eta^2-1)}\right]-\frac{1}{\eta^2-1}\frac{\partial^2G_\phi}{\partial\xi^2}-\frac{1}{1-\xi^2}\frac{\partial^2G_\phi}{\partial\eta^2}+\frac{\partial}{\partial\eta}\left[\frac{mG_\eta}{(1-\xi^2)(\eta^2-1)}\right]=\epsilon^2\frac{\eta^2-\xi^2}{(1-\xi^2)(\eta^2-1)}G_\phi. \tag{II-8}$$

If we differentiate (II-6) with respect to ξ, (II-7) with respect to η, and combine the two equations so obtained with (II-8), we get

$$\frac{\partial G_\xi}{\partial \xi}+\frac{\partial G_\eta}{\partial \eta}=\left[\frac{m}{1-\xi^2}+\frac{m}{\eta^2-1}\right]G_\phi, \tag{II-9}$$

which is just the solenoidal condition.

Eliminating G_ϕ from (II-6) and (II-7), we find

$$\left[\frac{1}{1-\xi^2}+\frac{1}{\eta^2-1}\right][SG_\xi+NG_\xi]-\frac{2\xi}{1-\xi^2}\left[\frac{\partial G_\xi}{\partial \xi}+\frac{\partial G_\eta}{\partial \eta}\right]+\frac{2\eta}{\eta^2-1}\left[\frac{\partial G_\xi}{\partial \eta}+\frac{\partial G_\eta}{\partial \xi}\right]=0, \tag{II-10}$$

$$\left[\frac{1}{1-\xi^2}+\frac{1}{\eta^2-1}\right][SG_\eta+NG_\eta]-\frac{2\xi}{1-\xi^2}\left[\frac{\partial G_\eta}{\partial \xi}+\frac{\partial G_\xi}{\partial \eta}\right]+\frac{2\eta}{\eta^2-1}\left[\frac{\partial G_\eta}{\partial \eta}+\frac{\partial G_\xi}{\partial \xi}\right]=0, \tag{II-11}$$

where S and N are the operators

$$S\equiv(1-\xi^2)\frac{\partial^2}{\partial \xi^2}-\frac{m^2}{1-\xi^2}+\epsilon^2(1-\xi^2),$$

$$N\equiv(\eta^2-1)\frac{\partial^2}{\partial \eta^2}-\frac{m^2}{\eta^2-1}+\epsilon^2(\eta^2-1).$$

Equations (II-10) and (II-11) admit two pairs of solutions in which the variables are separable. The first pair is obtained by putting $G_\xi=\xi G$, $G_\eta=-\eta G$ and the second pair by putting $G_\xi=\eta G$, $G_\eta=-\xi G$. In both cases G satisfies the equation

$$\frac{\partial}{\partial \xi}\left[(1-\xi^2)\frac{\partial G}{\partial \xi}\right]-\frac{m^2}{1-\xi^2}G-\epsilon^2\xi^2G+\frac{\partial}{\partial \eta}\left[(\eta^2-1)\frac{\partial G}{\partial \eta}\right]-\frac{m^2}{\eta^2-1}G+\epsilon^2\eta^2G=0. \tag{II-12}$$

So, if we put $G=u(\xi)v(\eta)$, we are left with the two ordinary differential equations

$$\frac{d}{d\xi}\left[(1-\xi^2)\frac{du}{d\xi}\right]-\frac{m^2}{1-\xi^2}u+\alpha u+\epsilon^2(1-\xi^2)u=0, \quad -1\leq\xi\leq1, \tag{II-13}$$

$$\frac{d}{d\eta}\left[(\eta^2-1)\frac{dv}{d\eta}\right]-\frac{m^2}{\eta^2-1}v-\alpha v+\epsilon^2(\eta^2-1)v=0, \quad 1<\eta<\infty, \tag{II-14}$$

which differ only in the range of the independent variable.

Finally, after G_ξ and G_η have been obtained, G_ϕ may be determined from (II-9).

Evidently the method fails when $m=0$. In this case, however, F_ξ, F_η, F_ϕ are not functions of ϕ, and (II-5) reduces to an equation in F_ϕ alone in which the variables are separable. If we put $F_\phi\equiv\{(1-\xi^2)(\eta^2-1)\}^{\frac{1}{2}}u(\xi)v(\eta)$, the differential equations satisfied by u and v are found to be just (II-13) and (II-14) with $m=1$. The functions F_ξ and F_η corresponding to this solution for F_ϕ are both zero since the field component proportional to F_ϕ is itself solenoidal. A second solution for the case where $m=0$ is obtained by taking the curl of the field intensity corresponding to the first solution.

For a given m, solutions of (II-13) and (II-14) exist only for a discrete set of values of the constant of separation α, corresponding to the various harmonics possible. In fact, we conclude from the similarity of these differential equations to that for the associated Legendrian functions that α is a function of two positive integral indices l and m such that $m\leqslant l$. The solutions of (II-13) and (II-14) for a given α_{lm} we shall designate by $u_{lm}(\xi)$ and $v_{lm}(\eta)$. Evidently each group of functions corresponding to a specified m constitutes an orthogonal set. If, then, we put

$$\begin{Bmatrix}E_\xi\\H_\xi\end{Bmatrix}\equiv\Xi(\xi,\eta)\begin{Bmatrix}\sin m\phi\\\cos m\phi\end{Bmatrix}, \quad \begin{Bmatrix}E_\eta\\H_\eta\end{Bmatrix}\equiv\mathrm{H}(\xi,\eta)\begin{Bmatrix}\sin m\phi\\\cos m\phi\end{Bmatrix}, \quad \begin{Bmatrix}E_\phi\\H_\phi\end{Bmatrix}\equiv\Phi(\xi,\eta)\begin{Bmatrix}\cos m\phi\\-\sin m\phi\end{Bmatrix},$$

with omission of the time factor, we have the following pairs of solutions, distinguished by single and double accents: For $m=0$,

$$\left.\begin{aligned}\Xi'_{l0}&=\frac{1}{(\eta^2-\xi^2)^{\frac{1}{2}}}u_{l1}(\xi)\frac{d}{d\eta}[(\eta^2-1)^{\frac{1}{2}}v_{l1}(\eta)],\\ \mathrm{H}'_{l0}&=-\frac{1}{(\eta^2-\xi^2)^{\frac{1}{2}}}\frac{d}{d\xi}[(1-\xi^2)^{\frac{1}{2}}u_{l1}(\xi)]v_{l1}(\eta),\\ \Phi'_{l0}&=0;\end{aligned}\right\} \tag{II-15}$$

$$\left.\begin{aligned}\Xi''_{l0}&=0,\\ \mathrm{H}''_{l0}&=0,\\ \Phi''_{l0}&=u_{l1}(\xi)v_{l1}(\eta);\end{aligned}\right\} \tag{II-16}$$

for $m>0$

$$\left.\begin{aligned}\Xi'_{lm}&=\frac{\xi}{\{(1-\xi^2)(\eta^2-\xi^2)\}^{\frac{1}{2}}}u_{lm}(\xi)v_{lm}(\eta),\\ \mathrm{H}'_{lm}&=-\frac{\eta}{\{(\eta^2-1)(\eta^2-\xi^2)\}^{\frac{1}{2}}}u_{lm}(\xi)v_{lm}(\eta),\\ \Phi'_{lm}&=\frac{\{(1-\xi^2)(\eta^2-1)\}^{\frac{1}{2}}}{m(\eta^2-\xi^2)}\left[\xi\frac{du_{lm}}{d\xi}v_{lm}(\eta)-\eta u_{lm}(\xi)\frac{dv_{lm}}{d\eta}\right];\end{aligned}\right\} \tag{II-17}$$

$$\left.\begin{aligned}\Xi''_{lm}&=\frac{\eta}{\{(1-\xi^2)(\eta^2-\xi^2)\}^{\frac{1}{2}}}u_{lm}(\xi)v_{lm}(\eta),\\ \mathrm{H}''_{lm}&=-\frac{\xi}{\{(\eta^2-1)(\eta^2-\xi^2)\}^{\frac{1}{2}}}u_{lm}(\xi)v_{lm}(\eta),\\ \Phi''_{lm}&=\frac{\{(1-\xi^2)(\eta^2-1)\}^{\frac{1}{2}}}{m(\eta^2-\xi^2)}\left[\eta\frac{du_{lm}}{d\xi}v_{lm}(\eta)-\xi u_{lm}(\xi)\frac{dv_{lm}}{d\eta}\right].\end{aligned}\right\} \tag{II-18}$$

2. SOLUTION OF THE EQUATION FOR $u_{lm}(\xi)$

The form of Eq. (II-13) for $u_{lm}(\xi)$ suggests a solution in the associated Legendrian functions $P_{lm}(\xi)$. Hence we put

$$\alpha_{lm}=l(l+1)+\epsilon^2\alpha'_{lm}+\epsilon^4\alpha''_{lm}+\epsilon^6\alpha'''_{lm}+\cdots,$$
$$u_{lm}=P_{lm}(\xi)+\epsilon^2\sum_k a_k'P_{km}(\xi)+\epsilon^4\sum_k a_k''P_{km}(\xi)+\epsilon^6\sum_k a_k'''P_{km}(\xi)+\cdots,$$

substitute in the differential equation,[2] and equate to zero the coefficient of each separate power of ϵ^2 after getting rid of the factor $1-\xi^2$ in the last term by means of the recurrence formula

$$(1-\xi^2)P_{lm}=\Gamma(-l-2)\Gamma(-l-1)[P_{lm}-P_{l+2,m}]+\Gamma(l-1)\Gamma(l)[P_{lm}-P_{l-2,m}],$$

where $\Gamma(x)\equiv(x+m)/(2x+1)$.

In this way we find the following formulas for the first four terms following $l(l+1)$ in the series for the characteristic value (eigenvalue) α_{lm}:

$$\alpha'_{lm}=-2\frac{l(l+1)+m^2-1}{(2l-1)(2l+3)}, \tag{II-19}$$

$$\alpha''_{lm}=\frac{\mathrm{H}(l-1)\mathrm{H}(l)}{2(2l-1)}-\frac{\mathrm{H}(l+1)\mathrm{H}(l+2)}{2(2l+3)}, \tag{II-20}$$

[2] This is a much simpler and easier method of solution than that given in I.

TABLE I. Characteristic values (eigenvalues).

$$\alpha_{11}=2-\frac{4}{5}\epsilon^2-\frac{4}{5^3\cdot 7}\epsilon^4+\frac{8}{3\cdot 5^5\cdot 7}\epsilon^6-\frac{124}{5^6\cdot 7^3\cdot 11}\epsilon^8+\cdots=2-0.800{,}000\epsilon^2-0.004{,}571\epsilon^4+0.000{,}122\epsilon^6-0.000{,}002\epsilon^8+\cdots,$$

$$\alpha_{21}=6-\frac{4}{7}\epsilon^2-\frac{4}{3\cdot 7^3}\epsilon^4+\frac{8}{3\cdot 7^5\cdot 11}\epsilon^6+\frac{5420}{3^4\cdot 7^7\cdot 11\cdot 13}\epsilon^8+\cdots=6-0.571{,}429\epsilon^2-0.003{,}887\epsilon^4+0.000{,}014\epsilon^6+0.000{,}001\epsilon^8+\cdots,$$

$$\alpha_{31}=12-\frac{8}{3\cdot 5}\epsilon^2+\frac{152}{3^4\cdot 5^3\cdot 11}\epsilon^4-\frac{115{,}568}{3^7\cdot 5^5\cdot 11\cdot 13}\epsilon^6+\frac{34{,}094{,}936}{3^{10}\cdot 5^6\cdot 11^3\cdot 13}\epsilon^8+\cdots=12-0.533{,}333\epsilon^2+0.001{,}365\epsilon^4$$
$$-0.000{,}118\epsilon^6+0.000{,}002\epsilon^8+\cdots,$$

$$\alpha_{41}=20-\frac{40}{7\cdot 11}\epsilon^2+\frac{7064}{7^3\cdot 11^3\cdot 13}\epsilon^4-\frac{462{,}736}{7^5\cdot 11^5\cdot 13}\epsilon^6+\cdots=20-0.519{,}481\epsilon^2+0.001{,}190\epsilon^4-0.000{,}013\epsilon^6+\cdots,$$

$$\alpha_{51}=30-\frac{20}{3\cdot 13}\epsilon^2+\frac{1108}{3^4\cdot 7\cdot 13^3}\epsilon^4-\frac{301{,}160}{3^7\cdot 7\cdot 13^5\cdot 17}\epsilon^6+\cdots=30-0.512{,}821\epsilon^2+0.000{,}889\epsilon^4-0.000{,}003\epsilon^6+\cdots,$$

$$\alpha_{22}=6-\frac{6}{7}\epsilon^2-\frac{2}{3\cdot 7^3}\epsilon^4+\frac{20}{3\cdot 7^5\cdot 11}\epsilon^6-\frac{5554}{3^4\cdot 7^7\cdot 11\cdot 13}\epsilon^8+\cdots=6-0.857{,}143\epsilon^2-0.001{,}944\epsilon^4+0.000{,}036\epsilon^6-0.000{,}001\epsilon^8+\cdots,$$

$$\alpha_{32}=12-\frac{2}{3}\epsilon^2-\frac{2}{3^4\cdot 11}\epsilon^4+\frac{4}{3^7\cdot 11\cdot 13}\epsilon^6+\frac{62}{3^{10}\cdot 11^3\cdot 13}\epsilon^8+\cdots=12-0.666{,}667\epsilon^2-0.002{,}245\epsilon^4+0.000{,}013\epsilon^6+0.000{,}000\epsilon^8+\cdots$$

$$\alpha''_{lm}=-\frac{4m^2-1}{(2l-1)(2l+3)}\left[\frac{\mathrm{H}(l-1)\mathrm{H}(l)}{(2l-5)(2l-1)^2}-\frac{\mathrm{H}(l+1)\mathrm{H}(l+2)}{(2l+3)^2(2l+7)}\right], \tag{II-21}$$

$$\alpha^{IV}_{lm}=\frac{\mathrm{H}(l-1)\mathrm{H}(l)}{2(2l-1)}\left[\frac{4(4m^2-1)^2}{(2l-5)^2(2l-1)^4(2l+3)^2}-\frac{\alpha''_{lm}}{2(2l-1)}+\frac{\mathrm{H}(l-3)\mathrm{H}(l-2)}{2\cdot 4(2l-1)(2l-3)}\right]$$
$$-\frac{\mathrm{H}(l+1)\mathrm{H}(l+2)}{2(2l+3)}\left[\frac{4(4m^2-1)^2}{(2l-1)^2(2l+3)^4(2l+7)^2}+\frac{\alpha''_{lm}}{2(2l+3)}+\frac{\mathrm{H}(l+3)\mathrm{H}(l+4)}{2\cdot 4(2l+3)(2l+5)}\right], \tag{II-22}$$

where $\mathrm{H}(x)\equiv\Gamma(x)\Gamma(-x)=(x^2-m^2)/(4x^2-1)$.

In fact, we can obtain by this method an equation for the entire characteristic value α_{lm}. Putting

$$k_s\equiv(l+s)(l+s+1)-\epsilon^2[\Gamma(-l-s-2)\Gamma(-l-s-1)+\Gamma(l+s-1)\Gamma(l+s)]-\alpha_{lm},$$

and

$$x_s\equiv\frac{\mathrm{H}(l+s)\mathrm{H}(l+s+1)}{k_{s-1}k_{s+1}},$$

this equation, involving two continued fractions, is

$$\cfrac{\epsilon^2x_{-1}}{1-\cfrac{\epsilon^2x_{-3}}{1-\epsilon^2x_{-5}/1-}}+\cfrac{\epsilon^2x_1}{1-\cfrac{\epsilon^2x_3}{1-\epsilon^2x_5/1-}}=1. \tag{II-23}$$

However, the first five terms of α_{lm} are sufficient for most purposes, and they are more easily calculated from (II-19) to (II-22) than from (II-23), the apparently simple form of which is deceptive.

We list in Table I characteristic values for $m=1$ and $l=1, 2, 3, 4, 5$, and for $m=2$ and $l=2, 3$.

When the characteristic functions in $u_{lm}(\xi)$ are expanded as a series in the associated Legendrian functions $P_{lm}(\xi)$, the coefficients are found to be much more complicated than when they are expanded in a simple power series in $s\equiv(1-\xi^2)^{\frac{1}{2}}$. So the latter expansion has been adopted. We have to consider separately the cases $l-m$ even and $l-m$ odd. In both cases it is found convenient to put

$$\beta_{lm}\equiv\frac{\alpha_{lm}-l(l+1)}{\epsilon^2}.$$

TABLE II. Characteristic functions (eigenfunctions).

$$u_{11}(\xi)=3!\sum_{p=1}^{\infty}\frac{p}{(2p+1)!}\epsilon^{2(p-1)}A_p s^{2p-1},$$

$$p_{11}(\eta)=3!\sum_{p=1}^{\infty}(-1)^{p-1}\frac{p}{(2p+1)!}\epsilon^{2(p-1)}A_p t^{2p-1},$$

$$f_{11}(\eta)=-\frac{12}{\alpha_{11}}(1+t^2)^{\frac{1}{2}}\sum_{p=1}^{\infty}(-1)^{p-1}\frac{p}{(2p+1)!}\epsilon^{2(p-1)}B_p t^{2p-1};$$

where

$$A_1=1,\quad A_2=-\frac{5}{4}\beta_{11},\quad A_3=1+\frac{2}{3^2\cdot 5^2}\epsilon^2-\frac{677}{3^2\cdot 5^4\cdot 7^2\cdot 11}\epsilon^4+\cdots,\quad A_4=1+\frac{3}{5^2\cdot 11}\epsilon^2+\cdots,\quad A_5=1+\cdots;$$

$$B_1=1,\quad B_2=1+\frac{81}{5^2\cdot 7}\epsilon^2-\frac{7474}{3^4\cdot 5^4\cdot 7}\epsilon^4+\cdots,\quad B_3=1+\frac{1858}{3^4\cdot 5^2}\epsilon^2+\cdots,\quad B_4=1+\cdots$$

$$u_{21}(\xi)=\frac{5!}{2!}(1-s^2)^{\frac{1}{2}}\sum_{p=1}^{\infty}\frac{p(p+1)}{(2p+3)!}\epsilon^{2(p-1)}A_p s^{2p-1},$$

$$p_{21}(\eta)=\frac{5!}{2!}(1+t^2)^{\frac{1}{2}}\sum_{p=1}^{\infty}(-1)^{p-1}\frac{p(p+1)}{(2p+3)!}\epsilon^{2(p-1)}A_p t^{2p-1},$$

$$f_{21}(\eta)=-\frac{12}{\alpha_{21}}\left[\frac{1}{3!}\frac{1}{t}+\frac{5!}{2\cdot 2!}\sum_{p=1}^{\infty}(-1)^{p-1}\frac{p(p+1)}{(2p+3)!}\epsilon^{2(p-1)}B_p t^{2p-1}\right];$$

where

$$A_1=1,\quad A_2=-\frac{7}{4}\beta_{21},\quad A_3=1+\frac{6}{7^2\cdot 11}\epsilon^2+\cdots,\quad A_4=1+\cdots;$$

$$B_1=1-\frac{5}{2\cdot 3\cdot 7}\epsilon^2+\frac{125}{2\cdot 3^2\cdot 7^2}\epsilon^4+\cdots,\quad B_2=1-\frac{517}{2^2\cdot 3^2\cdot 7^2}\epsilon^2+\cdots,\quad B_3=1+\cdots.$$

$$u_{31}(\xi)=s-\frac{5\cdot 7!}{2^2\cdot 3!}\sum_{p=1}^{\infty}\frac{p(p+1)(p+2)}{(2p+5)!}\epsilon^{2(p-1)}A_p s^{2p+1},$$

$$p_{31}(\eta)=t+\frac{5\cdot 7!}{2^2\cdot 3!}\sum_{p=1}^{\infty}(-1)^{p-1}\frac{p(p+1)(p+2)}{(2p+5)!}\epsilon^{2(p-1)}A_p t^{2p+1},$$

$$f_{31}(\eta)=-\frac{12}{\alpha_{31}}(1+t^2)^{\frac{1}{2}}\left[\frac{1}{3!}\frac{1}{t}+\frac{5\cdot 7!}{2^2\cdot 3!}\sum_{p=1}^{\infty}(-1)^{p-1}\frac{p(p+1)(p+2)}{(2p+5)!}\epsilon^{2(p-1)}B_p t^{2p-1}\right];$$

where

$$A_1=1+\frac{1}{2\cdot 5}\epsilon^2\beta_{31},\quad A_2=1-\frac{166}{3^2\cdot 5^2\cdot 11}\epsilon^2+\frac{1172}{3^6\cdot 5^4\cdot 13}\epsilon^4+\cdots,\quad A_3=1-\frac{98}{3^3\cdot 5^2\cdot 13}\epsilon^2+\cdots,\quad A_4=1+\cdots;$$

$$B_1=1-\frac{41}{3^2\cdot 5^2}\epsilon^2+\frac{4109}{3^6\cdot 5^4\cdot 11}\epsilon^4+\cdots,\quad B_2=1-\frac{767}{2\cdot 3^2\cdot 5^2\cdot 11}\epsilon^2+\cdots,\quad B_3=1+\cdots.$$

For $l-m$ even we put $u_{lm}(\xi)=s^m z$, getting

$$(1-s^2)\frac{d^2z}{ds^2}+\frac{2m+1}{s}\frac{dz}{ds}-2(m+1)s\frac{dz}{ds}+(l-m)(l+m+1)z+\epsilon^2(\beta_{lm}+s^2)z=0. \qquad \text{(II-24)}$$

Assuming a solution $z=\sum_p c_p s^p$, the recurrence formula for the coefficients is

$$p(p+2m)c_p-\{(p-l+m-2)(p+l+m-1)-\epsilon^2\beta_{lm}\}c_{p-2}+\epsilon^2 c_{p-4}=0,$$

giving a series that starts with c_0.

TABLE II.—*Continued.*

$$u_{41}(\xi)=(1-s^2)^{\frac{1}{2}}\left[s-\frac{7\cdot 9!}{2^3\cdot 4!}\sum_{p=1}^{\infty}\frac{p(p+1)(p+2)(p+3)}{(2p+7)!}\epsilon^{2(p-1)}A_p s^{2p+1}\right],$$

$$p_{41}(\eta)=(1+t^2)^{\frac{1}{2}}\left[t+\frac{7\cdot 9!}{2^3\cdot 4!}\sum_{p=1}^{\infty}(-1)^{p-1}\frac{p(p+1)(p+2)(p+3)}{(2p+7)!}\epsilon^{2(p-1)}A_p t^{2p+1}\right],$$

$$f_{41}(\eta)=-\frac{12}{\alpha_{41}}\left[\frac{1}{3!}\left\{\frac{1}{t}+\frac{95}{2\cdot 3}B't\right\}+\frac{35\cdot 9!}{2^3\cdot 3\cdot 4!}\sum_{p=1}^{\infty}(-1)^{p-1}\frac{p(p+1)(p+2)(p+3)}{(2p+7)!}\epsilon^{2(p-1)}B_p t^{2p+1}\right];$$

where

$$A_1=1+\frac{1}{2\cdot 7}\epsilon^2\beta_{41},\quad A_2=1-\frac{1446}{7^2\cdot 11^2\cdot 13}\epsilon^2+\cdots,\quad A_3=1+\cdots;$$

$$B'=1-\frac{241}{5\cdot 7\cdot 11\cdot 19}\epsilon^2+\cdots,\quad B_1=1-\frac{253}{2\cdot 3\cdot 7^2\cdot 11}\epsilon^2+\cdots,\quad B_2=1+\cdots.$$

$$u_{51}(\xi)=s-\frac{7}{2}A's^3+\frac{21\cdot 11!}{2^3\cdot 5!}\sum_{p=1}^{\infty}\frac{p(p+1)\cdots(p+4)}{(2p+9)!}\epsilon^{2(p-1)}A_p s^{2p+3},$$

$$p_{51}(\eta)=t+\frac{7}{2}A't^3+\frac{21\cdot 11!}{2^3\cdot 5!}\sum_{p=1}^{\infty}(-1)^{p-1}\frac{p(p+1)\cdots(p+4)}{(2p+9)!}\epsilon^{2(p-1)}A_p t^{2p+3},$$

$$f_{51}(\eta)=-\frac{12}{\alpha_{51}}(1+t^2)^{\frac{1}{2}}\left[\frac{1}{3!}\left\{\frac{1}{t}+\frac{105}{2^3}B't\right\}+\frac{105\cdot 11!}{2^4\cdot 5!}\sum_{p=1}^{\infty}(-1)^{p-1}\frac{p(p+1)\cdots(p+4)}{(2p+9)!}\epsilon^{2(p-1)}B_p t^{2p+1}\right];$$

where

$$A'=1+\frac{1}{2^3\cdot 7}\epsilon^2\beta_{51},\quad A_1=1-\frac{22}{3^3\cdot 13}\epsilon^2+\frac{47{,}321}{3^6\cdot 7^2\cdot 13^2}\epsilon^4+\cdots,\quad A_2=1-\frac{142}{3^3\cdot 13^2}\epsilon^2+\cdots,\quad A_3=1+\cdots;$$

$$B'=1-\frac{268}{3^3\cdot 5\cdot 7\cdot 13}\epsilon^2+\cdots,\quad B_1=1-\frac{19}{3^3\cdot 13}\epsilon^2+\cdots,\quad B_2=1+\cdots.$$

$$u_{22}(\xi)=\frac{5!}{2!}\sum_{p=1}^{\infty}\frac{p(p+1)}{(2p+3)!}\epsilon^{2(p-1)}A_p s^{2p},$$

$$p_{22}(\eta)=\frac{5!}{2!}\sum_{p=1}^{\infty}(-1)^{p-1}\frac{p(p+1)}{(2p+3)!}\epsilon^{2(p-1)}A_p t^{2p},$$

$$f_{22}(\eta)=4(1+t^2)^{\frac{1}{2}}\left[\frac{1}{3!}B'\frac{1}{t^2}-\frac{5!}{2^2\cdot 2!}\sum_{p=1}^{\infty}(-1)^{p-1}\frac{p(p+1)}{(2p+3)!}\epsilon^{2(p-1)}B_p t^{2p-2}\right.$$

where

$$A_1=1,\quad A_2=-\frac{7}{6}\beta_{22},\quad A_3=1+\cdots;$$

$$B'=1+\frac{4}{3\cdot 7}\epsilon^2+\frac{20}{3^2\cdot 7^2}\epsilon^4+\cdots,\quad B_1=1+\frac{1}{3\cdot 7}\epsilon^2-\frac{65}{3^3\cdot 7^2}\epsilon^4+\cdots,\quad B_2=1+\frac{55}{2\cdot 3^3\cdot 7^2}\epsilon^2+\cdots,\quad B_3=1+\cdots.$$

For $l-m$ odd we put $u_{lm}(\xi)=\xi s^m Z$, getting

$$(1-s^2)\frac{d^2Z}{ds^2}+\frac{2m+1}{s}\frac{dZ}{ds}-2(m+2)s\frac{dZ}{ds}+(l-m-1)(l+m+2)Z+\epsilon^2(\beta_{lm}+s^2)Z=0, \qquad \text{(II-25)}$$

which gives, when we put $Z=\sum_p c_p s^p$, the recurrence formula

$$p(p+2m)c_p-\{(p-l+m-1)(p+l+m)-\epsilon^2\beta_{lm}\}c_{p-2}+\epsilon^2 c_{p-4}=0,$$

representing a series that starts with c_0.

TABLE II.—*Concluded.*

$$u_{32}(\xi)=\frac{7!}{3!}(1-s^2)^{\frac{1}{2}}\sum_{p=1}^{\infty}\frac{p(p+1)(p+2)}{(2p+5)!}\epsilon^{2(p-1)}A_p s^{2p},$$

$$p_{32}(\eta)=\frac{7!}{3!}(1+t^2)^{\frac{1}{2}}\sum_{p=1}^{\infty}(-1)^{p-1}\frac{p(p+1)(p+2)}{(2p+5)!}\epsilon^{2(p-1)}A_p t^{2p},$$

$$f_{32}(\eta)=-\frac{4}{5}\left[\frac{1}{3!}\left\{B'\frac{1}{t^2}-\frac{5}{2}B''\right\}-\frac{5\cdot 7!}{2^2\cdot 3!}\sum_{p=1}^{\infty}(-1)^{p-1}\frac{p(p+1)(p+2)}{(2p+5)!}\epsilon^{2(p-1)}B_p t^{2p}\right];$$

where

$$A_1=1,\quad A_2=-\tfrac{3}{7}\beta_{32},\quad A_3=1+\cdots;$$

$$B'=1+\frac{4}{3^2\cdot 5}\epsilon^2+\frac{28}{3^3\cdot 5^2}\epsilon^4+\cdots,\qquad B''=1+\frac{1}{3^2\cdot 5}\epsilon^2-\frac{103}{3^3\cdot 5^2\cdot 11}\epsilon^4+\cdots,$$

$$B_1=1-\frac{1}{2\cdot 3^3}\epsilon^2-\frac{37}{2^2\cdot 3^4\cdot 5\cdot 11}\epsilon^4+\cdots,\quad B_2=1-\frac{5}{2^2\cdot 3^3\cdot 11}\epsilon^2+\cdots,\quad B_3=1+\cdots$$

The characteristic functions $u_{lm}(\xi)$ obtained from (II-24) and (II-25) are listed in Table II together with the functions $v_{lm}(\eta)$, the arbitrary coefficient c_0 in the tabulated functions $u_{lm}(\xi)$ being taken as unity.

3. SOLUTION OF THE EQUATION FOR $v_{lm}(\eta)$

Since we are interested primarily in conducting spheroids of eccentricity very close to unity (antenna), the objective in solving Eq. (II-14) for $v_{lm}(\eta)$ is to obtain series solutions representing diverging waves at $\eta=\infty$ which converge rapidly in the neighborhood of resonance for η nearly equal to unity.

By changing the independent variable from η to $p=\epsilon\eta$ the differential equation can be thrown into such a form that the zero-order terms are satisfied by the wave functions

$$S_l=(-1)^l p^l\left[\frac{1}{p}\frac{d}{dp}\right]^l e^{ip}.$$

Therefore, a solution can be constructed in the form of a series of these functions, which meets the first requirement stated above. Unfortunately, this series converges so slowly in the neighborhood of resonance for η nearly equal to unity as to be quite useless for the antenna problem.

Another possibility is to construct two independent solutions in series of associated Legendrian functions of the first and second kinds, respectively. The coefficients, however, turn out to be complicated, and difficult to calculate in the second case, and there remains the problem of finding what linear combination of the two independent primitives represents a diverging wave at infinity.

Finally, it was concluded that the most satisfactory method was that employed in I. First, we obtain two independent primitives in the independent variable[3] $t\equiv(\eta^2-1)^{\frac{1}{2}}$ which goes to zero as η goes to unity, and then determine the coefficients of the desired linear combination by comparison with the solution in $\rho=\epsilon t$ which represents a diverging wave at infinity. As in the case of the equation for $u_{lm}(\xi)$ we have to consider separately the cases $l-m$ even and $l-m$ odd.

For $l-m$ even we put $v_{lm}(\eta)=t^m y$, getting

$$(1+t^2)\frac{d^2y}{dt^2}+\frac{2m+1}{t}\frac{dy}{dt}+2(m+1)t\frac{dy}{dt}-(l-m)(l+m+1)y-\epsilon^2(\beta_{lm}-t^2)y=0. \qquad \text{(II-26)}$$

The first primitive for small t is the power series $y_1=\sum_p a_p t^p$ where

$$p(p+2m)a_p+\{(p-l+m-2)(p+l+m-1)-\epsilon^2\beta_{lm}\}a_{p-2}+\epsilon^2 a_{p-4}=0.$$

[3] Note that t used in this paper is the square root of the t in I.

A second primitive is obtained by putting

$$y_2=\tfrac{1}{2}y_1\log\frac{(1+t^2)^{\frac{1}{2}}+1}{(1+t^2)^{\frac{1}{2}}-1}+(1+t^2)^{\frac{1}{2}}x,$$

where x satisfies the equation

$$(1+t^2)\frac{d^2x}{dt^2}+\frac{2m+1}{t}\frac{dx}{dt}+2(m+2)t\frac{dx}{dt}-(l-m-1)(l+m+2)x-\epsilon^2(\beta_{lm}-t^2)x=2\left[\frac{1}{t}\frac{dy_1}{dt}+\frac{m}{t^2}y_1\right]. \quad \text{(II-27)}$$

For $l-m$ odd we put $v_{lm}(\eta)=\eta t^m Y$, getting

$$(1+t^2)\frac{d^2Y}{dt^2}+\frac{2m+1}{t}\frac{dY}{dt}+2(m+2)t\frac{dY}{dt}-(l-m-1)(l+m+2)\,Y-\epsilon^2(\beta_{lm}-t^2)\,Y=0. \quad \text{(II-28)}$$

The power series $Y_1=\sum_p a_p t^p$ supplies the first primitive for small t, where

$$p(p+2m)a_p+\{(p-l+m-1)(p+l+m)-\epsilon^2\beta_{lm}\}a_{p-2}+\epsilon^2a_{p-4}=0,$$

and the second primitive is

$$Y_2=\tfrac{1}{2}Y_1\log\frac{(1+t^2)^{\frac{1}{2}}+1}{(1+t^2)^{\frac{1}{2}}-1}+\frac{1}{(1+t^2)^{\frac{1}{2}}}X,$$

where X satisfies the equation

$$(1+t^2)\frac{d^2X}{dt^2}+\frac{2m+1}{t}\frac{dX}{dt}+2(m+1)t\frac{dX}{dt}-(l-m)(l+m+1)X-\epsilon^2(\beta_{lm}-t^2)X$$
$$=2\left[\left(t+\frac{1}{t}\right)\frac{dY_1}{dt}+\left(m+1+\frac{m}{t^2}\right)Y_1\right]. \quad \text{(II-29)}$$

To obtain the solution for large t for the case $l-m$ even we change the independent variable in (II-26) to $\rho\equiv\epsilon t$ and put

$$y=\rho^{-(m+1)}\Psi(\rho)e^{i\rho},$$

getting

$$z^2\frac{d^2\Psi}{dz^2}+2z^2\frac{d\Psi}{dz}-\alpha_{lm}\Psi=\epsilon^2\left[\frac{d^2\Psi}{dz^2}+\left(2-\frac{1}{z}\right)\frac{d\Psi}{dz}+\left(1-\frac{1}{z}-\frac{m^2-1}{z^2}\right)\Psi\right], \quad \text{(II-30)}$$

where $z\equiv i\rho$. The solution is of the form

$$\Psi=\sum_{p=0}^{\infty}c_pz^{-p}$$

where

$$2pc_p=\{(p+l)(p-l-1)-\epsilon^2(\beta_{lm}+1)\}c_{p-1}+\epsilon^2(2p-3)c_{p-2}-\epsilon^2\{(p-2)^2-m^2\}c_{p-3}.$$

After calculating the coefficients c_p we write the solution in the form

$$y=\frac{1}{\epsilon}\sum_n^{\text{even}}(-\epsilon^2)^{n/2}C_nt^{-m+n-1}+i\sum_n^{\text{odd}}(-\epsilon^2)^{(n-1)/2}C_nt^{-m+n-1}$$

for comparison with the primitives for t small, where

$$C_n=\frac{1}{n!}+\frac{c_1}{(n+1)!}+\frac{c_2}{(n+2)!}+\cdots,$$

$$C_{-n}=c_n+\frac{c_{n+1}}{1!}+\frac{c_{n+2}}{2!}+\cdots.$$

For $l-m$ odd we make the same change in independent variable in (II-28) and put

$$Y=\rho^{-(m+2)}\Psi(\rho)e^{i\rho},$$

getting

$$z^2\frac{d^2\Psi}{dz^2}+2z^2\frac{d\Psi}{dz}-\alpha_{lm}\Psi=\epsilon^2\left[\frac{d^2\Psi}{dz^2}+\left(2-\frac{3}{z}\right)\frac{d\Psi}{dz}+\left(1-\frac{3}{z}-\frac{m^2-4}{z^2}\right)\Psi\right]. \tag{II-31}$$

The recurrence formula for the coefficients in the solution

$$\Psi=\sum_{p=0}^{\infty}c_pz^{-p}$$

is

$$2pc_p=\{(p+l)(p-l-1)-\epsilon^2(\beta_{lm}+1)\}c_{p-1}+\epsilon^2(2p-1)c_{p-2}-\epsilon^2\{(p-1)^2-m^2\}c_{p-3},$$

and Y may be written in the form

$$Y=\frac{1}{\epsilon}\sum_{n}^{\text{even}}(-\epsilon^2)^{n/2}C_nt^{-m+n-2}+i\sum_{n}^{\text{odd}}(-\epsilon^2)^{(n-1)/2}C_nt^{-m+n-2},$$

where C_n has the same significance as before.

In calculating the coefficients a_p of y_1 or Y_1 the manner in which successive coefficients become of higher and higher order in ϵ^2 provides a perfect check on the arithmetic as well as on the previous calculation of α_{lm}. The same is true of the calculation of the coefficients c_p in the solution for large t, although here we have an additional check in the vanishing of those C_n's corresponding to negative powers of t in y_1. In every case at least one such vanishing coefficient was calculated as an arithmetical check. The arbitrary coefficient in the solution for large t was chosen in each instance so as to make $v_{lm}(\eta)$ equal to $(1/\rho)e^{i\rho}$ at infinity, whereas that in the solution for small t was determined by making a_0 equal to unity.

We shall designate by $p_{lm}(\eta)$ and $q_{lm}(\eta)$ the two independent solutions of the equation for $v_{lm}(\eta)$ for small t corresponding, in the case $l-m$ even, to y_1 and y_2, respectively, and, in the case $l-m$ odd, to Y_1 and Y_2, respectively. The function $p_{lm}(\eta)$ remains finite at $t=0$, while $q_{lm}(\eta)$ becomes infinite. For all values of the indices the latter has the form

$$q_{lm}(\eta)=\tfrac{1}{2}p_{lm}(\eta)\log\frac{(1+t^2)^{\frac{1}{2}}+1}{(1+t^2)^{\frac{1}{2}}-1}+f_{lm}(\eta).$$

Hence, in tabulating these functions it is sufficient to give $p_{lm}(\eta)$ and $f_{lm}(\eta)$. In Table II the three functions $u_{lm}(\xi)$, $p_{lm}(\eta)$, and $f_{lm}(\eta)$ are given for those values of the indices for which the characteristic values are listed in Table I. They are expressed in such a form that the first term in each of the series A_p or B_p which has been calculated is unity.

Finally we designate the function $v_{lm}(\eta)$ representing the diverging wave $(1/\rho)e^{i\rho}$ at infinity by $r_{lm}(\eta)$ and write

$$r_{lm}(\eta)=\frac{(i)^{l+1}}{2\cdot4\cdot6\cdots2m}\left[\frac{(l+m)!\epsilon^l}{(2l+1)\{1^2\cdot3^2\cdot5^2\cdots(2l-1)^2\}}a_{lm}p_{lm}(\eta)\right.$$
$$\left.+(-1)^{m+1}i^{\cdot}\frac{(2l+1)\{1^2\cdot3^2\cdot5^2\cdots(2l-1)^2\}}{(l-m)!\epsilon^{l+1}}b_{lm}q_{lm}(\eta)\right]. \tag{II-32}$$

The coefficients a_{lm} and b_{lm} are listed in Table III. Evidently the function representing the converging wave $(1/\rho)e^{-i\rho}$ at infinity is just the complex conjugate of $r_{lm}(\eta)$.

It will be observed that, for $m=1$, the equation

$$a_{l1}b_{l1}=\alpha_{l1}/l(l+1)$$

holds for all five cases. This relation provides a valuable check on the arithmetical computations. Also, for $m=2$, we have a check in the relation

$$a_{12}b_{12}=1/B',$$

although here each coefficient was calculated by two independent methods to preclude the possibility of arithmetical error.

4. ZEROS OF CERTAIN CHARACTERISTIC VALUES (EIGENVALUES)

The zeros of the coefficients b_{l1} are very important in the applications of the theory to the antenna problem. The series for b_{11} and for the characteristic value α_{11} have been carried far enough to show that they have a common zero $\epsilon=\pi/2$ accurate to five significant figures. To a lesser degree of accuracy the given series indicates that b_{21} and α_{21} have a common zero $\epsilon=\pi$ and b_{31} and α_{31} a common zero $\epsilon=3\pi/2$. We shall now prove rigorously that b_{l1} and α_{l1} have a common zero and shall find its exact value.

If we make $m=1$ in Eq. (II-14) for v and put $v=z/(\eta^2-1)^{\frac{1}{2}}$, the resulting equation for z is

$$(\eta^2-1)\left[\frac{d^2z}{d\eta^2}+\epsilon^2 z\right]-\alpha z=0.$$

If ϵ_0 is a zero of α, then, the complete solution of (II-14) for this value of the parameter is

$$v=\frac{A}{(\eta^2-1)^{\frac{1}{2}}}\exp(i\epsilon_0\eta)+\frac{B}{(\eta^2-1)^{\frac{1}{2}}}\exp(-i\epsilon_0\eta), \tag{II-33}$$

and the solution representing a diverging wave of amplitude $1/\rho$ at infinity, where $\rho\equiv\epsilon(\eta^2-1)^{\frac{1}{2}}$, is

$$v_{l1}(\eta)=\frac{1}{\rho(\epsilon_0)}\exp(i\epsilon_0\eta), \tag{II-34}$$

exact for all values of η. This function, therefore, must be identical with the function $r_{l1}(\eta)$ given by (II-32) for $\epsilon=\epsilon_0$, for all values of the index l. Consequently the coefficient of the logarithmic term in $q_{l1}(\eta)$ must vanish for $\epsilon=\epsilon_0$, that is,

$$b_{l1}(\epsilon_0)=0,$$

proving that α_{l1} and b_{l1} have a common zero.

Furthermore, if we replace η by $(1+t^2)^{\frac{1}{2}}$ in (II-34) and use the power series expansion for the exponential factor, we find, on separating real and imaginary parts,

$$v_{l1}(\eta)=\frac{1}{\epsilon_0 t}\cos\epsilon_0-\tfrac{1}{2}t\sin\epsilon_0+\tfrac{1}{8}t^3\{\sin\epsilon_0-\epsilon_0\cos\epsilon_0\}+\cdots$$
$$+i(1+t^2)^{\frac{1}{2}}\left[\frac{1}{\epsilon_0 t}\sin\epsilon_0-\frac{1}{2}\frac{t}{\epsilon_0}\{\sin\epsilon_0-\epsilon_0\cos\epsilon_0\}+\frac{1}{8}\frac{t^3}{\epsilon_0}\{(3-\epsilon_0^2)\sin\epsilon_0-3\epsilon_0\cos\epsilon_0\}+\cdots\right]. \tag{II-35}$$

Now the function $p_{l1}(\eta)$ contains no term in negative powers of t. Therefore, comparing with (II-32), we find that when l is odd, $\cos\epsilon_0=0$ and consequently ϵ_0 is equal to $(n+\frac{1}{2})\pi$, whereas, when l is even, $\sin\epsilon_0=0$ and consequently $\epsilon_0=n\pi$. The value of the integer n is easily ascertained from the series for the characteristic values given in Table I. We find, for l odd or even, that $\epsilon_0=l\pi/2$.

When l is odd the part of $r_{l1}(\eta)$ containing $p_{l1}(\eta)$ is real, and the first term in the power series for this function is t. Hence, comparing (II-32) with (II-35), we find that

$$a_{l1}(\epsilon_0)=\frac{(2l+1)\{1^2\cdot3^2\cdot5^2\cdots(2l-1)^2\}}{(l+1)!\epsilon_0^{\,l}}. \tag{II-36}$$

TABLE III. Coefficients of diverging wave functions.

$$a_{11}=1-\frac{1}{2\cdot 5^2}\epsilon^2+\frac{187}{2^3\cdot 5^4\cdot 7^2}\epsilon^4-\frac{26{,}021}{2^4\cdot 3^4\cdot 5^6\cdot 7^2}\epsilon^6+\cdots=1-0.020{,}000\epsilon^2+0.000{,}763\epsilon^4-0.000{,}026\epsilon^6+\cdots,$$

$$b_{11}=1-\frac{19}{2\cdot 5^2}\epsilon^2-\frac{2609}{2^3\cdot 5^4\cdot 7^2}\epsilon^4+\frac{32{,}593}{2^4\cdot 3^4\cdot 5^6\cdot 7^2}\epsilon^6+\cdots=1-0.380{,}000\epsilon^2-0.010{,}649\epsilon^4+0.000{,}164\epsilon^6+\cdots;$$

$$a_{21}=1-\frac{3}{2\cdot 7^2}\epsilon^2+\frac{389}{2^3\cdot 3^3\cdot 7^4}\epsilon^4+\cdots=1-0.030{,}612\epsilon^2+0.000{,}750\epsilon^4+\cdots,$$

$$b_{21}=1-\frac{19}{2\cdot 3\cdot 7^2}\epsilon^2-\frac{1751}{2^3\cdot 3^3\cdot 7^4}\epsilon^4+\cdots=1-0.064{,}626\epsilon^2-0.003{,}376\epsilon^4+\cdots;$$

$$a_{31}=1-\frac{23}{2\cdot 3^3\cdot 5^2}\epsilon^2-\frac{113{,}549}{2^3\cdot 3^6\cdot 5^4\cdot 11^2}\epsilon^4+\cdots=1-0.017{,}037\epsilon^2-0.000{,}257\epsilon^4+\cdots,$$

$$b_{31}=1-\frac{37}{2\cdot 3^3\cdot 5^2}\epsilon^2-\frac{42{,}233}{2^3\cdot 3^6\cdot 5^4\cdot 11^2}\epsilon^4+\cdots=1-0.027{,}407\epsilon^2-0.000{,}096\epsilon^4+\cdots;$$

$$a_{41}=1-\frac{127}{2\cdot 7^2\cdot 11^2}\epsilon^2+\cdots=1-0.010{,}710\epsilon^2+\cdots,\quad b_{41}=1-\frac{181}{2\cdot 7^2\cdot 11^2}\epsilon^2+\cdots=1-0.015{,}264\epsilon^2+\cdots;$$

$$a_{51}=1-\frac{67}{2\cdot 3^3\cdot 13^2}\epsilon^2+\cdots=1-0.007{,}342\epsilon^2+\cdots,\quad b_{51}=1-\frac{89}{2\cdot 3^3\cdot 13^2}\epsilon^2+\cdots=1-0.009{,}752\epsilon^2+\cdots;$$

$$a_{22}=1-\frac{1}{2\cdot 7^2}\epsilon^2+\frac{121}{2^3\cdot 3^3\cdot 7^4}\epsilon^4+\cdots=1-0.010{,}204\epsilon^2+0.000{,}233\epsilon^4+\cdots,$$

$$b_{22}=1-\frac{53}{2\cdot 3\cdot 7^2}\epsilon^2+\frac{14{,}381}{2^3\cdot 3^3\cdot 7^4}\epsilon^4+\cdots=1-0.180{,}272\epsilon^2+0.027{,}730\epsilon^4+\cdots;$$

$$a_{32}=1-\frac{1}{2\cdot 3^3}\epsilon^2+\frac{223}{2^3\cdot 3^6\cdot 11^2}\epsilon^4+\cdots=1-0.018{,}519\epsilon^2+0.000{,}316\epsilon^4+\cdots,$$

$$b_{32}=1-\frac{19}{2\cdot 3^3\cdot 5}\epsilon^2+\frac{5903}{2^3\cdot 3^6\cdot 5\cdot 11^2}\epsilon^4+\cdots=1-0.070{,}370\epsilon^2+0.001{,}673\epsilon^4+\cdots$$

When l is even, the part of $r_{l1}(\eta)$ containing $p_{l1}(\eta)$ is imaginary, and the first term in the series for this function is $(1+l^2)^{\frac{1}{2}}l$. Therefore, comparing again with (II-35), we find that (II-36) holds for l even as well as l odd.

When l is odd, it is evident from Table II that the first term in $f_{l1}(\eta)$ is $-\{2(1+l^2)^{\frac{1}{2}}\}/\{\alpha_{l1}l\}$. Hence

$$\frac{b_{l1}(\epsilon_0)}{\alpha_{l1}(\epsilon_0)}=\frac{(l-1)!\epsilon_0{}^l}{(2l+1)\{1^2\cdot 3^2\cdot 5^2\cdots(2l-1)^2\}}. \tag{II-37}$$

On the other hand, when l is even, the first term in $f_{l1}(\eta)$ is $-2/\{\alpha_{l1}l\}$. Therefore, (II-37) holds for l even as well as for l odd.

Similarly we can find exact values of the other coefficients in $p_{l1}(\eta)$ and $f_{l1}(\eta)$ for $\epsilon=\epsilon_0$. Thus we have a criterion of the rapidity with which the series given in the tables converge in the neighborhood of ϵ_0. This is illustrated in Table IV, where the exact values and the series values of some of the coefficients are given for $\epsilon=\epsilon_0$. The figures in parentheses indicate the number of terms used in the series. Of course the agreement becomes worse the larger l, partly because ϵ_0 becomes larger and partly because fewer terms of the series have been calculated. In fact, the functions for $l>1$ were not computed

TABLE IV. Coefficients at zero of α_{l1}.

l	ϵ_0	Coefficient	Exact value	Series value	
1	$\pi/2$	a_{11}	0.95493···	0.95491	(4)
		A_2	1.013212···	1.013210	(4)
		b_{11}/α_{11}	0.5236···	0.5241	(4)
		B_2	2.026···	2.014	(3)
		B_3	3.06···	3.26	(2)
2	π	a_{21}	0.76···	0.77	(3)
		A_2	1.0639···	1.0637	(4)
		b_{21}/α_{21}	0.219···	0.220	(3)
		B_1	0	0.5	(3)
3	$3\pi/2$	a_{31}	0.63···	0.71	(4)
		A_1	−0.200	−0.195	(4)
		b_{31}/α_{31}	0.133···	0.137	(3)
		B_1	−0.07···	0.05	(3)

primarily for evaluation at the zeros of their characteristic values, but rather as correction terms in the neighborhood of the important first resonance ($\epsilon=\pi/2$) for $t>0$. Here the convergence is entirely satisfactory. Therefore, the coefficients for which it is important that the series should give accurate values in the neighborhood of ϵ_0 are those for which $l=1$. In judging these, it must be remembered that the terms in $f_{11}(\eta)$ involving B_2 and B_3, as compared with that in B_1, have numerical coefficients 1/10 and 1/280, respectively. Hence, for small t, the accuracy is not less than that of the series for b_{11}/α_{11}, the first four terms of which show an error of only one part in one thousand.

Turning now to Eq. (II-13) for u for the case $m=1$, we note that, if we put $u=z/(1-\xi^2)^{\frac{1}{2}}$, we get for z the equation

$$(1-\xi^2)\left[\frac{d^2z}{d\xi^2}+\epsilon^2 z\right]+\alpha z=0,$$

which yields a solution, when $\alpha=0$, of the same form as that previously obtained in η. Hence we conclude, when l is odd, that

$$[u_{l1}(\xi)]_{\epsilon=\epsilon_0}=(-1)^{(l-1)/2}\frac{2(2l+1)\{1^2\cdot 3^2\cdot 5^2\cdots(2l-1)^2\}}{(l+1)!\epsilon_0{}^{l+1}a_{l1}(\epsilon_0)}\frac{\cos\epsilon_0\xi}{(1-\xi^2)^{\frac{1}{2}}},$$

and, when l is even, that

$$[u_{l1}(\xi)]_{\epsilon=\epsilon_0}=(-1)^{(l-2)/2}\frac{2(2l+1)\{1^2\cdot 3^2\cdot 5^2\cdots(2l-1)^2\}}{(l+1)!\epsilon_0{}^{l+1}a_{l1}(\epsilon_0)}\frac{\sin\epsilon_0\xi}{(1-\xi^2)^{\frac{1}{2}}}.$$

Using the value of $a_{l1}(\epsilon_0)$ specified by (II-36) these reduce to

$$[u_{l1}(\xi)]_{\epsilon=\epsilon_0}=(-1)^{(l-1)/2}\frac{2}{\epsilon_0}\frac{\cos\epsilon_0\xi}{(1-\xi^2)^{\frac{1}{2}}} \tag{II-38}$$

for l odd, and

$$[u_{l1}(\xi)]_{\epsilon=\epsilon_0}=(-1)^{(l-2)/2}\frac{2}{\epsilon_0}\frac{\sin\epsilon_0\xi}{(1-\xi^2)^{\frac{1}{2}}} \tag{II-39}$$

for l even.

The method followed in this section does not succeed when $m>1$.

PHYSICAL REVIEW VOLUME 65, NUMBERS 3 AND 4 FEBRUARY 1 AND 15, 1944

The Electrical Oscillations of a Prolate Spheroid. Paper III

The Antenna Problem

LEIGH PAGE
Sloane Physics Laboratory, Yale University, New Haven, Connecticut
(Received October 4, 1943)

The straight wire antenna is approximated by a perfectly conducting prolate spheroid of eccentricity very close to unity. (1) The first three harmonics of the axially symmetrical free oscillations are discussed, with calculation of the wave-length λ and the logarithmic decrement δ. (2) The tangential electric field component of a plane wave with **E** parallel to the axis of the spheroid is expanded in the prolate spheroidal wave functions of Paper II. (3) The oscillations forced by such a plane wave are discussed for frequencies in the neighborhood of resonance with reference to current distribution, radiation resistance, and scattered field.

1. FREE OSCILLATIONS

WE shall discuss briefly the axially symmetrical free oscillations of a perfectly conducting prolate spheroid so thin that the squares and higher powers of the value t_0 of $t\equiv(\eta^2-1)^{\frac{1}{2}}$ at the surface[1] can be neglected as compared with unity. Under these circumstances t_0 represents effectively the ratio of the minor semi-axis b of the spheroid to the major semi-axis a. We are concerned with the wave functions (II-15), in which v_{l1} stands for the function r_{l1} representing a diverging wave as given by (II-32).

The sole boundary condition is $E_\xi=0$ for $t=t_0$, that is,

$$\frac{d}{dt}\{tr_{l1}(\eta)\}=0, \quad t=t_0. \tag{III-1}$$

a. Fundamental or First Harmonic

For $l=1$, Eq. (III-1) becomes

$$b_{11}=(4/3^2)i\epsilon^3 l_{11}a_{11}, \tag{III-2}$$

where

$$l_{11}\equiv\left[\log\frac{(1+t_0^2)^{\frac{1}{2}}+1}{(1+t_0^2)^{\frac{1}{2}}-1}-2-\frac{1}{5}\epsilon^2+\frac{9}{5^3\cdot 7}\epsilon^4-\frac{886}{3^4\cdot 5^5\cdot 7}\epsilon^6+\cdots\right]^{-1}$$

if we neglect squares and higher powers of t_0.

For the limiting case $t_0=0$ of an infinitely thin antenna $l_{11}=0$ and hence $b_{11}=0$. Hence, as shown in II, $\epsilon=\pi/2$. Consequently, if λ is the wave-length and δ the logarithmic decrement of the free oscillations,

$$\lambda=4a, \quad \delta=0. \tag{III-3}$$

To discuss antennas of finite thickness we put $t_0\equiv(10)^{-n}$ and make $\epsilon=\pi/2$ everywhere except in the factor of b_{11} which vanishes for this value of ϵ. This approximation yields results accurate to within one percent for $n\geq 3$ and to within two or three percent for $n=2$. Then we find from (III-2) that

$$\epsilon=\frac{\pi}{2}\left[1-\frac{0.1685i}{n-0.228}\right].$$

[1] See Paper II for definitions of the symbols appearing in this paper. References to Paper II will be indicated by II and to Paper I by I.

In terms of the wave-length and the logarithmic decrement

$$\epsilon=\frac{\pi}{2}\frac{4a}{\lambda}\left[1-i\frac{\delta}{2\pi}\right]. \tag{III-4}$$

Therefore

$$\lambda=4a, \quad \delta=1.059/(n-0.228). \tag{III-5}$$

b. Second Harmonic

For $l=2$ we have the boundary condition

$$b_{21}=\frac{4}{3^3\cdot 5^2}i\epsilon^5 l_{21}a_{21}, \tag{III-6}$$

where

$$l_{21}\equiv\left[\log\frac{(1+t_0^2)^{\frac{1}{2}}+1}{(1+t_0^2)^{\frac{1}{2}}-1}-3+\frac{1}{3\cdot 7}\epsilon^2-\frac{95}{3^3\cdot 7^3}\epsilon^4+\cdots\right]^{-1}.$$

For a thin antenna this gives approximately

$$\epsilon=\pi\left[1-\frac{0.107i}{n-0.5}\right],$$

from which it follows that

$$\lambda=2a, \quad \delta=0.67/(n-0.5). \tag{III-7}$$

c. Third Harmonic

For $l=3$ the boundary condition becomes

$$b_{31}=\frac{32}{3^3\cdot 5^4\cdot 7^2}i\epsilon^7 l_{31}a_{31}, \tag{III-8}$$

where

$$l_{31}\equiv\left[\log\frac{(1+t_0^2)^{\frac{1}{2}}+1}{(1+t_0^2)^{\frac{1}{2}}-1}-\frac{11}{3}+\frac{1}{2\cdot 3\cdot 5}\epsilon^2-\frac{59}{2\cdot 3^4\cdot 5^2\cdot 11}\epsilon^4+\cdots\right]^{-1}.$$

As the series for b_{31} converges too slowly for $\epsilon=3\pi/2$, we have used (II-37). For a thin antenna we get, approximately,

$$\epsilon=\frac{3\pi}{2}\left[1-\frac{0.086i}{n-0.4}\right]$$

from which it follows that

$$\lambda=(4a/3), \quad \delta=0.54/(n-0.4). \tag{III-9}$$

The series given in II have not been carried far enough to calculate even rough values of the logarithmic decrement for higher harmonics than the third. However, the wave-length for a thin antenna is given by $\lambda=4a/l$ for the lth harmonic, however great the integer l may be.

2. INCIDENT WAVE

Preparatory to the investigation of the electrical oscillations of a perfectly conducting prolate spheroid forced by a plane electromagnetic wave of angular frequency ω with the electric vector parallel to the long axis of the spheroid, it is necessary to expand the field components of the incident wave in the prolate spheroidal wave-functions specified by Eqs. (II-15) to (II-18). Evidently $v_{lm}(\eta)=p_{lm}(\eta)$ since $q_{lm}(\eta)$ becomes infinite at the origin.

Designating unit vectors in the directions of increasing ξ, η, ϕ by ξ_1, η_1, ϕ_1, respectively, and putting $s\equiv(1-\xi^2)^{\frac{1}{2}}$, $t\equiv(\eta^2-1)^{\frac{1}{2}}$, $\epsilon\equiv(\kappa\mu)^{\frac{1}{2}}(\omega f/c)=2\pi f/\lambda$, as before, we find the electric and magnetic

field intensities in the incident plane wave are

$$\mathbf{E}^i=\left[\xi_1\frac{\eta s}{(\eta^2-\xi^2)^{\frac{1}{2}}}+\mathbf{n}_1\frac{\xi t}{(\eta^2-\xi^2)^{\frac{1}{2}}}\right]e^{ikst\sin\phi}, \tag{III-10}$$

$$\mathbf{H}^i=\left[-\xi_1\frac{\xi t\cos\phi}{(\eta^2-\xi^2)^{\frac{1}{2}}}+\mathbf{n}_1\frac{\eta s\cos\phi}{(\eta^2-\xi^2)^{\frac{1}{2}}}-\boldsymbol{\phi}_1\sin\phi\right]e^{ikst\sin\phi}, \tag{III-11}$$

for a wave of unit amplitude. As usual we have omitted the time factor $e^{-i\omega t}$.

Expanding the exponential as a power series we find for the two components of the electric field of the incident plane wave:

$$E_\xi{}^i=\frac{\eta}{(\eta^2-\xi^2)^{\frac{1}{2}}}\left[s-\frac{\epsilon^2t^2}{2^2}s^3+\frac{\epsilon^4t^4}{2^2\cdot4^2}s^5-\frac{\epsilon^6t^6}{2^2\cdot4^2\cdot6^2}s^7+\cdots+i\epsilon\sin\phi\left\{ts^2-\frac{\epsilon^2t^3}{2\cdot2^2}s^4+\cdots\right\}\right.$$
$$\left.+\frac{\epsilon^2}{2^2}\cos2\phi\left\{t^2s^3-\frac{\epsilon^2t^4}{3\cdot2^2}s^5+\cdots\right\}+i\frac{\epsilon^3}{2^3\cdot3}\sin3\phi\{t^3s^4-\cdots\}+\cdots\right],$$

$$E_\eta{}^i=\frac{\xi}{(\eta^2-\xi^2)^{\frac{1}{2}}}\left[t-\frac{\epsilon^2t^3}{2^2}s^2+\frac{\epsilon^4t^5}{2^2\cdot4^2}s^4-\frac{\epsilon^6t^7}{2^2\cdot4^2\cdot6^2}s^6+\cdots+i\epsilon\sin\phi\left\{t^2s-\frac{\epsilon^2t^4}{2\cdot2^2}s^3+\cdots\right\}\right.$$
$$\left.+\frac{\epsilon^2}{2^2}\cos2\phi\left\{t^3s^2-\frac{\epsilon^2t^5}{3\cdot2^2}s^4+\cdots\right\}+i\frac{\epsilon^3}{2^3\cdot3}\sin3\phi\{t^4s^3-\cdots\}+\cdots\right].$$

Since the boundary conditions involve $E_\xi{}^i$ only, we need concern ourselves with this component alone. In order to obtain the coefficients with the desired accuracy, it is necessary to calculate the first few terms of $u_{71}(\xi)$ and $p_{71}(\eta)$ in addition to the functions given in Table II of II.

We find for the desired expansion

$$E_\xi{}^i=\frac{1}{(\eta^2-\xi^2)^{\frac{1}{2}}}\left\{\frac{\eta}{2t}\left[M'_{10}u_{11}(\xi)\frac{d}{dt}\{tp_{11}(\eta)\}+\frac{2}{5^2}\epsilon^2M'_{30}u_{31}(\xi)\frac{d}{dt}\{tp_{31}(\eta)\}+\frac{3}{7^2\cdot9^2}\epsilon^4M'_{50}u_{51}(\xi)\frac{d}{dt}\{tp_{51}(\eta)\}+\cdots\right]\right.$$
$$+i\epsilon\sin\phi\left[\frac{\eta}{s}M''_{11}u_{11}(\xi)p_{11}(\eta)+\frac{2}{5^2}\frac{\eta}{s}\epsilon^2M''_{31}u_{31}(\xi)p_{31}(\eta)+\cdots-\frac{\xi}{s}M'_{21}u_{21}(\xi)p_{21}(\eta)\right.$$
$$\left.-\frac{2}{7^2}\frac{\xi}{s}\epsilon^2M'_{41}u_{41}(\xi)p_{41}(\eta)+\cdots\right]-\frac{\epsilon^2}{2^2}\cos2\phi\left[\frac{\eta}{s}M''_{22}u_{22}(\xi)p_{22}(\eta)+\cdots\right.$$
$$\left.\left.-\frac{\xi}{s}M'_{32}u_{32}(\xi)p_{32}(\eta)-\cdots\right]+\cdots\right\}, \tag{III-12}$$

where

$$M'_{10}\equiv1-\frac{2}{5^2}\epsilon^2+\frac{93}{5^4\cdot7^2}\epsilon^4-\frac{446}{3^4\cdot5^5\cdot7^2}\epsilon^6+\cdots,$$

$$M'_{30}\equiv1-\frac{32}{3^3\cdot5^2}\epsilon^2+\frac{742}{3^4\cdot5^3\cdot11^2}\epsilon^4+\cdots,$$

$$M'_{50}\equiv1-\frac{10}{3\cdot13^2}\epsilon^2+\cdots,$$

$$M''_{11}\equiv1-\frac{2}{5^2}\epsilon^2+\cdots,$$

$$M'_{21}\equiv1-\frac{2}{7^2}\epsilon^2+\cdots,$$

$$M''_{31}\equiv1+\cdots,\quad M'_{41}\equiv1+\cdots,\quad M''_{22}\equiv1+\cdots,\quad M'_{32}\equiv1+\cdots.$$

3. THIN RECEIVING ANTENNA

In this section we shall investigate the current produced in a very eccentric perfectly conducting prolate spheroid by an incident plane electromagnetic wave of angular frequency ω and unit amplitude, the electric field of which is parallel to the long axis of the spheroid. We shall be particularly interested in the frequency of resonance and frequencies close to resonance. Since the eccentricity of the spheroidal conductor under consideration is close to unity, the value t_0 of the parameter t at its surface is effectively equal to the ratio of the minor semi-axis b of the conducting spheroid to the major semi-axis a. We shall confine our discussion to conductors for which $t_0<(10)^{-2}$, with particular attention to the limiting case attained as t_0 goes to zero. Therefore we can neglect terms of order t_0^2 as compared with terms of order unity.

Remembering that the first term in $p_{l1}(\eta)$ for l odd is t, it is clear, then, that we need retain only this first term in the part of the expression (III-12) for $E_\xi{}^i$ which is independent of ϕ. As regards the part of this expression involving $\sin\phi$, terms in the first power of t appear, but this part of the expression determines only the distribution of the current in azimuth and has no effect on the total current through any cross section of the conductor. Therefore we shall neglect it. The same is true of the part of the expression involving $\cos 2\phi$, which, however, contains no terms of order less than t^2 and is negligible on that account. Similar considerations apply *a fortiori* to the remaining parts of the expression.

Hence we write as a sufficiently good approximation

$$E_\xi{}^i=\frac{\eta}{(\eta^2-\xi^2)^{\frac{1}{2}}}\left[M'_{10}u_{11}(\xi)+\frac{2}{5^2}\epsilon^2M'_{30}u_{31}(\xi)+\frac{3}{7^2\cdot 9^2}\epsilon^4M'_{50}u_{51}(\xi)+\cdots\right]. \tag{III-13}$$

The corresponding component of the electric field intensity in the scattered wave must be

$$E_\xi{}^r=\frac{\eta}{(\eta^2-\xi^2)^{\frac{1}{2}}}\left[N'_{10}u_{11}(\xi)\frac{1}{t}\frac{d}{dt}\{tr_{11}(\eta)\}+\epsilon^2N'_{30}u_{31}(\xi)\frac{1}{t}\frac{d}{dt}\{tr_{31}(\eta)\}\right.$$
$$\left.+\epsilon^4N'_{50}u_{51}(\xi)\frac{1}{t}\frac{d}{dt}\{tr_{51}(\eta)\}+\cdots\right] \tag{III-14}$$

in order to satisfy the boundary condition $E_\xi{}^i+E_\xi{}^r=0$ for $t=t_0$. Consequently, if terms in t^2 and higher powers are neglected,

$$N'_{10}=\frac{2}{3}\epsilon^2l_{11}M'_{10}\frac{\frac{4}{3^2}\epsilon^3l_{11}a_{11}-ib_{11}}{\left(\frac{4}{3^2}\epsilon^3l_{11}a_{11}\right)^2+b_{11}^2},$$

$$N'_{30}=-\frac{8}{3^2\cdot 5^4\cdot 7}\epsilon^4l_{31}M'_{30}\frac{\frac{32}{3^3\cdot 5^4\cdot 7^2}\epsilon^7l_{31}a_{31}-ib_{31}}{\left(\frac{32}{3^3\cdot 5^4\cdot 7^2}\epsilon^7l_{31}a_{31}\right)^2+b_{31}^2},$$

$$N'_{50}=\frac{16}{3^8\cdot 5^2\cdot 7^4\cdot 11}\epsilon^6l_{51}M'_{50}\frac{\frac{256}{3^9\cdot 5^3\cdot 7^4\cdot 11^2}\epsilon^{11}l_{51}a_{51}-ib_{51}}{\left(\frac{256}{3^9\cdot 5^3\cdot 7^4\cdot 11^2}\epsilon^{11}l_{51}a_{51}\right)^2+b_{51}^2},$$

where l_{11} and l_{31} are defined in Section 1 of this paper, and

$$l_{51}\equiv\left[\log\frac{(1+t_0^2)^{\frac{1}{2}}+1}{(1+t_0^2)^{\frac{1}{2}}-1}-\frac{137}{2\cdot 3\cdot 5}+\frac{1}{5\cdot 13}\epsilon^2+\cdots\right]^{-1}.$$

The magnetic field strength in the scattered wave corresponding to (III-14) consists of the single component

$$H_\phi{}^r=-i\left(\frac{\kappa}{\mu}\right)^{\frac{1}{2}}\epsilon[N'_{10}u_{11}(\xi)r_{11}(\eta)+\epsilon^2N'_{30}u_{31}(\xi)r_{31}(\eta)+\epsilon^4N'_{50}u_{51}(\xi)r_{51}(\eta)+\cdots], \qquad \text{(III-15)}$$

and the current is

$$I=[2\pi cfstH_\phi{}^r]_{t=t_0}.$$

This gives

$$I=2\pi\left(\frac{\kappa}{\mu}\right)^{\frac{1}{2}}cf\epsilon\left[\frac{M'_{10}l_{11}}{a_{11}}\frac{\frac{4}{3^2}\epsilon^3l_{11}a_{11}-ib_{11}}{\left(\frac{4}{3^2}\epsilon^3l_{11}a_{11}\right)^2+b_{11}^2}\{su_{11}(\xi)\}+\frac{\epsilon^2}{3\cdot5^2}\frac{M'_{30}l_{31}}{a_{31}}\frac{\frac{32}{3^3\cdot5^4\cdot7^2}\epsilon^7l_{31}a_{31}-ib_{31}}{\left(\frac{32}{3^3\cdot5^4\cdot7^2}\epsilon^7l_{31}a_{31}\right)^2+b_{31}^2}\{su_{31}(\xi)\}\right.$$

$$\left.+\frac{\epsilon^4}{5\cdot7^2\cdot9^2}\frac{M'_{50}l_{51}}{a_{51}}\frac{\frac{256}{3^9\cdot5^3\cdot7^4\cdot11^2}\epsilon^{11}l_{51}a_{51}-ib_{51}}{\left(\frac{256}{3^9\cdot5^3\cdot7^4\cdot11^2}\epsilon^{11}l_{51}a_{51}\right)^2+b_{51}^2}\{su_{51}(\xi)\}+\cdots\right]e^{-i\omega\tau} \qquad \text{(III-16)}$$

with inclusion of the time factor.

We consider first the limiting case of an antenna of length $2a=2f$ and zero thickness. Then $l_{11}=l_{31}=l_{51}=0$, and the current is zero except for those wave-lengths which make one of the coefficients b_{11}, b_{31}, b_{51} vanish. It was shown in II that b_{11} vanishes for $\epsilon=\pi/2$, b_{31} vanishes for $\epsilon=3\pi/2$, and b_{51} vanishes for $\epsilon=5\pi/2$. Hence, as $\epsilon\equiv2\pi f/\lambda$ and $a=f$ when $t_0=0$, it follows that the first three resonances occur at wave-lengths equal to twice, two-thirds, and two-fifths the length of the antenna. The resonance is infinitely sharp but not infinitely high.

a. First Resonance

We shall discuss the first resonance in some detail, as it is by far the most important. First consider an infinitely thin antenna. Making use of Eqs. (II-34) and (II-38), we find for the current at first resonance

$$\begin{aligned}I&=\left[2\pi c\left(\frac{\kappa}{\mu}\right)^{\frac{1}{2}}a\right]M'_{10}(\epsilon_0)(1-\xi^2)^{\frac{1}{2}}u_{11}(\xi)\cos\omega\tau\\&=\left[2\pi c\left(\frac{\kappa}{\mu}\right)^{\frac{1}{2}}a\right]1.045\cos\left(\frac{\pi}{2}\xi\right)\cos\omega\tau,\end{aligned} \qquad \text{(III-17)}$$

in exact agreement with the result of the approximate method employed in I.

Since the element of length $d\lambda_\xi$ corresponding to the increment $d\xi$ is

$$d\lambda_\xi=f\left(\frac{\eta_0{}^2-\xi^2}{1-\xi^2}\right)^{\frac{1}{2}}d\xi,$$

the applied electromotive force along $d\lambda_\xi$ is

$$E_\xi{}^id\lambda_\xi=\frac{ad\xi}{(1-\xi^2)^{\frac{1}{2}}}\left[M'_{10}u_{11}(\xi)+\frac{2}{5^2}\epsilon^2M'_{30}u_{31}(\xi)+\frac{3}{7^2\cdot9^2}\epsilon^4M'_{50}u_{51}(\xi)+\cdots\right]\cos\omega\tau.$$

Remembering that the functions $u_{l1}(\xi)$ are orthogonal, we find that the mean time rate of absorption of energy is

$$\pi c\left(\frac{\kappa}{\mu}\right)^{\frac{1}{2}}a^2[M'_{10}(\epsilon_0)]^2\int_{-1}^{1}[u_{11}(\xi)]^2d\xi.$$

The radiation resistance R is defined as the ratio of this quantity to one-half the square of the current amplitude at the center of the antenna. Hence,

$$R=\frac{1}{2\pi c}\left(\frac{\mu}{\kappa}\right)^{\frac{1}{2}}\frac{\int_{-1}^{1}[u_{11}(\xi)]^2d\xi}{[u_{11}(0)]^2}=\frac{1.2188}{2\pi c}\left(\frac{\mu}{\kappa}\right)^{\frac{1}{2}}. \tag{III-18}$$

If R_p is the radiation resistance in ohms

$$R_p=4\pi c^2(10)^{-9}R=73.08\left(\frac{\mu}{\kappa}\right)^{\frac{1}{2}}\text{ ohms}, \tag{III-19}$$

in exact agreement with the result of the approximate method employed in I.

Finally we obtain, with the aid of (II-34) and (II-38), the following simple expressions for the three non-vanishing field components in the wave scattered by an infinitely thin antenna at resonance:

$$E_\xi^r=-\frac{4\eta_0M'_{10}(\epsilon_0)}{\pi\{(\eta^2-\xi^2)(1-\xi^2)\}^{\frac{1}{2}}}\cos\left(\frac{\pi}{2}\xi\right)\cos\left\{\frac{\pi}{2}(\eta-\eta_0)-\omega\tau\right\}, \tag{III-20}$$

$$E_\eta^r=-\frac{4\eta_0M'_{10}(\epsilon_0)}{\pi\{(\eta^2-\xi^2)(\eta^2-1)\}^{\frac{1}{2}}}\sin\left(\frac{\pi}{2}\xi\right)\sin\left\{\frac{\pi}{2}(\eta-\eta_0)-\omega\tau\right\}, \tag{III-21}$$

$$H_\phi^r=\frac{4\eta_0M'_{10}(\epsilon_0)}{\pi\{(1-\xi^2)(\eta^2-1)\}^{\frac{1}{2}}}\left(\frac{\kappa}{\mu}\right)^{\frac{1}{2}}\cos\left(\frac{\pi}{2}\xi\right)\cos\left\{\frac{\pi}{2}(\eta-\eta_0)-\omega\tau\right\}, \tag{III-22}$$

where $M'_{10}(\epsilon_0)=0.8206$ and, for the limiting case of an infinitely thin antenna, $\eta_0=1$. These expressions are valid at resonance for all $\eta>1$.

Next we pass to the case of an antenna of small but finite thickness. As in Section 1 we put $t_0=(10)^{-n}$. If $n\geq 3$ we do not incur an error as great as one percent if we retain the expressions for the wave-length of resonance and for the radiation resistance at resonance which were found for the infinitely thin antenna, and even for $n=2$ the error is only about two percent. But now the resonance peak in the current is no longer infinitely sharp. To determine its form we shall use only the first term in the general expression (III-16) for the current, ignoring a small but almost negligible asymmetry due to succeeding terms. We find

$$I=\left[2\pi c\left(\frac{\kappa}{\mu}\right)^{\frac{1}{2}}a\right]\frac{1.045\cos\left(\frac{\pi}{2}\xi\right)}{1+35.2(n-0.228)^2\left(\frac{\delta\lambda}{\lambda_r}\right)^2}\cos(\omega\tau+\phi) \tag{III-23}$$

for the current, where $\lambda_r=4a$ is the wave-length of resonance and $\delta\lambda$ the deviation from λ_r. The lead ϕ of the current ahead of the electromotive-force is given by

$$\tan\phi=5.93(n-0.228)\frac{\delta\lambda}{\lambda_r}. \tag{III-24}$$

These expressions are valid, of course, only for values of the ratio $\delta\lambda/\lambda_r$ small compared with unity. They represent quite typical resonance curves.

b. Second Resonance

In discussing the second resonance we shall consider only the case of an infinitely thin antenna, and, as the series involved converges more slowly in this region, we can do no more than calculate

a rough value of the current amplitude at resonance. We find for the current at resonance

$$I=-\left[2\pi c\left(\frac{\kappa}{\mu}\right)^{\frac{1}{2}}a\right]0.04\cos\left(\frac{3\pi}{2}\xi\right)\cos\omega\tau. \qquad \text{(III-25)}$$

The current is in phase with the impressed electromotive force in the two extreme thirds of the antenna, but out of phase in the middle third. As the current amplitude at the center of the antenna is only some 4 percent of that at first resonance, the second and higher order resonances are evidently of little importance as compared with the first resonance.

PHYSICAL REVIEW VOLUME 65, NUMBERS 3 AND 4 FEBRUARY 1 AND 15, 1944

Crystal Statistics. I. A Two-Dimensional Model with an Order-Disorder Transition

LARS ONSAGER
Sterling Chemistry Laboratory, Yale University, New Haven, Connecticut

(Received October 4, 1943)

The partition function of a two-dimensional "ferromagnetic" with scalar "spins" (Ising model) is computed rigorously for the case of vanishing field. The eigenwert problem involved in the corresponding computation for a long strip crystal of finite width (n atoms), joined straight to itself around a cylinder, is solved by direct product decomposition; in the special case $n=\infty$ an integral replaces a sum. The choice of different interaction energies ($\pm J, \pm J'$) in the (0 1) and (1 0) directions does not complicate the problem. The two-way infinite crystal has an order-disorder transition at a temperature $T=T_c$ given by the condition

$$\sinh(2J/kT_c)\sinh(2J'/kT_c)=1.$$

The energy is a continuous function of T; but the specific heat becomes infinite as $-\log|T-T_c|$. For strips of finite width, the maximum of the specific heat increases linearly with $\log n$. The order-converting dual transformation invented by Kramers and Wannier effects a simple automorphism of the basis of the quaternion algebra which is natural to the problem in hand. In addition to the thermodynamic properties of the massive crystal, the free energy of a (0 1) boundary between areas of opposite order is computed; on this basis the mean ordered length of a strip crystal is

$$(\exp(2J/kT)\tanh(2J'/kT))^n.$$

INTRODUCTION

THE statistical theory of phase changes in solids and liquids involves formidable mathematical problems.

In dealing with transitions of the first order, computation of the partition functions of both phases by successive approximation may be adequate. In such cases it is to be expected that both functions will be analytic functions of the temperature, capable of extension beyond the transition point, so that good methods of approximating the functions may be expected to yield good results for their derivatives as well, and the heat of transition can be obtained from the difference of the latter. In this case, allowing the continuation of at least one phase into its metastable range, the heat of transition, the most appropriate measure of the discontinuity, may be considered to exist over a range of temperatures.

It is quite otherwise with the more subtle transitions which take place without the release of latent heat. These transitions are usually marked by the vanishing of a physical variable, often an asymmetry, which ceases to exist beyond the transition point. By definition, the strongest possible discontinuity involves the specific heat. Experimentally, several types are known. In the $\alpha-\beta$ quartz transition,[1] the specific heat becomes infinite as $(T_c-T)^{-\frac{1}{2}}$; this may be the rule for a great many structural transformations in crystals. On the other hand, supraconductors exhibit a clear-cut finite discontinuity of the specific heat, and the normal state can be continued at will below the transition

[1] H. Moser, Physik. Zeits. **37**, 737 (1936).

point by the application of a magnetic field.[2] Ferromagnetic Curie points[1, 3] and the transition of liquid helium to its suprafluid state[4] are apparently marked by essential singularities of the specific heats; in either case it is difficult to decide whether the specific heat itself or its temperature coefficient becomes infinite. Theoretically, for an ideal Bose gas the temperature coefficient of the specific heat should have a finite discontinuity at the temperature where "Einstein condensation" begins.

In every one of these cases the transition point is marked by a discontinuity which does not exist in the same form at any other temperature; for even when a phase can be continued beyond its normal range of stability, the transition in the extended range involves a finite heat effect.

Whenever the thermodynamic functions have an essential singularity any computation by successive approximation is difficult because the convergence of approximation by analytic functions in such cases is notoriously slow.

When the existing dearth of suitable mathematical methods is considered, it becomes a matter of interest to investigate models, however far removed from natural crystals, which yield to exact computation and exhibit transition points.

It is known that no model which is infinite in one dimension only can have any transition.[5, 6]

The two-dimensional "Ising model," originally intended as a model of a ferromagnetic,[7] is known to be more properly representative of condensation phenomena in the two-dimensional systems formed by the adsorption of gases on the surfaces of crystals.[8] It is known that this model should have a transition.[9] Recently, the transition point has been located by Kramers and Wannier.[10] In the following, the partition function and derived thermodynamic functions will be computed for a rectangular lattice with different interaction constants in two perpendicular directions; this generalization is of some interest and does not add any difficulties.

The similar computation of the partition functions for hexagonal and honeycomb lattices involves but relatively simple additional considerations. A general form of the dual transformation invented by Kramers and Wannier together with a rather obvious "star-triangle" transformation are used in this connection, and the transition points can be computed from the transformations alone. While these were a great help to the discovery of the present results, the logical development of the latter is best relieved of such extraneous topics, and the subject of transformations will be reserved for later communication.

OUTLINE OF METHOD

As shown by Kramers and Wannier,[10] the computation of the partition function can be reduced to an eigenwert problem. This method will be employed in the following, but it will be convenient to emphasize the abstract properties of relatively simple operators rather than their explicit representation by unwieldy matrices.

For an introduction to the language we shall start with the well-known problem of the linear lattice and proceed from that to a rectangular lattice on a finite base. For symmetry we shall wrap the latter on a cylinder, only straight rather than in the screw arrangement preferred by Kramers and Wannier.

The special properties of the operators involved in this problem allow their expansion as linear combinations of the generating basis elements of an algebra which can be decomposed into direct products of quaternion algebras. The representation of the operators in question can be reduced accordingly to a sum of direct products of two-dimensional representations, and the roots of the secular equation for the problem in hand are obtained as products of the roots of certain quadratic equations. To find all the roots requires complete reduction, which is best performed by the explicit construction of a transforming matrix, with valuable by-products of

[2] W. H. Keesom, Zeits. f. tech. Physik **15**, 515 (1934); H. G. Smith and R. O. Wilhelm, Rev. Mod. Phys. **7**, 237 (1935).
[3] H. Klinkhardt, Ann. d. Physik [4], **84**, 167 (1927).
[4] W. H. and A. P. Keesom, Physica **2**, 557 (1935); J. Satterly, Rev. Mod. Phys. **8**, 347 (1938); K. Darrow, *ibid.* **12**, 257 (1940).
[5] E. Montroll, J. Chem. Phys. **9**, 706 (1941).
[6] K. Herzfeld and M. Goeppert-Mayer, J. Chem. Phys. **2**, 38 (1934).
[7] E. Ising, Zeits. f. Physik **31**, 253 (1925).
[8] R. Peierls, Proc. Camb. Phil. Soc. **32**, 471 (1936).
[9] R. Peierls, Proc. Camb. Phil. Soc. **32**, 477 (1936).
[10] H. A. Kramers and G. H. Wannier, Phys. Rev. **60**, 252, 263 (1941).

FIG. 1. Linear crystal model. Spin of entering atom ○ depends statistically on spin of atom in previous end position ●.

identities useful for the computation of averages pertaining to the crystal. This important but formidable undertaking will be reserved for a later communication. It so happens that the representations of maximal dimension, which contain the two largest roots, are identified with ease from simple general properties of the operators and their representative matrices. The largest roots whose eigenvectors satisfy certain special conditions can be found by a moderate elaboration of the procedure; these results will suffice for a qualitative investigation of the spectrum. To determine the thermodynamic properties of the model it suffices to compute the largest root of the secular equation as a function of the temperature.

The passage to the limiting case of an infinite base involves merely the substitution of integrals for sums. The integrals are simplified by elliptic substitutions, whereby the symmetrical parameter of Kramers and Wannier[10] appears in the modulus of the elliptic functions. The modulus equals unity at the "Curie point"; the consequent logarithmic infinity of the specific heat confirms a conjecture made by Kramers and Wannier. Their conjecture regarding the variation of the maximum specific heat with the size of the crystal base is also confirmed.

THE LINEAR ISING MODEL

As an introduction to our subsequent notation we shall consider a one-dimensional model which has been dealt with by many previous authors.[7,10] (See Fig. 1.)

Consider a chain of atoms where each atom (k) possesses an internal coordinate $\mu^{(k)}$ which may take the values ± 1. The interaction energy between each pair of successive atoms depends on whether their internal coordinates are alike or different:

$$u(1,1)=u(-1,-1)=-u(1,-1)$$
$$=-u(-1,1)=-J,$$

or

$$u(\mu^{(k)},\mu^{(k-1)})=-J\mu^{(k)}\mu^{(k-1)}. \tag{1}$$

The partition function of this one-dimensional crystal equals

$$e^{-F/kT}=Q(T) \tag{2}$$
$$=\sum_{\mu^{(1)},\mu^{(2)},\cdots,\mu^{(N)}=\pm 1}\exp(-\sum_k u(\mu^{(k)},\mu^{(k-1)})/kT).$$

Following Kramers and Wannier,[10] we express this sum in terms of a matrix whose elements are

$$(\mu\,|\,V\,|\,\mu')=e^{-u(\mu,\mu')/kT}. \tag{3}$$

Then the summation over $(\mu^{(2)},\cdots,\mu^{(N-1)})$ in (2) is equivalent to matrix multiplication, and we obtain

$$Q(T)=\sum_{\mu 1,\,\mu N}(\mu^{(1)}\,|\,V^{N-1}\,|\,\mu^{(N)})=\lambda_m{}^N O(1), \tag{4}$$

where λ_m is the greatest characteristic number of the matrix V. Since all the elements of this matrix are positive, λ_m will be a simple root of the secular equation

$$|\,V-\lambda\,|=0,$$

and the identity

$$\lambda_m\psi_m(\mu)=(V,\psi_m(\mu)) \tag{5}$$

will be satisfied by a function (eigenvector) $\psi_m(\mu)$ which does not change sign.[11] In the present case we have

$$\psi_m(1)=\psi_m(-1)$$
$$\lambda_m=2\cosh(J/kT). \tag{6}$$

It will be convenient to use the abbreviation

$$J/kT=H. \tag{7}$$

The matrix V, written explicitly

$$V=\begin{pmatrix} e^H, & e^{-H} \\ e^{-H}, & e^H \end{pmatrix}, \tag{8}$$

represents an operator on functions $\psi(\mu)$, which has the effect

$$(V,\psi(\mu))=e^H\psi(\mu)+e^{-H}\psi(-\mu). \tag{9}$$

This operator is therefore a function of the "complementary" operator C which replaces μ by $-\mu$

$$(C,\psi(\mu))=\psi(-\mu);\quad C^2=1, \tag{10}$$

[11] S. B. Frobenius, Preuss. Akad. Wiss. pp. 514–518 (1909); R. Oldenberger, Duke Math. J. 6, 357 (1940). See also E. Montroll, reference 5.

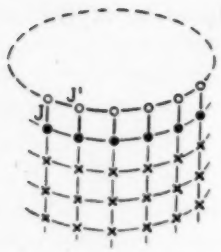

FIG. 2. Cylindrical crystal model. Configuration of added tier—○—○—○— depends on that of tier —●—●—●— in previous marginal position.

and whose eigenfunctions are the (two) different powers of μ

$$(C, 1)=1, \quad (C, \mu)=-\mu, \tag{11}$$

with the characteristic numbers $+1$ and -1, respectively. The linearized expression of V in terms of C is evident from (9), which is now written more compactly

$$V=e^{H}+e^{-H}C. \tag{12}$$

The eigenfunctions of V are of course the same as those of C, given by (11); the corresponding characteristic numbers are

$$\begin{aligned}\lambda_m=\lambda_+&=e^{H}+e^{-H}=2\cosh H\\ \lambda_-&=e^{H}-e^{-H}=2\sinh H.\end{aligned} \tag{13}$$

We shall deal frequently with *products* of many operators of the type (12). It is therefore a matter of great interest to linearize the *logarithm* of such an operator. Following Kramers and Wannier,[10] we introduce the function of H

$$H^*=\tfrac{1}{2}\log\coth H=\tanh^{-1}(e^{-2H}), \tag{14}$$

and obtain

$$V=e^{H}(1+e^{-2H}C)=e^{H}(1+(\tanh H^*)C),$$

which may be written

$$\begin{aligned}V&=(e^{H}/\cosh H^*)\exp(H^*C)\\ &=(2\sinh 2H)^{\frac{1}{2}}\exp(H^*C).\end{aligned} \tag{15}$$

The first, less symmetrical form serves to keep a record of the sign when H is not a positive real number. For example,

$$\begin{aligned}(-H)^*&=H^*\pm\tfrac{1}{2}\pi i\\ \cosh((-H)^*)&=\pm i\sinh H^*.\end{aligned} \tag{16}$$

For reference, we tabulate here the relations given by Kramers and Wannier.

$$\begin{aligned}\sinh 2H\sinh 2H^*&=\cosh 2H\tanh 2H^*\\ &=\tanh 2H\cosh 2H^*=1.\end{aligned} \tag{17}$$

Alternatively, we can express the hyperbolic functions in terms of the gudermannian angle

$$\operatorname{gd} u\equiv 2\tan^{-1}(e^{u})-\tfrac{1}{2}\pi=2\tan^{-1}(\tanh\tfrac{1}{2}u), \tag{18}$$

whereby

$$\begin{aligned}\sinh u\cot(\operatorname{gd} u)&=\coth u\sin(\operatorname{gd} u)\\ &=\cosh u\cos(\operatorname{gd} u)=1.\end{aligned} \tag{19}$$

Then the relation between H and H^* may be written in the form

$$\operatorname{gd} 2H+\operatorname{gd} 2H^*=\tfrac{1}{2}\pi. \tag{20}$$

THE RECTANGULAR ISING MODEL

We consider n parallel chains of the same type as before. We shall build up these chains simultaneously, tier by tier, adding one atom to each chain in one step (see Fig. 2). With the last atom in the jth chain is associated the variable μ_j capable of the values ± 1. A complete set of values assigned to the n variables describes a configuration $(\mu)=(\mu_1, \cdots, \mu_n)$ of the last tier of atoms. The operator which describes the addition of a new tier with the interaction energy

$$u_1((\mu), (\mu'))=-\sum_{j=1}^{n} J\mu_j\mu_j'=-kTH\sum\mu_j\mu_j' \tag{21}$$

is now

$$\begin{aligned}V_1&=\prod_{j=1}^{n}(e^{H}+e^{-H}C_j)\\ &=(2\sinh 2H)^{n/2}\exp(H^*B),\end{aligned} \tag{22}$$

whereby

$$B\equiv\sum_{j=1}^{n} C_j, \tag{23}$$

and the individual operators $C_1, \cdots, C_n$ have the effect

$$\begin{aligned}&(C_j, \psi(\mu_1, \cdots, \mu_j, \cdots, \mu_n))\\ &\quad=\psi(\mu_1, \cdots, \mu_{j-1}, -\mu_j, \mu_{j+1}, \cdots, \mu_n).\end{aligned} \tag{24}$$

Next, let us assume a similar interaction between adjacent atoms in a tier, only with an independent value J' for the pairwise energy of interaction. For symmetry, let the nth atom be neighbor to the first; then with the convention

that the atoms in a tier are numbered modulo n,

$$\mu_{j+n}=\mu_j,$$

the total tierwise interaction energy will be

$$u_2(\mu_1, \cdots, \mu_n) = -J'\sum_{j=1}^{n}\mu_j\mu_{j+1} = -kTH'\sum_{j=1}^{n}\mu_j\mu_{j+1}. \quad (25)$$

The effect of this interaction is simply to multiply the general term of the partition function, represented by one of the 2^n vector components $\psi(\mu_1, \cdots, \mu_n)$, by the appropriate factor $\exp(-u_2(\mu_1, \cdots, \mu_n)/kT)$; the corresponding operator V_2 has a diagonal matrix in this representation. It can be constructed from the simple operators $s_1, \cdots, s_n$ which multiply ψ by its first, $\cdots$, nth argument, as follows

$$(s_j, \psi(\mu_1, \cdots, \mu_n)) = \mu_j\psi(\mu_1, \cdots, \mu_n) \quad (26)$$

$$A=\sum_{j=1}^{n} s_j s_{j+1}, \quad (27)$$

$$V_2=\exp(H'A). \quad (28)$$

We now imagine that we build the crystal in alternate steps. We first add a new tier of atoms (see Fig. 3), next introduce interaction among atoms in the same tier, after that we add another tier, etc. The alternate modifications of the partition function are represented by the product

$$\cdots V_2\ V_1\ V_2\ V_1\ V_2\ V_1$$

with alternating factors; the addition of one tier of atoms with interaction both ways is represented by $(V_2V_1)=V$. The eigenwert problem which yields the partition function of the crystal is accordingly

$$\lambda\psi=(V,\psi)=(V_2V_1,\psi)$$
$$=(2\sinh 2H)^{n/2}(\exp(H'A)\exp(H^*B),\psi). \quad (29)$$

Viz., in the more explicit matrix notation used by previous authors[12]

$$\lambda\psi(\mu_1\cdots\mu_n)=\exp\left(H'\sum_1^n\mu_j\mu_{j+1}\right)$$
$$\times\sum_{\mu_1'\cdots\mu_n'=\pm1}\exp\left(H\sum_1^n\mu_j\mu_j'\right)\psi(\mu_1'\cdots\mu_n').$$

[12] See H. A. Kramers and G. H. Wannier (reference 10). E. Montroll (reference 5); E. N. Lassettre and J. P. Howe, J. Chem. Phys. 9, 747 (1941).

This 2^n-dimensional problem we shall reduce to certain sets of 2-dimensional problems. So far, we have expressed A and B rather simply by the generating elements $s_1, C_1, \cdots, s_n, C_n$ of a certain abstract algebra, which is easily recognized as a direct product of n quaternion algebras. However, the expansion (27) of A is not linear. Following a preliminary study of the basis group, we shall therefore construct a new basis for a part of the present algebra, which allows linear expansions of both A and B in terms of its generating elements.

QUATERNION ALGEBRA

We have introduced two sets of linear operators $s_1, \cdots, s_n$ and $C_1, \cdots, C_n$ by the definitions

$$\begin{aligned}(s_j, \psi(\mu_1, \cdots, \mu_j, \cdots, \mu_n)) &= \mu_j\psi(\mu_1, \cdots, \mu_j, \cdots, \mu_n),\\ (C_j, \psi(\mu_1, \cdots, \mu_j, \cdots, \mu_n)) &= \psi(\mu_1, \cdots, -\mu_j, \cdots, \mu_n).\end{aligned} \quad (30)$$

We shall see that the group generated by these operators forms a complete basis for the algebra of linear operators in the 2^n-dimensional vector space of the functions $\psi(\mu_1, \cdots, \mu_n)$. Their abstract properties are

$$\begin{aligned} &s_j^2=C_j^2=1, \quad s_jC_j=-C_js_j;\\ &s_js_k=s_ks_j, \quad C_jC_k=C_kC_j;\\ &s_jC_k=C_ks_j; \quad (j\neq k).\end{aligned} \quad (31)$$

The algebra based on one of the subgroups $(1, s_j, C_j, s_jC_j)$ is a simple quaternion algebra. The group of its basis elements includes $(-1, -s_j, -C_j, C_js_j)$ as well; but this completion of the group adds no new independent element for the purpose of constructing a basis. If we disregard

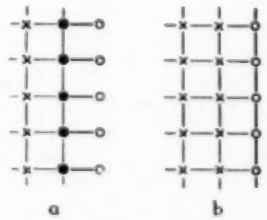

FIG. 3. Two-step extension of a two-dimensional crystal. (a) A new tier of atoms ○ is added (V_1); their configuration depends on that of atoms ● in previous marginal position. (b) Interaction energy between marginal atoms ○ is introduced (V_2), which modifies the distribution of configurations in this tier of atoms.

the sign, each element is its own inverse. Except for the invariant element (-1) and the unit proper, each element together with its negative constitutes a class. This algebra has just one irreducible representation

$$\mathbf{D}_2(1)=\begin{pmatrix}1&0\\0&1\end{pmatrix};\qquad \mathbf{D}_2(s_j)=\begin{pmatrix}1&0\\0&-1\end{pmatrix};$$

$$\mathbf{D}_2(C_j)=\begin{pmatrix}0&1\\1&0\end{pmatrix};\quad \mathbf{D}_2(s_jC_j)=\begin{pmatrix}0&1\\-1&0\end{pmatrix}.$$

Our algebra of operators in 2^n-dimensional space can be described accordingly as the direct product of n simple quaternion algebras, which is still referred to as a (general) quaternion algebra. Each one of its 4^n independent basis elements can be expressed uniquely as a product of n factors, one from each set $(1, s_j, C_j, s_jC_j)$. Still, each element furnishes its own inverse and, except for (-1) and the unit, each element with its negative constitutes a class, which immediately characterizes all possible representations of the algebra: *The characters of all basis elements with the sole exception of the unit must vanish.* This of course is a consequence of the direct product construction. Another is the recognition that the algebra has only one irreducible representation

$$\mathbf{D}_2\times\mathbf{D}_2\times\cdots\times\mathbf{D}_2=\mathbf{D}_{2^n}$$

which is of 2^n dimensions; our definitions (30) describe an explicit version of it.

With the customary restriction that the elements of the basis group are to be represented by unitary matrices, the representations of the 4^n independent basis elements must be orthogonal to each other (in the hermitian sense) on the 2^{2n} (or more) matrix elements as a vector basis. For the vector product in question is nothing but

$$\sum_{r,s=1}^{2^n}\mathbf{D}(Q_1)_{rs}\overline{\mathbf{D}}(Q_2)_{rs}=\mathrm{Tr.}\,(\mathbf{D}(Q_1Q_2^{-1}))=\mathrm{Tr.}\,(\mathbf{D}(Q_3)),$$

and if Q_1 and Q_2 are independent elements of the basis group, then their quotient Q_3 is an element different from the unit and (-1), so that its character vanishes.

Since orthogonality guarantees linear independence, the irreducible 2^n-dimensional representation of our 4^n independent basis elements will suffice for the construction of any $2^n\times 2^n$ matrix by linear combination; *our quaternion algebra is equivalent to the complete matrix algebra of 2^n dimensions*. The choice between the two forms is a matter of convenience; the quaternion description seems more natural to the problem in hand. One of the main results obtained by Kramers and Wannier will be derived below; the comparison with their derivation is instructive.

In the following, the entire basis group will not be needed. Since our operator A involves only products of pairs of the generating elements $s_1, \cdots, s_n$ and B does not involve any of these but only $C_1, \cdots, C_n$, we shall have to deal only with that subgroup of the basis which consists of elements containing an *even* number of factors s_j. This "even" subgroup, which comprises half the previous basis, may be characterized equally well by the observation that it consists of those basis elements which commute with the operator

$$C=C_1C_2\cdots C_n \tag{32}$$

which reverses all spins at once

$$(C,\psi(\mu_1,\cdots,\mu_n))=\psi(-\mu_1,\cdots,-\mu_n). \tag{32a}$$

The representation (30) is now reducible because the 2^{n-1} *even* functions satisfying

$$(C,\psi)=\psi$$

are transformed among themselves as are the *odd* functions satisfying

$$(C,\psi)=-\psi.$$

The corresponding algebras are both of the same type as before, with $(n-1)$ pairs of generating elements

$$s_1s_n,\ s_2s_n,\ \cdots,\ s_{n-1}s_n;\quad C_1, C_2, \cdots, C_{n-1}$$

and either algebra is equivalent to the complete matrix algebra of 2^{n-1} dimensions. The previously independent operator C_n is now expressible by the others because either $C=1$ or $C=-1$, according to whether we are dealing with even or odd functions. This choice of sign determines the only difference between the two versions of the algebra in question. Moreover, the operator

$$A=\sum_{j=1}^{n}s_js_{j+1}$$

is the same in both versions, but obviously

$$B=\sum_{j=1}^{n} C_j$$

is not; here the interpretation of C_n makes a difference.

The arbitrary elimination of one of the sets of operators which enter symmetrically into the problem causes much inconvenience. The symmetry can be retained if we start with the two series of operators

$$s_1s_2,\ s_2s_3,\ \cdots,\ s_ns_1;\quad C_1,\ C_2,\ \cdots,\ C_n \tag{33}$$

required to satisfy the identities

$$s_1s_2s_2s_3\cdots s_ns_1=s_1^2s_2^2\cdots s_n^2=1$$

$$C_1C_2\cdots C_n=C=\begin{cases}1; & \text{(even functions)}\\ -1; & \text{(odd functions).}\end{cases} \tag{34}$$

The commutation rules are simply described when the two sets are arranged in the interlacing cyclic sequence

$$s_ns_1,\ C_1,\ s_1s_2,\ C_2,\ \cdots,\ s_{n-1}s_n,\ C_n,\ (s_ns_1,\ \cdots). \tag{35}$$

Here each element anticommutes with its neighbors and commutes with all other elements in the sequence.

Dual Transformation

The fundamental algebraic reason for the dual relation found by Kramers and Wannier is now readily recognized: *In the representation which belongs to even functions*, the two sets (33) are alike because the starting point of the sequence (35) is immaterial. Neither does it matter if the sequence is reversed, so that the general rules of computation remain unchanged if each member of the sequence (35) is replaced by the corresponding member of the sequence

$$C_k,\ s_ks_{k\pm1},\ C_{k\pm1},\ s_{k\pm1}s_{k\pm2},\ \cdots.$$

Accordingly, the correspondence

$$s_js_{j+1}\rightarrow C_{k\pm j},\quad C_j\rightarrow s_{k\pm(j-1)}s_{k\pm j} \tag{36}$$

describes an automorphism of the whole algebra. Under this automorphism we have in particular

$$A\rightarrow B$$
$$B\rightarrow A$$

or, compactly

$$f(A, B)\rightarrow f(B, A),$$

all in the algebra of even functions. Similarity can be inferred from the additional observation that the characters of all representations are determined by the commutation rules, or equally well from the theorem that every automorphism of a complete matrix algebra is an internal automorphism. When we return to our original mixed algebra of even and odd functions, our result takes the form

$$(1+C)f(A, B)\sim(1+C)f(B, A). \tag{37}$$

Application to the operator V given by (29) shows that the two operators

$$(\sinh 2H)^{-n/2}(1+C)\,V(H', H)$$
$$=2^{-n/2}(1+C)\exp(H'A)\exp(H^*B),$$
$$(\sinh 2H')^{n/2}(1+C)\,V'(H^*, H'^*)$$
$$=2^{-n/2}(1+C)\exp(H'B)\exp(H^*A)$$

are similar, so that the part of the spectrum of $V(H^*, H'^*)$ which belongs to even functions can be obtained from the corresponding part of the spectrum of $V(H', H)$ by the relation

$$\lambda_+(H^*, H'^*)$$
$$=(\sinh 2H\sinh 2H')^{-n/2}\lambda_+(H', H). \tag{38}$$

This result applies in particular to the largest characteristic numbers of the operators in question because both can be represented by matrices with all positive elements so that, by Frobenius' theorem,[11] the corresponding eigenvectors cannot be odd.

In the "screw" construction of a crystal preferred by Kramers and Wannier,[10] the addition of one atom is accomplished by the operator ($\mathfrak{M}$ in their notation)

$$\exp(Hs_{n-1}s_n)(\sinh 2H)^{\frac{1}{4}}\exp(H^*C_n)T$$
$$=(\sinh 2H)^{\frac{1}{4}}\exp(Hs_{n-1}s_n)T\exp(H^*C_1),$$

where T is a permutation operator which turns the screw through the angle $2\pi/n$. They indicate in explicit matrix form a transformation which effects one of the automorphisms (36), namely,

$$s_js_{j+1}\rightarrow C_{n-j},\quad C_j\rightarrow s_{n-j+1}s_{n-j}$$

whereby naturally

$$T\rightarrow T^{-1}.$$

The equivalent of (38) follows. In consequence, if the crystal is disordered at high temperatures (small H), a transition must occur at the temperature where the equality

$$H=H^*=\tfrac{1}{2}\log\cot\pi/8 \tag{39a}$$

is satisfied.

Unfortunately, our simplified derivation fails to exhibit one of the most important properties of the "dual" transformation: When applied to large two-dimensional (∞^2) crystal models, it *always* converts order into disorder and vice versa; this result is readily obtained by detailed inspection of the matrix representation. The consequent determination of the transition point for the rectangular crystal by the generalization of (39a)

$$H'=H^*;\quad (kT=kT_c) \tag{39b}$$

will be verified in the following by other means.

On the other hand, the given results are still but special applications of a transformation which applies to all orientable graphs, not just rectangular nets. Except for its "order-converting" property, this transformation is best obtained and discussed in simple topological terms. The properties of the "dual" and certain other transformations will be given due attention in a separate treatise; it would be too much of a digression to carry the subject further at this point.

Fundamental Vector Systems

We shall give brief consideration to the vector basis of our quaternion algebra, as described by the operator formulation (30). The systems of eigenvector which belong to the two sets of operators $(s_1, \cdots, s_n)$ and $(C_1, \cdots, C_n)$ are easily identified. The representations (30) of the former are already diagonal, so that their eigenvectors are δ functions

$$(s_j,\ \delta(\mu_1-\mu_1',\ \cdots,\ \mu_j-\mu_j',\ \cdots,\ \mu_n-\mu_n'))$$
$$=\mu_j'\delta(\mu_1-\mu_1',\ \cdots,\ \mu_j-\mu_j',\ \cdots,\ \mu_n-\mu_n'). \tag{40}$$

The eigenvectors of $(C_1, \cdots, C_n)$ are the different products of $\mu_1, \cdots, \mu_n$, with the normalizing factor $2^{-n/2}$

$$(C_j,\ (\mu_1^{\nu_1}\cdots\mu_n^{\nu_n}))=(-)^{\nu_j}(\mu_1^{\nu_1}\cdots\mu_n^{\nu_n}). \tag{41}$$

The explicit representation of a transformation which leads from one of these systems to the other is obtained from the expansion of the identity

$$\delta(\mu_1-\mu_1',\ \cdots,\ \mu_n-\mu_n')$$
$$=2^{-n}(1+\mu_1'\mu_1)\cdots(1+\mu_n'\mu_n). \tag{42}$$

This product description of a δ function is often more convenient. The two systems (40) and (41) yield diagonal representations of the operators A and B, respectively. The construction of the latter is a little simpler. With a slight variation of the notation we find

$$(B,\ (\mu_{j_1}\mu_{j_2}\cdots\mu_{j_k}))=(n-2k)(\mu_{j_1}\mu_{j_2}\cdots\mu_{j_k}), \tag{43a}$$

so that any homogeneous function of $(\mu_1, \cdots, \mu_n)$ is an eigenvector of B. With no repeated factors allowed, the number of independent homogeneous functions of degree k is the binomial coefficient $\binom{n}{k}$. Accordingly, the secular polynomial is

$$|B-\lambda|\equiv\prod_{k=0}^{n}(n-2k-\lambda)^{\binom{n}{k}}. \tag{43b}$$

Whereas B measures the degree of a function $\psi(\mu_1, \cdots, \mu_n)$, the operator A simply counts alternations of sign in the configuration $(\mu_1, \cdots, \mu_n)$. The analog of (43a) is now

$$\left(A,\ \left(\prod_{1}^{j_1}(1+\mu_j)\prod_{j_1+1}^{j_2}(1-\mu_j)\cdots\prod_{j_{2k}+1}^{n}(1+\mu_j)\right)\right)$$
$$=(n-4k)\left(\prod_{1}^{j_1}(1+\mu_j)\prod_{j_1+1}^{j_2}(1-\mu_j)\cdots\right.$$
$$\left.\times\prod_{j_{2k}+1}^{n}(1+\mu_j)\right). \tag{44a}$$

The alternations of sign are located arbitrarily behind $j_1, j_2, \cdots j_{2k}$; but their total number must be even $=2k$. On the other hand, the result (44a) is equally valid when μ_j is replaced throughout by $-\mu_j$; so that the spectrum of A repeats in duplicate that part of the spectrum of B which belongs to even functions, and its secular polynomial is

$$|A-\lambda|\equiv\prod_{k=0}^{[n/2]}(n-4k-\lambda)^{2\binom{n}{2k}}. \tag{44b}$$

By an obvious transformation, one-half of the

paired characteristic numbers of A may be assigned to even functions and the other, identical half to odd functions. We note again that the three operators

$$(1-C)A \sim (1+C)A \sim (1+C)B$$

are similar, whereas $(1-C)B$ has a different structure.

Some Important Elements of the Basis

As a preliminary to the simultaneous reduction of the representation of the operators A and B, we shall consider certain elements of the basis group which will recur frequently in the process and introduce a special notation for them. We have already encountered

$$P_{aa} = -C_a, \quad P_{a,a+1} = s_a s_{a+1}.$$

In general we define P_{ab} as the product

$$P_{ab} = s_a C_{a+1} C_{a+2} \cdots C_{b-1} s_b; \qquad (a, b = 1, 2, \cdots, 2n). \quad (45)$$

These operators are elements of the "even" basis and commute with C. They satisfy the recurrence formula

$$P_{a,b+1} = P_{ab} P_{bb} P_{b,b+1} = P_{ab} s_b C_b s_{b+1}. \quad (45a)$$

The period of this recurrence formula is $2n$; increasing either index by n has the effect of a multiplication by $(-C)$

$$P_{a,b+n} = P_{a+n,b} = -CP_{ab} = -P_{ab}C. \quad (46)$$

The product (45) obviously may be written in reverse order when $(b-a) \leqq n$, and by (46), this result is easily extended to all (a, b). Accordingly,

$$P_{ab}^2 = s_a C_{a+1} \cdots C_{b-1} s_b s_b C_{b-1} \cdots C_{a+1} s_a = 1. \quad (47)$$

More generally, we thus obtain the "rule of the wild index"

$$P_{ac} P_{bc} = P_{ad} P_{bd}, \quad P_{ac} P_{ad} = P_{bc} P_{bd}. \quad (48)$$

The analogous result for indices congruent (mod $=n$) is obtained immediately by combination with (46)

$$\begin{aligned} P_{ac} P_{b,c+n} &= P_{ad} P_{b,d+n} = P_{ad} P_{b+n,d}, \\ P_{ac} P_{a+n,d} &= P_{bc} P_{b+n,d} = P_{bc} P_{b,d+n}. \end{aligned} \quad (49)$$

While the period of the recurrence formula (45a) is $2n$, it is evident from (46) that the period of the commutation rules will be just n; for the factor C commutes with all the operators P_{ab}. For this reason we shall need a modified Kronecker symbol with the period n, as follows

$$D(0) = D(n) = 1, \quad D(m) \sin(m\pi/n) = 0. \quad (50)$$

Indices which differ by 0 or n (mod $=2n$) will be called *congruent*; (in the former case we call them equal). Only the congruence of *corresponding* indices matters; no important identity results from the accident that a front index coincides with a rear index. The distinction between front and rear indices represents the distinction between the opposite directions of rotation (1, 2, 3, $\cdots$, n) and (1, n, $n-1$, $\cdots$, 2) around the base of the "crystal."

The effect of simultaneous congruence is evident from (47) together with (46); one obtains either the unit (1) or the invariant basis element $(-C)$. More generally, a product of the form

$$P_{aa'} P_{bb'} \cdots P_{kk'}$$

with any number of factors equals one of the invariant elements ± 1, $\pm C$ if both front and rear indices congruent to each of the possible values 1, 2, $\cdots$, n occur an even number (0, 2, 4, $\cdots$) of times. This rule can be obtained from (48) by simple manipulation; compare the derivation of exchange rules below. In addition, thanks to the relation

$$P_{11} P_{22} \cdots P_{nn} = (-)^n C_1 C_2 \cdots C_n = (-)^n C, \quad (51)$$

an invariant element also results if both front and rear indices congruent to each of the numbers 1, 2, $\cdots$, n occur an *odd* number of times. A count of the group elements shows that there can be no further identities of this sort; accordingly, if a product satisfies neither of the given conditions, it must be a basis element different from ± 1 and $\pm C$.

The commutation rules for the operators P_{ab} can be broken up into rules which govern the exchange of indices between adjacent factors in a product. These in turn can be obtained by the rule of the wild index from the commutation rules which involve $P_{aa} = -C_a$. We first consider the product

$$P_{ab} P_{bb} = -P_{ab} C_b = -s_a C_{a+1} \cdots C_{b-1} s_b C_b.$$

When $a \equiv b$, the commutative character of the multiplication is trivial. Otherwise, there is only one factor s_b in P_{ab}; so that this operator anticommutes with $C_b = -P_{bb}$. Accordingly,

$$P_{ab}P_{bb} + (-)^{D(a-b)}P_{bb}P_{ab} = 0.$$

In view of (48) this may be written equally well

$$P_{ac}P_{bc} + (-)^{D(a-b)}P_{bc}P_{ac} = 0.$$

However, the result does not depend on the presence of a wild index, because

$$P_{ac}P_{bd} = P_{ac}P_{ad}P_{ad}P_{bd} = P_{bc}P_{bd}P_{ad}P_{bd} = -(-)^{D(a-b)}P_{bc}P_{ad}P_{bd}^2.$$

The same reasoning applies to the exchange of rear indices, and we obtain the general rule

$$P_{ac}P_{bd} = -(-)^{D(a-b)}P_{bc}P_{ad} = -(-)^{D(c-d)}P_{ad}P_{bc} = (-)^{D(a-b)+D(c-d)}P_{bd}P_{ac}. \quad (52)$$

Accordingly, the exchange of indices between adjacent factors in a product takes place with change of sign unless the trivial exchange of congruent (wild) indices is involved.

The product $P_{ac}P_{bd}$ is seen to be commutative when neither $(a-b)$ nor $(c-d)$ divides n, and in the trivial case when both do. When one and only one congruence exists, the factors anticommute.

For future reference we give here the direct operational definition of P_{ab}. In the case

$$\cot(a-\tfrac{1}{2})\pi/n > \cot(b-\tfrac{1}{2})\pi/n$$

we have

$$(P_{ab}, \psi(\mu_1, \cdots, \mu_n)) = \mu_a\mu_b\psi(\mu_1, \cdots, \mu_a, -\mu_{a+1}, \cdots, -\mu_{b-1}, \mu_b, \cdots, \mu_n); \quad (53a)$$
$$(\sin((b-a-\tfrac{1}{2})\pi/n) > 0)$$

$$(P_{ab}, \psi(\mu_1, \cdots, \mu_n)) = -\mu_a\mu_b\psi(-\mu_1, \cdots, -\mu_a, \mu_{a+1}, \cdots, \mu_{b-1}, -\mu_b, \cdots, -\mu_n); \quad (53b)$$
$$(\sin((b-a-\tfrac{1}{2})\pi/n) < 0).$$

When $\cot(a-\tfrac{1}{2})\pi/n \leqq \cot(b-\tfrac{1}{2})\pi/n$, substantially the same formulas apply, only the changes of sign are arranged $(-\mu_1, \cdots, -\mu_{b-1}, \mu_b, \cdots, \mu_a, -\mu_{a+1}, \cdots, -\mu_n)$ in the case (a) and $(\mu_1, \cdots, \mu_{b-1}, -\mu_b, \cdots, -\mu_a, \mu_{a+1}, \cdots, \mu_n)$ in the case (b).

The given formulas describe the effect of P_{ab} in terms of the vector basis (40). The effect of this same operator on a vector which belongs to the fundamental system (41) can be described conveniently with the aid of functions which introduce a change of sign once in a period $(1, 2, \cdots, n)$. Individually, these functions have the period $2n$. We shall use the standard notation

$$\operatorname{sgn} x = \begin{cases} -1; & x<0 \\ 0; & x=0 \\ 1; & x>0. \end{cases}$$

Then the function

$$\operatorname{sgn}(\sin(j\pi/n))$$

changes sign at $j=0$ and $j=n$ and vanishes for these values of j, while the function

$$\operatorname{sgn}(\sin(j-\tfrac{1}{2})\pi/n)$$

has everywhere the absolute value 1, with changes of sign between 0 and 1, and between n and $n+1$. With this notation we obtain

$$(P_{ab}, \mu_{j_1}\mu_{j_2}\cdots\mu_{j_k}) = \operatorname{sgn}[\sin((b-a-\tfrac{1}{2})\pi/n) \times \prod_{h=1}^{k} (\sin(j_h-a-\tfrac{1}{2})\pi/n \sin(j_h-b+\tfrac{1}{2})\pi/n)] \times \mu_a\mu_b\mu_{j_1}\cdots\mu_{j_k}. \quad (54)$$

This formula can be verified by direct count of the sign changes caused by the operator

$$C_{a+1}C_{a+2}\cdots C_{b-1}$$

acting on each factor of the product

$$\mu_b\mu_{j_1}\mu_{j_2}\cdots\mu_{j_k}.$$

THE BASIS OF A REDUCED REPRESENTATION

Some Important Commutators

The operators

$$A = \sum_1^n s_j s_{j+1} = \sum_1^n P_{a,a+1}, \quad B = \sum_1^n C_j = -\sum_1^n P_{aa}$$

are invariant against the dihedral (rotation-reflection) group of transformations

$$\mu_j \rightarrow \mu_{k\pm j}; \quad (j=1, 2, \cdots, n). \quad (55)$$

From the operators P_{ab} we can form $2n$ linear combinations which exhibit the same symmetry,

most simply as follows:

$$A_m=\sum_{a=1}^{n} P_{a,a+m}, \tag{56}$$

whereby

$$A_0=-B, \quad A_1=A. \tag{56a}$$

In view of (46) we have

$$A_{m+n}=-CA_m=-A_mC. \tag{57}$$

From the commutators

$$[P_{ac}, P_{bd}]=P_{ac}P_{bd}-P_{bd}P_{ac}$$

which vanish unless exactly one congruence between the indices is satisfied, we can form $n-1$ independent linear combinations of dihedral symmetry, which may be written most compactly

$$G_m=\tfrac{1}{4}\sum_{a=1}^{n}([P_{ax}, P_{a+m,x}]-[P_{xa}, P_{x,a+m}])$$
$$=\tfrac{1}{2}\sum_{a=1}^{n}(P_{ax}P_{a+m,x}-P_{xa}P_{x,a+m}). \tag{58}$$

While the definition of $G_1, G_2, \cdots$ will be extended conventionally to the complete period $m=1, 2, \cdots, 2n$, they satisfy the identities

$$G_{-m}=-G_m; \quad G_0=G_n=0 \tag{58a}$$

so that there are only $n-1$ independent operators included in the set. The analog of (57)

$$G_{m+n}=-CG_m=-G_mC \tag{59}$$

is valid. The commutators of $A_1, A_2, \cdots, A_{2n}$ with each other necessarily can be expressed in terms of the set (58). By definition

$$[A_m, A_m]=0.$$

By (57) we have also

$$[A_m, A_{m+n}]=0.$$

If we exclude these trivial cases, the congruences

$$a\equiv b; \quad a+k\equiv b+m$$

will not be satisfied simultaneously when we compute

$$[A_k, A_m]=\sum_{a,b=1}^{n}[P_{a,a+k}, P_{b,b+m}]$$
$$=\sum_{c=1}^{n}[P_{xc}, P_{x,c+m-k}]+\sum_{a=1}^{n}[P_{ax}, P_{a-m+k,x}]$$

whence

$$[A_k, A_m]=4G_{k-m}, \tag{60}$$

With the convention (58a) this is also valid in the trivial case $k\equiv m$. Conversely, the commutators of $A_1, A_2, \cdots, A_{2n}$ with their own commutators $G_1, G_2, \cdots, G_{n-1}$ can be expressed in terms of the former as follows:

$$2[G_m, A_k]=\sum_{a,b=1}^{n}([P_{ax}P_{a+m,x}, P_{b,b+k}]$$
$$-[P_{xa}P_{x,a+m}, P_{b-k,b}]).$$

Again if we exclude the trivial case $m\equiv 0$, the congruences $b\equiv a$, $b\equiv a+m$ will not be satisfied simultaneously. Hence,

$$2[G_m, A_k]=\sum_{a=1}^{n}([P_{ax}P_{a+m,x}, P_{a,a+k}]$$
$$+[P_{ax}P_{a+m,x}, P_{a+m,a+k+m}]$$
$$-[P_{xa}P_{x,a+m}, P_{a-k,a}]$$
$$-[P_{xa}P_{x,a+m}, P_{a-k+m,a+m}]).$$

Here

$$[P_{ax}P_{a+m,x}, P_{a,a+k}]=-2P_{a,a+k}P_{ax}P_{a+m,x}$$
$$=-2P_{a,a+k}P_{a,a+k}P_{a+m,a+k}=-2P_{a+m,a+k},$$
$$[P_{ax}P_{a+m,x}, P_{a+m,a+k+m}]$$
$$=2P_{ax}P_{a+m,x}P_{a+m,a+k+m}=2P_{a,a+k+m},$$

etc., and we obtain

$$2[G_m, A_k]=\sum_{a=1}^{n}(-2P_{a+m,a+k}+2P_{a,a+k+m}$$
$$+2P_{a-k,a+m}-2P_{a-k+m,a})$$
$$=\sum_{a=1}^{n}(4P_{a,a+k+m}-4P_{a,a+k-m}),$$

or, simply

$$[G_m, A_k]=2A_{k+m}-2A_{k-m} \tag{61}$$

which is also valid in the trivial case $m\equiv 0$. It is easily shown from (60) and (61) that the commutators $G_1, \cdots, G_{n-1}$ commute with each other. We have generally

$$[G_m, [A_k, A_0]]=[[G_m, A_k], A_0]+[A_k, [G_m, A_0]].$$

Using this together with (60) and (61) we find

$$[G_m, G_k]=[(2A_{k+m}-2A_{k-m}), A_0]$$
$$+[A_k, (2A_m-2A_{-m})]$$
$$=8G_{k+m}-8G_{k-m}$$
$$+8G_{k-m}-8G_{k+m}=0. \tag{61a}$$

A Set of Generating Basis Elements

The commutation rules (60) and (61) suggest the introduction of the operators $X_0, X_1, \cdots, X_n, Y_1, \cdots, Y_{n-1}, Z_1, \cdots, Z_{n-1}$ defined as follows:

$$X_r=(4n)^{-1}\sum_{a,b=1}^{2n}\cos((a-b)r\pi/n)P_{ab},$$

$$Y_r=(4n)^{-1}\sum_{a,b=1}^{2n}\sin((a-b)r\pi/n)P_{ab}, \tag{62}$$

$$Z_r=(-i/8n)\sum_{a,b=1}^{2n}\sin((a-b)r\pi/n)\times(P_{ax}P_{bx}-P_{xa}P_{xb}).$$

Again these definitions will apply conventionally for the entire period $r=1, 2, \cdots, 2n$, whereby

$$\begin{aligned}&X_{-r}=X_r,\\ &Y_{-r}=-Y_r;\quad Y_0=Y_n=0,\\ &Z_{-r}=-Z_r;\quad Z_0=Z_n=0.\end{aligned} \tag{62a}$$

Comparison of (62) with (56) and (58) yields directly

$$\begin{aligned}X_r&=(2n)^{-1}\sum_{m=1}^{2n}\cos(mr\pi/n)A_m,\\ Y_r&=-(2n)^{-1}\sum_{m=1}^{2n}\sin(mr\pi/n)A_m,\\ Z_r&=(i/2n)\sum_{m=1}^{2n}\sin(mr\pi/n)G_m.\end{aligned} \tag{63a}$$

Conversely, from the orthogonal properties of the coefficients

$$\begin{aligned}A_m&=\sum_{r=1}^{2n}(X_r\cos(mr\pi/n)-Y_r\sin(mr\pi/n)),\\ G_m&=-i\sum_{r=1}^{2n}Z_r\sin(mr\pi/n).\end{aligned} \tag{63b}$$

In particular, A and B admit the expansions

$$\begin{aligned}B=-A_0&=-\sum_{1}^{2n}X_r=-X_0-2X_1\\ &\quad-\cdots-2X_{n-1}-X_n,\\ A=A_1&=\sum_{1}^{2n}(X_r\cos(r\pi/n)-Y_r\sin(r\pi/n))\\ &=X_0+2(X_1\cos(\pi/n)\\ &\quad-Y_1\sin(\pi/n))+\cdots\\ &\quad+2(X_{n-1}\cos((n-1)\pi/n)\\ &\quad-Y_{n-1}\sin((n-1)\pi/n))-X_n.\end{aligned} \tag{63c}$$

Conversely, the operators (62) can be constructed from A and B by means of (60), (61), and (63a).

The relations (57) and (59) now become

$$\begin{aligned}(1+(-)^rC)X_r&=(1+(-)^rC)Y_r\\ &=(1+(-)^rC)Z_r=0\end{aligned} \tag{64}$$

so that the operators (62) belong to the algebra of even functions when r is odd, and vice versa; they annihilate even functions for even r and odd functions for odd r. We could deal with each set independently, but the two have many properties in common, and it is often convenient to keep them together.

The commutation rules for the operators (62) are easily obtained from (60) and (61). Thanks to the orthogonal properties of the trigonometric coefficients, we find

$$\begin{aligned}&[X_r, X_s]=[Y_r, Y_s]=[Z_r, Z_s]=0,\\ &[X_r, Y_s]=[Y_r, Z_s]=[Z_r, X_s]=0;\\ &\qquad\cos(r\pi/n)\neq\cos(s\pi/n).\end{aligned} \tag{65a}$$

The only commutators which do not vanish are

$$\begin{aligned}&[X_r, Y_r]=-2iZ_r,\\ &[Y_r, Z_r]=-2iX_r,\quad(r=1, 2, \cdots, n-1)\\ &[Z_r, X_r]=-2iY_r.\end{aligned} \tag{65b}$$

We shall show next that the operators (X_r, Y_r, Z_r), which commute with the members of other sets (X_s, Y_s, Z_s), anticommute among themselves. For this purpose we compute

$$(X_r+iY_r)^2=(4n)^{-2}\sum_{a,b=1}^{2n}e^{(a+b-c-d)r\pi i/n}P_{ac}P_{bd}$$

by the definition (62). In the given expansion we may interchange (a, b) and (c, d) independently without disturbing the coefficient. Taking the mean of the four alternatives we obtain

$$(8n)^{-2}\sum_{a,b=1}^{2n}e^{(a+b-c-d)r\pi i/n}\times(P_{ac}P_{bd}+P_{ad}P_{bc}+P_{bc}P_{ad}+P_{bd}P_{ac})$$

and by the exchange rule (52), this equals

$$(8n)^{-2}\sum_{a,b=1}^{2n}e^{(a+b-c-d)r\pi i/n}\times(1-(-)^{D(a-b)})(1-(-)^{D(c-d)})P_{ac}P_{bd}.$$

The only products which contribute to this sum

are those for which $a \equiv b$ as well as $c \equiv d$, whereby according to (46) and (47)

$$P_{ac}^2 = P_{ac}P_{a+n,c+n} = 1; \quad P_{ac}P_{a,c+n} = P_{ac}P_{a+n,c} = -C$$

and we obtain

$$(X_r + iY_r)^2 = (8n)^{-2} \sum_{a,c=1}^{2n} 8e^{2(a-c)r\pi i/n}(1-(-)^r C),$$

whence, observing (62a)

$$X_0^2 = \tfrac{1}{2}(1-C) = R_0, \tag{66}$$

$$X_n^2 = \tfrac{1}{2}(1-(-)^n C) = R_n = \begin{cases} R_0; & (n \text{ even}) \\ 1-R_0; & (n \text{ odd}) \end{cases}$$

$$(X_r \pm iY_r)^2 = 0; \quad (r = 1, 2, \cdots, n-1). \tag{67}$$

The latter result implies that X_r, Y_r anticommute

$$X_r Y_r = -Y_r X_r \tag{67a}$$

and that their squares are identical

$$X_r^2 = Y_r^2 = R_r. \tag{67b}$$

Now (65b) implies

$$X_r Y_r = -Y_r X_r = -iZ_r$$

and since the product in turn must anticommute with either factor, e.g.,

$$X(YX) = (XY)X = -(YX)X,$$

we have similarly

$$Y_r Z_r = -Z_r Y_r = -iX_r; \quad Z_r X_r = -X_r Z_r = -iY_r.$$

These results together imply (67b) as well as its extension

$$Z_r^2 = iX_r Y_r Z_r = X_r^2 = Y_r^2 = R_r.$$

The operator R_r thus defined satisfies the relations appropriate to the unit of a quaternion algebra with the hermitian basis (R_r, X_r, Y_r, Z_r), *viz.*, the real basis (R_r, X_r, Y_r, iZ_r) because

$$R_r X_r = Y_r Y_r X_r = iY_r Z_r = X_r,$$

etc., and

$$R_r^2 = R_r X_r X_r = X_r^2 = R_r.$$

The multiplication table is accordingly

$$\begin{aligned} R_r &= R_r^2 = X_r^2 = Y_r^2 = Z_r^2, \\ X_r &= R_r X_r = X_r R_r = iY_r Z_r = -iZ_r Y_r, \\ Y_r &= R_r Y_r = Y_r R_r = iZ_r X_r = -iX_r Z_r, \\ Z_r &= R_r Z_r = Z_r R_r = iX_r Y_r = -iY_r X_r. \end{aligned} \tag{68}$$

For $r = 0$ and $r = n$ the operators Y_r and Z_r vanish; in either case we obtain a commutative algebra with a degenerate basis (R_0, X_0) or (R_n, X_n); cf. (66).

In the original quaternion algebra described by (31) the operators $R_0, R_1, \cdots, R_{n-1}, R_n$ are projections. It remains to enumerate the dimensions of these projections [in the irreducible representation (30)]. By (66), R_0 and R_n are 2^{n-1} dimensional. By (64), the others have at most that many dimensions, because R_r is contained in R_0 or in $(1-R_0)$ as r is even or odd. Further information can be obtained from suitable explicit expansions of R_r in terms of the basis elements P_{ab}. A very compact expression is obtained by evaluating

$$R_r = \tfrac{1}{2}(X_r^2 + Y_r^2)$$

directly from the expansions (62), which yields

$$R_r = 2^{-5}n^{-2} \sum_{a,b,c,d=1}^{2n} \cos[(a-b-c+d)r\pi/n] P_{ac}P_{bd}. \tag{69}$$

To obtain an interesting modification of this formula we interchange the pairs of indices (a, b) and (c, d) independently. By (52) the mean of the four alternatives equals

$$\begin{aligned} R_r = 2^{-7}n^{-2} \sum_{a,b,c,d} & (\cos((a-b-c+d)r\pi/n) \\ & -(-)^{D(a-b)} \cos((a-b+c-d)r\pi/n)) \\ & \times (1+(-)^{D(a-b)+D(c-d)}) P_{ac}P_{bd}. \end{aligned}$$

The anticommuting product terms in which either $a \equiv b$ but not $c \equiv d$, or vice versa, cancel out. The terms for which neither congruence is satisfied yield

$$2^{-5}n^{-2} \sum_{a,b,c,d} \sin((a-b)r\pi/n) \sin((c-d)r\pi/n) P_{ac}P_{bd}.$$

The terms for which both congruences are satisfied yield either the identity or $-(-)^r C$ and add up to $\tfrac{1}{4}(1-(-)^r C)$. Accordingly,

$$\begin{aligned} R_r = (1-(-)^r C) & \\ \times (\tfrac{1}{4} + (8n)^{-2} & \sum_{a,b,c,d=1}^{2n} \sin((a-b)r\pi/n) \\ & \times \sin((c-d)r\pi/n) P_{ac}P_{bd}). \end{aligned} \tag{70}$$

The dimensions (character) of the projection R_r are simply enumerated from (70). When $n > 2$,

we have $-1 \neq P_{ac}P_{bd} \neq 1$ unless $a \equiv b$; $c \equiv d$, so that the dimension of R_r is one fourth of the total 2^n.

$$\mathrm{Dim}(R_r) = 2^{n-2}; \quad (r = 1, 2, \cdots, n-1); \quad (n > 2). \quad (71)$$

For the case $n = 2$; $r = 1$ we have from (63c) and (64)

$$B(1+C) = -4X_1; \quad (n = 2).$$

By (43a), the even eigenvectors of B are the two possible even homogeneous functions: (1) and $(\mu_1\mu_2)$; the corresponding characteristic numbers of B are 2 and -2. Neither vanishes, so that in this case R_1 contains all of $1-R_0$, and we have the "exceptional" result

$$R_1 = 1 - R_0; \quad \mathrm{Dim}(R_1) = 2; \quad (n = 2). \quad (71a)$$

Irreducible Representations

In the previous section we have completed the abstract theory of the algebra generated by the operators A and B defined by (27) and (23), which are involved in the eigenwert problem (29). Apart from illustrative references to the representation (30), our main results have been derived from the abstract commutation rules (31). Now the task before us is to apply these results to the solution of problems such as (29), which can be formulated explicitly in terms of A and B. For this purpose we shall again think of the abstract numbers $s_1, s_2, \cdots, s_n, C_1, C_2, \cdots, C_n$ as linear operators in a 2^n-dimensional vector space, defined by the matrix representation (30).

Essentially, the problem of reduction consists in finding the vector spaces which are invariant towards A and B, in the sense that neither A nor B operating on any member of an invariant set can yield anything but a linear combination of the vectors which belong to the same set. Since the set of operators (62) can be constructed from A and B and vice versa [cf. (63c)], it is evident that the invariant sets in question must be invariant towards all the operators (62). In view of the commutation rules (65), we may specify for added convenience that the matrices representing the operators (62) and their products shall be direct products of irreducible representations of the factor groups (R_r, X_r, Y_r, Z_r).

To answer the main questions dealt with in the present communication it will suffice to find the largest solution to the problem (29). The identification of the corresponding irreducible representation of the operators (62) is an easier task than the complete reduction, which we shall leave aside for future attention. We shall go a little further and identify separately for the vector spaces of even and odd functions the representations of maximal dimensions.

By (64) we may consider the sets of even and odd functions separately. The former are annihilated by (R_r, X_r, Y_r, Z_r) for even $r = (0, 2, 4, \cdots)$, the latter for odd $r = (1, 3, 5, \cdots)$. By (66), the space of even functions is formed by the projection $1 - R_0 = \frac{1}{2}(1+C)$, that of odd functions by $R_0 = \frac{1}{2}(1-C)$.

In the representation (30) the operator of (29) has a matrix whose elements are all positive. Accordingly, by Frobenius' theorem[11] the components of the "maximal" eigenvector must be all of one sign in this representation. It follows immediately that the vector in question cannot be odd. More precisely, it cannot be orthogonal to the even vector

$$\chi_0(\mu_1, \cdots, \mu_n) = \mathrm{const} = 2^{-n/2}$$

(normalized), which happens to be the only function of degree zero. By (43a), this is an eigenvector of B corresponding to the simple characteristic number n

$$(B, \chi_0) = (B(1-R_0), \chi_0) = n\chi_0. \quad (72)$$

Since by (63c) and (64)

$$\begin{aligned} -B &= X_1 + X_2 + \cdots + X_{2n}, \\ -B(1-R_0) &= X_1 + X_3 + \cdots + X_{2n-1} \\ &= \begin{cases} 2X_1 + 2X_3 + \cdots + 2X_{2m-1}; \\ \qquad\qquad (n = 2m) \\ 2X_1 + 2X_3 + \cdots + 2X_{2m-1} \\ \quad + X_{2m+1}; \quad (n = 2m+1) \end{cases} \end{aligned} \quad (73)$$

and $X_0, X_1, \cdots, X_n$ commute with each other, they commute with B. Accordingly, operation with X_r on χ_0 will either annihilate it or convert it into some function of the same degree. But χ_0 is the only function of degree zero. Hence, χ_0 is a common eigenvector of $X_0, X_1, \cdots X_n$ satisfying

$$(X_r, \chi_0) = \xi_r\chi_0; \quad (r = 0, 1, \cdots, n).$$

By (68) and (66) the operators X_r all satisfy the identity

$$X_r^3 - X_r = X_r(X_r-1)(X_r+1) = 0, \qquad (74)$$

so that $\xi_0, \xi_1, \cdots, \xi_n$ are to be selected from the numbers 0, 1, −1. Since χ_0 is an even vector we have

$$\xi_0 = \xi_2 = \xi_4 = \cdots = 0$$

and by comparison with (73)

$$\xi_1 + \xi_3 + \cdots + \xi_{2n-1} = -n.$$

There is just one way to satisfy this requirement

$$\begin{gathered} \xi_1 = \xi_3 = \cdots = \xi_{2n-1} = -1, \\ (X_r, \chi_0) = -\chi_0; \\ (r = 1, 3, \cdots, 2[(n-1)/2]+1). \end{gathered} \qquad (75)$$

Having identified one common eigenvector χ_0 of $X_1, X_3, \cdots$, we proceed to construct others which belong to the same invariant set by operations with $Y_1, Y_3, \cdots$. In general if χ satisfies

$$(X_r, \chi) = \xi_r \chi; \quad (r = 1, 3, \cdots),$$

then by (68) and (65)

$$\begin{aligned} (X_r, (Y_r, \chi)) &= (X_r Y_r, \chi) = (-Y_r X_r, \chi) \\ &= -\xi_r (Y_r, \chi), \\ (X_s, (Y_r, \chi)) &= (X_s Y_r, \chi) = (Y_r X_s, \chi) \\ &= \xi_s (Y_r, \chi); \quad (s \neq r) \end{aligned}$$

so that the operation with Y_r gives a new common eigenvector; the sign of the corresponding ξ_r is reversed and the others are unchanged. If ξ_r vanishes, Y_r will only annihilate χ because by (68)

$$(Y_r, \chi) = (Y_r X_r^2, \chi) = (Y_r, \xi_r^2 \chi).$$

For this reason it is useless to operate with $Y_2, Y_4, \cdots$ on χ_0. It is equally useless to operate more than once with any one Y_r because by (68) Y_r is its own inverse in the subspace R_r

$$Y_r^2 = X_r^2 = R_r,$$

so that the second operation at best undoes the effect of the first. Finally, since

$$Z_r = iX_r Y_r$$

the operation with Z_r can only give us such eigenfunctions of X_r as we can obtain with Y_r alone. Accordingly, the vectors which we can obtain by operating with various combinations of $(Y_1, Y_3, \cdots)$ on χ_0—at most once apiece—form an invariant set. The vectors thus obtained can be distinguished from each other by their different sets of characteristic numbers; when necessary we shall designate them individually

$$\chi(\xi_1, \xi_3, \cdots, \xi_{2m-1}; (\mu)); \quad (n \geqq 2m \geqq n-1).$$

In the case of odd n we have $\xi_n = -1$ for every vector in the set; there is no Y_n. For the rest, every combination occurs exactly once, as is expressed by the following formulation of the relations derived above

$$\begin{aligned} &(X_r, \chi(\xi_1, \xi_3, \cdots, \xi_{2m-1}; (\mu))) \\ &\qquad = \xi_r \chi(\xi_1, \xi_3, \cdots, \xi_{2m-1}; (\mu)), \\ &(Y_r, \chi(\xi_1, \xi_3, \cdots, \xi_{2m-1}; (\mu))) \\ &\qquad = \chi(\xi_1, \cdots, -\xi_r, \cdots, \xi_{2m-1}; (\mu)), \\ &(X_n, \chi(\xi_1, \xi_3, \cdots, \xi_{n-2}; (\mu))) \\ &\qquad = -\chi(\xi_1, \cdots, \xi_{n-2}; (\mu)). \end{aligned} \qquad (76)$$

A more explicit description of the functions χ is not necessary. The relations (76) in conjunction with the verified construction of the one vector

$$\chi(-1, -1, \cdots, -1; (\mu)) = 2^{-n/2} \qquad (76a)$$

suffice for definition. From the one given vector, the construction is in effect completed by means of the formal relations (68).

The representation (76) is analogous to (30); but it has only $m = [n/2]$ factors and the number of dimensions is $2^{[n/2]}$, if we denote by $[x]$ the greatest integer which does not exceed x. Moreover, denoting by Q_r a general function of the factor basis (R_r, X_r, Y_r, Z_r), the representation (76) is a direct product of the two-dimensional representations

$$\begin{aligned} &\mathbf{D}_{\max} = \mathbf{D}_2(Q_1) \times \mathbf{D}_2(Q_3) \times \cdots \times \mathbf{D}_2(Q_{n-1}); \\ &\qquad\qquad (n = 2m) \\ &\mathbf{D}_{\max} = \mathbf{D}_2(Q_1) \times \mathbf{D}_2(Q_3) \times \cdots \\ &\qquad \times \mathbf{D}_2(Q_{n-2}) \times \mathbf{D}_-(Q_n); \quad (n = 2m+1) \\ &\mathbf{D}_2(X_r) = \begin{pmatrix} -1 & 0 \\ 0 & 1 \end{pmatrix}; \quad \mathbf{D}_2(Y_r) = \begin{pmatrix} 0 & 1 \\ 1 & 0 \end{pmatrix}; \\ &\mathbf{D}_+(X_r) = (1); \quad \mathbf{D}_-(X_r) = (-1) \end{aligned} \qquad (77)$$

supplemented by the one-dimensional representation $\mathbf{D}_-(Q_n)$ when n is odd.

An invariant vector space may be constructed by the same procedure from any common eigenvector of $(X_0, X_1, \cdots, X_n)$. The characters of the representation will be determined by the initial ξ_0 and ξ_n, which are common to all members of an invariant set, together with the values (0 or 1) of $\xi_1^2, \xi_2^2, \cdots, \xi_{n-1}^2$. For the signs of $\xi_1, \xi_2, \cdots, \xi_{n-1}$ can be changed independently by operation with $Y_1, Y_2, \cdots, Y_{n-1}$, excepting those which vanish in the first place. To put it in geometrical language, the general type of the representation is determined by an intersection of projections

$$P_0P_1\cdots P_n$$

where for $r=1, 2, \cdots, n-1$, P_r is either R_r or $1-R_r$, while R_0 is subdivided into $\frac{1}{2}(R_0+X_0)$ and $\frac{1}{2}(R_0-X_0)$, and R_n is similarly subdivided. The vector space constructed above from χ_0 is the only intersection common to all of the projections $R_1, R_3, \cdots, R_{[n/2]-1}$. For every such intersection must contain an even eigenvector of B corresponding to the characteristic number n when n is even or $n-1-\xi_n$ when n is odd, in either case an even function of degree less than 2, and the only function that satisfies this specification is const. $=\chi_0$.

We have already pointed out that by Frobenius' theorem, that eigenvector which corresponds to the largest solution of (29) cannot be orthogonal to χ_0. Therefore, this eigenvector belongs to the invariant set constructed above, which contains χ_0. The expectation of a *simple* largest characteristic number is in accord with our finding that the invariant vector space which corresponds to the maximal representation (77) is unique.

In connection with the considerations of Lassettre and Howe,[13] it ia a matter of interest to identify not only the largest solution λ_{max} of (29), but in addition the largest solution $\bar{\lambda}_{max}$ which belongs to an *odd* eigenvector. As it happens, this solution is the second largest in magnitude. We shall prefer a slight variation of the above procedure. From one common eigenvector of the operators

$$X_r^* = -X_r\cos(r\pi/n)+Y_r\sin(r\pi/n); \quad (r=0, 1, \cdots, n-1, n) \tag{78}$$
$$X_0^* = -X_0; \quad X_n^* = X_n$$

we shall construct others by operations with, say, $Z_1, \cdots, Z_{n-1}$, which anticommute with the corresponding X_r^*. Then instead of B we consider

$$A=\sum_{j=1}^{n} s_js_{j+1} = -\sum_{r=1}^{2n} X_r^* = X_0 - \sum_{r=1}^{n-1} 2X_r^* - X_n,$$

$$R_0A = \tfrac{1}{2}(1-C)A \tag{79}$$
$$= \begin{cases} X_0-2X_2^*-2X_4^*-\cdots-2X_{n-2}^*-X_n; & (n=2m) \\ X_0-2X_2^*-2X_4^*-\cdots-2X_{n-1}^*; & (n=2m+1) \end{cases}$$

[cf. (63c)]. By (68) the operators (78) satisfy

$$X_r^{*2}=R_r=X_r^2; \quad X_r^{*3}-X_r^*=0. \tag{80}$$

The matrix which represents the operator

$$\exp(H'A)=\prod_{j=1}^{n}(\cosh H'+s_js_{j+1}\sinh H')$$

in terms of the vector basis (41) which renders B diagonal consists of two 2^{n-1}-dimensional matrices which transform even functions among themselves and odd functions among themselves, respectively. In either matrix all elements are positive (provided $H'>0$), so that Frobenius' theorem applies in the vector spaces of even and odd functions separately. The modification by the factor $\exp(H^*B)$ in (29) does not affect this conclusion because this factor is represented here by a diagonal matrix whose elements are all positive.

By (44) the largest characteristic number n of A is double and belongs to the two configurations $(+, +, \cdots, +)$, $(-, -, \cdots, -)$, which are free from alternations of sign. When the corresponding even and odd eigenvectors

$$\left.\begin{matrix} \chi_0^* \\ \chi_0^{(-)*} \end{matrix}\right\} = 2^{-1}(2^{-n}\prod_{1}^{n}(1+\mu_j) \pm 2^{-n}\prod_{1}^{n}(1-\mu_j)) \tag{81}$$

are expanded in terms of the vector basis (41), their components are all positive, so that the representations which correspond to the characteristic numbers λ_{max} and $\bar{\lambda}_{max}$ of (29) must

[13] E. N. Lassettre and J. P. Howe, reference 12.

belong to unique invariant vector spaces which contain χ_0^* and $\chi_0^{(-)*}$, respectively. The former has been constructed above from χ_0. The odd vector $\chi_0^{(-)*}$ is a common eigenvector of all X_r^* and satisfies

$$n\chi_0^{(-)*}=(A,\ \chi_0^{(-)*})$$
$$=-\sum_{q=1}^{n}(X_{2q}^*,\ \chi_0^{(-)*})=-\left(\sum_{q=1}^{n}\xi_{2q}^*\right)\chi_0^{(-)*}$$

which requires

$$\xi_0=-\xi_0^*=1,$$
$$\xi_{2q}^{*2}=1;\quad (0<q<\tfrac{1}{2}n)$$
$$\xi_n=\xi_n^*=-1;\quad (n=2m),$$

so that the vector $\chi_0^{(-)*}$ is included in the projection

$$\tfrac{1}{2}(R_0+X_0)R_2R_4\cdots R_{2[n/2]}$$

and in $\frac{1}{2}(R_n-X_n)$ when n is even. The "maximal odd" representation is therefore

$$\mathbf{D}_{\max}^{-}=\mathbf{D}_+(Q_0)\times\mathbf{D}_2(Q_2)\times\cdots\times\mathbf{D}_2(Q_{n-1});\quad (n=2m+1)$$
$$\mathbf{D}_{\max}^{-}=\mathbf{D}_+(Q_0)\times\mathbf{D}_2(Q_2)\times\cdots\times\mathbf{D}_2(Q_{n-2})\times\mathbf{D}_-(Q_n);\quad (n=2m) \tag{82}$$

with the notation of (77). When n is odd, $\mathbf{D}_{\max}^{-}$ has $2^{(n-1)/2}$ dimensions, the same number as $\mathbf{D}_{\max}$, and there can be no further representation with this number of dimensions, for there is only one pair of configurations with less than two alternations of sign. For even n the representation $\mathbf{D}_{\max}^{-}$ has only $2^{(n-2)/2}$ dimensions; it is still unique. However, one other representation with the same number of dimensions is compatible with the known spectrum (44) of A, namely,

$$\mathbf{D}_{\text{alt}}=\mathbf{D}_-(Q_0)\times\mathbf{D}_2(Q_2)\times\cdots\times\mathbf{D}_2(Q_{n-2})\times\mathbf{D}_+(Q_n). \tag{82a}$$

The count of configurations with n (even) alternations yields one pair: $(+\ -\ +\ -\ \cdots\ +\ -)$ and $(-\ +\ -\ +\ \cdots\ -\ +)$; reasoning analogous to the above shows that exactly one invariant vector space belongs to (82a).

The identification of the remaining invariant vector spaces involves more elaborate calculations; the complete theory will be given in a later publication. However, in order to settle an interesting question which will arise, we shall complete the discussion of those n vector spaces which contain the n functions of degree one

$$\chi_1(2r;\mu_1,\cdots,\mu_n)=n^{-\frac{1}{2}}\sum_{k=1}^{n}\exp(2rk\pi i/n)\mu_k. \tag{83a}$$

These functions may be classified according to the representations of the dihedral symmetry group (55). To the identical representation of (55) belongs $\chi_1(0;(\mu))$; the corresponding representation of the algebra (68) is (82). For even n, $\chi_1(n;(\mu))$ belongs to another one-dimensional representation of (55) and to the representation (82a) of (68). The remaining functions (83a) belong pairwise to two-dimensional representations of (55). To show that the pair of similar representations which belong to the pair $\chi_1(\pm 2r;(\mu))$ are described by

$$\mathbf{D}_-(Q_0)\times\mathbf{D}_0(Q_{2r})\times\prod_{s\neq r}\mathbf{D}_2(Q_{2s});\quad (n\text{ odd})$$
$$\mathbf{D}_-(Q_0)\times\mathbf{D}_-(Q_n)\times\mathbf{D}_0(Q_{2r})\times\prod_{s\neq r}\mathbf{D}_2(Q_{2s});\quad (n\text{ even}) \tag{83b}$$

one may verify that the vectors in question are annihilated by X_{2r}

$$(X_{2r},\ \chi_1(2r;(\mu)))=(X_{2r},\ \chi_1(-2r;(\mu)))=0;\quad (0<2r<n). \tag{83c}$$

The direct calculation by means of (62) and (54) is not too laborious; since X_{2r} commutes with B, only the terms of first degree have to be computed. The remaining factors in (83b) are then determined as before by the relation

$$(B,\ \chi_1)=(n-2)\chi_1.$$

SOLUTION OF THE EIGENWERT PROBLEM

It is a simple matter now to compute those solutions of the eigenwert problem (29) which belong to the representations (77), (82), and (83); we only have to solve a set of quadratic equations.

As to the "physical" significance of the solutions, we recall that the characteristic number itself yields the partition function and with it the thermodynamic functions of the crystal. Moreover, as shown by Kramers and Wannier, the individual components $\psi(\mu_1,\cdots,\mu_n)$ of the

eigenvector which belongs to λ_{max} describe the statistical distribution of configurations of the last tier of atoms added to the crystal.[10] On the other hand, if we know in addition the eigenvector $\psi'(\mu_1, \cdots, \mu_n)$ which belongs to λ_{max} for the adjoint operator $V' = V_1' V_2' = V_1 V_2$, then the component products

$$\psi(\mu_1, \cdots, \mu_n)\psi'(\mu_1, \cdots, \mu_n)$$

describe the statistical distribution of configurations in the *interior* of the crystal.[13]

With the latter result in mind, we first transform V to self-adjoint form by operation with $V_1^{\frac{1}{2}}$; then

$$\bar{V} = V_1^{\frac{1}{2}} V V_1^{-\frac{1}{2}} = V_1^{\frac{1}{2}} V_2 V_1^{\frac{1}{2}}$$
$$= (2 \sinh 2H)^{n/2}$$
$$\times \exp(\tfrac{1}{2}H'A)\exp(H^*B)\exp(\tfrac{1}{2}H'A) \quad (84)$$

has the same characteristic numbers as V, and the squares

$$\psi^2(\mu_1, \cdots, \mu_n) = f(\mu_1, \cdots, \mu_n)$$

of the components of its principal eigenvector will describe the distribution of configurations in the interior of the crystal.

To solve the eigenwert problem we may transform $\bar{V}$ into a function of the operators $X_0, X_1, \cdots, X_n$ alone, or equally well into a function of $X_0^*, X_1^*, \cdots, X_n^*$. The latter procedure involves slightly simpler relations; either result is readily converted into the other by means of the real orthogonal operator[14]

$$\exp\left(\sum_{r=1}^{n-1}((n-r)/2n)\pi i Z_r\right)$$
$$= \prod_{r=1}^{n-1}(1-(1-\sin(r\pi/2n))R_r + \cos(r\pi/2n) i Z_r).$$

For reference we observe here the somewhat more general rule

$$\exp(i\alpha Z_r)(X_r \cos\beta + Y_r \sin\beta)\exp(-i\alpha Z_r)$$
$$= X_r \cos(2\alpha+\beta) + Y_r \sin(2\alpha+\beta) \quad (85)$$

which is easily verified by means of the multiplication table (68). The latter—and (85)—are also valid if X_r, Y_r, Z_r are replaced throughout by

$$X_r^* = -X_r \cos(r\pi/n) + Y_r \sin(r\pi/n),$$
$$Y_r^* = X_r \sin(r\pi/n) + Y_r \cos(r\pi/n), \quad (86)$$
$$Z_r^* = -Z_r$$

(dual transformation). We now recall the expansions

$$A = -X_0^* - 2X_1^* - \cdots - 2X_{n-1}^* - X_n^*$$
$$B = -X_0 - 2X_1 - \cdots - 2X_{n-1} - X_n$$
$$= X_0^* + 2\sum_{r=1}^{n-1}(\cos(r\pi/n)X_r^* - \sin(r\pi/n)Y_r^*) - X_n^*.$$

Substitution in (84) yields

$$\bar{V} = (2\sinh 2H)^{n/2}\exp((H^*-H')X_0^*)$$
$$\prod_{r=1}^{n-1}(U_r)\exp(-(H^*+H')X_n^*) \quad (87)$$

where

$$U_r = \exp(-H'X_r^*)\exp(-2H^*X_r)\exp(-H'X_r^*)$$
$$= (1-R_r) + (\cosh 2H' \cosh 2H^*$$
$$-\sinh 2H' \sinh 2H^* \cos(r\pi/n))R_r$$
$$-(\sinh 2H' \cosh 2H^*$$
$$-\cosh 2H' \sinh 2H^* \cos(r\pi/n))X_r^*$$
$$-\sinh 2H^* \sin(r\pi/n)Y_r^*. \quad (87a)$$

By inspection of the factored form we note that transformation with $(1-R_r+iZ_r)$ changes U_r into U_r^{-1}, which differs from U_r in the signs of the coefficients of X_r^* and Y_r^*. Adding the two together we obtain

$$U_r + U_r^{-1} = 2(1-R_r+(\cosh 2H' \cosh 2H^*$$
$$-\sinh 2H' \sinh 2H^* \cos(r\pi/n))R_r)$$
$$= 2(1-R_r) + 2\cosh\gamma_r R_r$$

whence the characteristic numbers of U_r belonging to the subspace R_r are e^{γ_r} and $e^{-\gamma_r}$, of equal multiplicity. (Those which belong to $(1-R_r)$ are trivial, all equal to unity.) Accordingly we may write

$$U_r = 1 - R_r + \cosh\gamma_r R_r - \sinh\gamma_r \cos\delta_r^* X_r^*$$
$$-\sinh\gamma_r \sin\delta_r^* Y_r^*$$
$$= \exp(-\gamma_r(\cos\delta_r^* X_r^* + \sin\delta_r^* Y_r^*)) \quad (88)$$

where γ_r and δ_r^* can be computed from $2H'$,

[14] This is not exactly the dual transformation; it takes a further transformation with $\Pi(1-R_r+X_r)$ to obtain (86).

$2H^*$, $\omega_r = r\pi/n$ by the rules of hyperbolic trigonometry, as indicated by Fig. 4. We note in particular the trigonometric relations[15]

$$\cosh\gamma = \cosh 2H' \cosh 2H^* - \sinh 2H' \sinh 2H^* \cos\omega, \quad \text{(a)}$$

$$\sinh\gamma \cos\delta^* = \sinh 2H' \cosh 2H^* - \cosh 2H' \sinh 2H^* \cos\omega, \quad \text{(b)} \tag{89}$$

$$\sin\omega/\sinh\gamma = \sin\delta^*/\sinh 2H^* = \sin\delta'/\sinh 2H', \quad \text{(c)}$$

$$\cot\delta^* = (\sinh 2H' \coth 2H^* - \cosh 2H' \cos\omega)/\sin\omega. \quad \text{(d)}$$

With the aid of (85) and (86) we find immediately the transformations which reduce U_r to diagonal form with regard to the eigenvectors of either X_r^* or X_r as a vector basis,

$$U_r = \exp(-\tfrac{1}{2}\delta_r^* iZ_r)\exp(-\gamma_r X_r^*)\exp(\tfrac{1}{2}\delta_r^* iZ_r), \tag{90a}$$

$$U_r = \exp(\tfrac{1}{2}(\pi-\omega_r - \delta_r^*)iZ_r)\exp(-\gamma_r X_r)\exp(-\tfrac{1}{2}(\pi-\omega_r-\delta_r^*)iZ_r), \quad (r=1, 2, \cdots, n-1) \tag{90b}$$

and by substitution in (87)

$$\exp\left(\sum_{r=1}^{n-1}\tfrac{1}{2}\delta_r^* iZ_r\right)\bar{V}\exp\left(-\sum_{r=1}^{n-1}\tfrac{1}{2}\delta_r^* iZ_r\right) = (2\sinh 2H)^{n/2}\exp\left((H^*-H')X_0^* - \sum_{r=1}^{n-1}\gamma_r X_r^* - (H'+H^*)X_n^*\right), \tag{91a}$$

$$\exp\left(-\sum_{r=1}^{n-1}\tfrac{1}{2}(\pi-\omega_r - \delta_r^*)iZ_r\right)\bar{V}\exp\left(\sum_{r=1}^{n-1}\tfrac{1}{2}(\pi-\omega_r-\delta_r^*)iZ_r\right) = (2\sinh 2H)^{n/2}\exp\left((H'-H^*)X_0 - \sum_{r=1}^{n-1}\gamma_r X_r - (H'+H^*)X_n\right). \tag{91b}$$

[15] The formulas of hyperbolic trigonometry are obtained from those of spherical trigonometry by the substitution of imaginary lengths for the sides. See F. Klein, *Vorlesungen über Nicht-Euklidische Geometrie* (Springer, Berlin, 1928), p. 195.

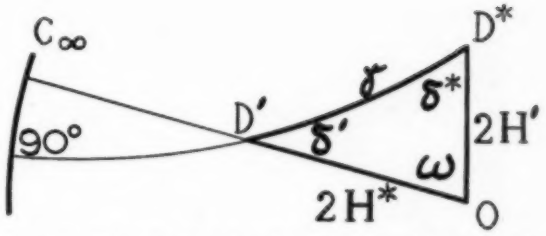

FIG. 4. Hyperbolic triangle. Stereographic projection, conformal. Circles are represented by circles, geodetics by circles invariant towards inversion in the limiting circle $C\infty$ of the projection. See F. Klein, reference 15, pp. 293–299.

The spectrum of $\bar{V}$ is now known to the extent that the common eigenvectors χ of $(X_0, X_1, \cdots, X_{n-1}, X_n)$ and the corresponding sets of characteristic numbers $(\xi_0, \xi_1, \cdots, \xi_{n-1}, \xi_n)$ are known. For every solution χ to that problem $\bar{V}$ has an eigenvector ψ with characteristic number λ given by

$$\psi = \left(\exp\left(-\sum_{r=1}^{n-1}\tfrac{1}{2}(\pi-\omega_r-\delta_r^*)iZ_r\right), \chi\right), \qquad (\bar{V}, \psi) = \lambda\psi, \tag{92}$$

$$\log\lambda = \tfrac{1}{2}n\log(2\sinh 2H) + (H'-H^*)\xi_0 - \sum_{r=1}^{n-1}\gamma_r\xi_r - (H'+H^*)\xi_n.$$

In the previous section we were able to show that the largest characteristic number of $\bar{V}$ belongs to the representation (77). In view of (76) and (76a) we must put $\xi_0 = \xi_2 = \xi_4 = \cdots = 0$. All the others may be taken negative, which calls for $\chi = \chi_0$, and obviously this is the best choice. Accordingly,

$$\log\lambda_{\max} - \tfrac{1}{2}n\log(2\sinh 2H) = \begin{cases}\gamma_1+\gamma_3+\cdots+\gamma_{2m-1}; & (n=2m)\\ \gamma_1+\gamma_3+\cdots+\gamma_{2m-1}+(H'+H^*); & (n=2m+1).\end{cases} \tag{93}$$

These two results can be combined if we adopt the natural conventions

$$\gamma_{-r} = \gamma_r; \quad \gamma_n = 2H'+2H^*. \tag{94}$$

Then (93) takes the compact form

$$\log\lambda_{\max} - \tfrac{1}{2}n\log(2\sinh 2H) = \tfrac{1}{2}\sum_{r=1}^{n}\gamma_{2r-1} = \tfrac{1}{2}\sum_{r=1}^{n}\cosh^{-1}(\cosh 2H'\cosh 2H^* - \sinh 2H'\sinh 2H^*\cos((2r-1)\pi/2n)). \tag{95}$$

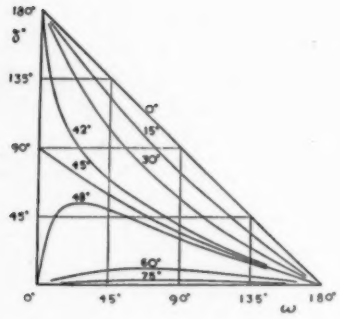

FIG. 5. Variation of δ^* with ω for the quadratic crystal, at various reduced temperatures $(k/J)T=1/H$.

gd $2H$	$1/H$
0°	∞
15°	7.551
30°	3.641
42°	2.472
45°	2.269
48°	2.089
66°†	1.29
77°‡	0.92

† By mistake marked 60° on figure.
‡ By mistake marked 75° on figure.

The corresponding eigenvector can be described by either of the two formulas

$$\psi_{\max}=\left(\exp\left(-\sum_{0<2r<n}\tfrac{1}{2}(\pi-\omega_{2r-1}-\delta^*_{2r-1})iZ_{2r-1}\right),\chi_0\right), \quad (96a)$$

$$\psi_{\max}=\left(\exp\left(\sum_{0<2r<n}\tfrac{1}{2}\delta^*_{2r-1}iZ_{2r-1}\right),\chi_0^*\right). \quad (96b)$$

Here we have omitted operations with $\exp((\text{const})Z_{2r})$; $(r=1, 2, \cdots)$, because these have no effect on χ_0 or any other even vector. The somewhat simpler form (96b) involves construction from the even δ function χ_0^* given by (81); one easily verifies that ξ_1^*, ξ_3^*, $\cdots$ are all negative for this vector.

The Principal Eigenvector

The result (96) describes explicitly the distribution of configurations (ψ^2) of one row of atoms in a crystal. The terms of the description are quite unfamiliar. We should not regret this; for among the main objects of the development of this theory is the invention of more suitable methods for the description of such distributions. Even so, we must try to establish the connection with more familiar types of description in terms of more tangible quantities. Moreover, the result (96) fails to describe the statistical correlation of configurations in different rows of atoms. Methods of dealing with these two tasks have been perfected to a considerable degree; but the algebraic apparatus involved is elaborate enough to make a separate publication advisable.

One quite tangible result is readily obtained from (96b): The probability of a configuration free from alternations is

$$2\psi^2(++\cdots+)=2\psi^2(----\cdots-)=\prod(\cos^2(\tfrac{1}{2}\delta^*_{2r-1})).$$

Similarly, when n is even so that a configuration free from persistencies of sign is possible, the probability of such a configuration is

$$2\psi^2(+-+-\cdots+-)=2\psi^2(-+-+\cdots-+)=\prod(\sin^2(\tfrac{1}{2}\delta^*_{2r-1})).$$

Presumably, the probabilities of the 2^n-4 remaining configurations are intermediate between the given limits. One can show from the commutation rules that the probabilities of configurations with 2, 4, 6, $\cdots$ alternations of sign can be computed successively from those terms in the expansion of (96b) which contain, respectively, 1, 2, 3, $\cdots$ factors of the type $(Z_r \sin\tfrac{1}{2}\delta_r^*)$. However, the labor involved increases rapidly with the number of steps.

Of greater interest is the fact that the description (96) brings out a striking qualitative difference between those distributions which occur for $n(H'-H^*)\gg 1$ and those which occur for $n(H^*-H')\gg 1$.

The variation of δ^* with $\omega=r\pi/n$ is given analytically by (89d); but a qualitative inspection of Fig. 4 is even more convenient. Let us keep the side $OD^*=2H'$ of the triangle OD^*D' fixed; then the positions of the vertex D' for $\omega=\pi/n$, $\omega=3\pi/n$, $\cdots$ are equidistant points on a circle of radius $OD'=2H^*$. Now if $2H^*>2H'$, then $\delta^*=\pi$ for $\omega=0$, and δ^* decreases from π to 0 as ω increases from 0 to π. On the other hand, if $2H^*<2H'$, then $\delta^*=0$ for $\omega=0$. As ω increases, δ^* increases to a maximum value

$$\sin^{-1}(\sinh 2H^*/\sinh 2H')=\delta^*_{\max}<\tfrac{1}{2}\pi$$

given by (89c) for $\delta'=\frac{1}{2}\pi$; with further increase of ω, δ^* decreases again until $\delta^*=0$ for $\omega=\pi$.

As regards the angle $\frac{1}{2}(\pi-\delta^*-\omega)$ which occurs in (96a), the axiom

$$\delta'+\delta^*+\omega<\pi$$

of hyperbolic geometry implies

$$\pi-\omega-\delta^*>0.$$

A graphical representation of δ^* as a function of ω at various temperatures is given in Fig. 5 for a quadratic crystal ($H'=H$). As regards the variation of δ^* with the temperature for a fixed ω, we note that as the former increases from 0 to ∞, δ^* increases from 0 to $\pi-\omega$. *For small values of ω, nearly all of this increase takes place over a small interval of temperatures which includes the critical point.* A detailed inspection of the operators Z_r can be made to show that those for which r is small are the most effective in introducing pairs of alternations far apart, which is just what it takes to convert order into disorder.

Concerning the extreme cases of low and high temperatures, one sees easily that in the former case δ^* and in the latter case $\pi-\omega-\delta^*$ will remain small for all ω. This is neither new nor surprising; it means that the low temperature distribution consists mostly of configurations which resemble the perfectly ordered arrangement represented by $\chi_0{}^*$, while the high temperature distribution resembles the completely random distribution described by χ_0.

Propagation of Order

The principal characteristic number (95) of the eigenwert problem (29) yields the partition function, and the principal eigenvector determines the distribution of configurations. Nevertheless, the remaining 2^n-1 characteristic numbers are of some interest. In general, these describe the propagation of order.[16] In particular, if long-range order is present, at least one of the subsidiary characteristic numbers should be very nearly equal to the principal.[17] Moreover, at the transition point where long-range order appears, one may expect a phenomenon analogous to the branching of multiple-valued analytic functions such as $z^{1/n}$, whereby the order of the branch-point bears a relation to the type of the singularity. A survey of the solutions which belong to the representations (77), (82), and (83) will answer the most important questions.

To obtain all the solutions which belong to (77b), the angles $\frac{1}{2}\delta_1{}^*$, $\frac{1}{2}\delta_3{}^*$, $\cdots$ in (96) may be replaced independently by $\frac{1}{2}\delta_1{}^*+\frac{1}{2}\pi$, $\frac{1}{2}\delta_3{}^*+\frac{1}{2}\pi$, $\cdots$; the corresponding characteristic numbers are given by the formula

$$\log\lambda-\tfrac{1}{2}n\log(2\sinh 2H)$$
$$=\begin{cases}\pm\gamma_1\pm\gamma_3\pm\cdots\pm\gamma_{2m-1}; & (n=2m)\\ \pm\gamma_1\pm\gamma_3\pm\cdots\pm\gamma_{2m-1}+\frac{1}{2}\gamma_{2m+1}; & (n=2m+1)\end{cases}\tag{97}$$

where the optional signs are independent and each combination occurs once.

That part of the spectrum of V which belongs to the representation (82) is obtained similarly. The result is

$$\log\lambda-\tfrac{1}{2}n\log(2\sinh 2H)$$
$$=\begin{cases}(H'-H^*)\pm\gamma_2\pm\gamma_4\pm\cdots\pm\gamma_{2m-2}+\frac{1}{2}\gamma_{2m}; & \\ \qquad\qquad (n=2m)\\ (H'-H^*)\pm\gamma_2\pm\gamma_4\pm\cdots\pm\gamma_{2m}; & \\ \qquad\qquad (n=2m+1).\end{cases}\tag{98}$$

For the largest of these we find the counterpart of (95)

$$\log\lambda_{\max}^{(-)}-\tfrac{1}{2}n\log(2\sinh 2H)$$
$$=(H'-H^*)+\tfrac{1}{2}\sum_{r=1}^{n-1}\gamma_{2r}=$$
$$=\tfrac{1}{2}\left(\gamma_0\operatorname{sgn}(H'-H^*)+\sum_{r=1}^{n-1}\gamma_{2r}\right)\tag{99}$$

with the natural notation

$$\gamma_0=\cosh^{-1}(\cosh 2H'\cosh 2H^*$$
$$-\sinh 2H'\sinh 2H^*)=2|H'-H^*|.\tag{100}$$

First of all, this differs from (95) in the substitution of $\gamma_0, \gamma_2, \cdots$ for $\gamma_1, \gamma_3, \cdots$. Moreover, the sign of $\frac{1}{2}\gamma_0$ is mandatory and changes at the critical point. This leads to a most remarkable limiting result for large values of n. The two sums

$$\gamma_1+\gamma_3+\cdots+\gamma_{2n-1}=\gamma(\pi/n)+\gamma(3\pi/n)+\cdots,$$
$$\gamma_0+\gamma_2+\cdots+\gamma_{2n-2}=\gamma(0)+\gamma(2\pi/n)+\cdots$$

[16] F. Zernike, Physica **7**, 565 (1938).
[17] See reference 13. See also E. Montroll, J. Chem. Phys. **10**, 61 (1942).

may be considered as different numerical quadratures of

$$(n/2\pi)\int_0^{2\pi}\gamma(\omega)d\omega$$

by the trapeze rule. For periodic, analytic functions the approximation to the integral improves very rapidly (exponentially) with increasing number of intervals. Hence, with rapid convergence

$$\lim_{n=\infty}(\lambda_{\max}^{(-)}/\lambda_{\max})=\begin{cases}1; & (H'>H^*)\\ \exp(2H^*-2H'); & (H'<H^*).\end{cases} \quad (101)$$

The distribution of the logarithms of the remaining characteristic numbers which belong to (77) and (82)

$$\log\lambda_{\max}-2\gamma_1,\ \log\lambda_{\max}-2\gamma_3,\ \cdots,\ \log\lambda_{\max}-2\gamma_1-2\gamma_3,\ \cdots,$$
$$\log\lambda_{\max}^{(-)}-2\gamma_2,\ \log\lambda_{\max}^{(-)}-2\gamma_4,\ \cdots,\ \log\lambda_{\max}^{(-)}-2\gamma_2-2\gamma_4,\ \cdots$$

becomes *dense* as $n\to\infty$. These "continua" remain distinct from the two largest characteristic numbers as long as $H'\neq H^*$. However, for $H'<H^*$ the representations (83b) give rise to a continuum

$$\log\lambda=\log\lambda_{\max}^{(-)}+\gamma_0-\gamma_{2r};\quad (H'<H^*) \quad (102)$$

which contains $\lambda_{\max}^{(-)}$ as a superior limit. Further complications due to representations which we have not investigated here are excluded by (43) and (63c).

At the critical point $H'=H^*$, we have $\gamma_0=0$; $\gamma_r=O(r/n)$. In this exceptional case both $\lambda_{\max}^{(-)}$ and $\lambda_{\max}$ itself are limits of "continua." The following scheme summarizes the results

$$\begin{aligned}&\lambda_{\max}=\lambda_{\max}^{(-)}>(\text{continuum});\quad (H'>H^*)\\ &\lambda_{\max}=\lambda_{\max}^{(-)}=\lim(\text{continuum});\quad (H'=H^*)\\ &\lambda_{\max}>\lambda_{\max}^{(-)}=\lim(\text{continuum});\quad (H'<H^*).\end{aligned} \quad (103)$$

At temperatures below the critical point ($H'>H^*$), we have "asymptotic degeneracy" of order 2, as a symptom of long-range order. Above the critical point, there is no degeneracy of the principal characteristic number. At the critical point we observe branching associated with an "asymptotic degeneracy" of *infinite order*.

In regard to the "propagation of order," the mean distance to which a local disturbance in the crystal is propagated is inversely proportional to $\log(\lambda_{\max}/\lambda)$. We note that this "range" of the "short-range order" becomes infinite at the critical point.

Since the functions (83a) belong to different representations of the dihedral group (55), —and the same is necessarily true for their respective invariant vector spaces—, the result (102) ought to contain information about the anisotropy of the propagation of order. A tentative computation leads to the implicit formula

$$\cosh 2H\cosh 2H'-\sinh 2H\cosh(\beta\sin\varphi)-\sinh 2H'\cosh(\beta\cos\varphi)=0 \quad (104)$$

for the mean range $(1/\beta)$ of the short-range correlation in the direction φ, when $H'<H^*$.

THERMODYNAMIC PROPERTIES OF A LARGE CRYSTAL

To compute the partition function per atom

$$\lambda=\lambda_\infty=\lim_{n=\infty}(\lambda_{\max})^{1/n} \quad (105)$$

for an infinite crystal we replace the sum (95) by the integral

$$\log\lambda_\infty=\tfrac{1}{2}\log(2\sinh 2H)+\frac{1}{2\pi}\int_0^\pi\gamma(\omega)d\omega \quad (106)$$

where

$$\cosh\gamma(\omega)=\cosh 2H'\cosh 2H^*-\sinh 2H'\sinh 2H^*\cos\omega.$$

There are several ways to show that (106) actually describes a symmetrical function of H and H'. For example, with the aid of the useful identity

$$\int_0^{2\pi}\log(2\cosh x-2\cos\omega)d\omega=2\pi x \quad (107)$$

we can convert (106) into the double integral

$$\log(\lambda/2)=\tfrac{1}{2}\pi^{-2}\int_0^\pi\int_0^\pi\log(\cosh 2H\cosh 2H'-\sinh 2H\cos\omega-\sinh 2H'\cos\omega')d\omega d\omega'. \quad (108)$$

It seems rather likely that this result could be derived from direct algebraic and topological considerations without recourse to the operator

method used in the present work. Such a development might well amount to a great improvement of the theory.

A generalization of the expansion whose initial terms were given by Kramers and Wannier is easily obtained from (108). With the notation

$$\begin{aligned} 2\kappa &= \tanh 2H/\cosh 2H' = \sin g \cos g', \\ 2\kappa' &= \tanh 2H'/\cosh 2H = \cos g \sin g' \end{aligned} \tag{109a}$$

we expand the logarithm in powers of κ and κ' and integrate term by term to obtain

$$\begin{aligned} &\log \lambda - \tfrac{1}{2}\log(4\cosh 2H \cosh 2H') \\ &= \tfrac{1}{2}\pi^{-2}\int_0^\pi\int \log(1-2\kappa\cos\omega - 2\kappa'\cos\omega')d\omega d\omega' \\ &= -\tfrac{1}{2}\sum_{r+s>0}(2r+2s-1)!(r!)^{-2}(s!)^{-2}\kappa^{2r}\kappa'^{2s}. \end{aligned} \tag{109b}$$

Specialization to the case $H=H'$; $\kappa=\kappa'$ of quadratic symmetry yields

$$\begin{aligned} &\log\lambda - \log(2\cosh 2H) \\ &= \tfrac{1}{2}\pi^{-2}\int_0^\pi\int \log(1-4\kappa\cos\omega_1\cos\omega_2)d\omega_1 d\omega_2 \\ &= -\sum_{n=1}^{\infty}\left(\binom{2n}{n}^2 \Big/ 4n\right)\kappa^{2n} \\ &= \log(1-\kappa^2-4\kappa^4-29\kappa^6-265\kappa^8-2745\kappa^{10} \\ &\qquad -30773\kappa^{12}-364315\kappa^{14}-\cdots) \end{aligned} \tag{109c}$$

which confirms the result given previously to the order κ^{10} by Kramers and Wannier.[10]

These expansions converge for all values of H and H' because

$$|2\kappa\cos\omega + 2\kappa'\cos\omega'| \leqq 2\kappa+2\kappa' = \sin(g+g') \leqq 1.$$

The limit of convergence of the series is given by the transition point,[18] and it converges even at the limit. Of course it is not very suitable for computation in the critical region; much better formulas for this purpose will be obtained.

The partition function (106) yields directly the free energy F of the crystal; the energy U and the specific heat C are obtained by differentiation with regard to the temperature T. For a crystal of N atoms

$$\begin{aligned} F &= U - TS = -NkT\log\lambda, \\ U &= F - T(dF/dT) = NkT^2 d(\log\lambda)/dT, \\ C &= dU/dT. \end{aligned} \tag{110}$$

For the purpose of differentiation it will be convenient to consider λ, given by (106), as a function of two independent variables $H=J/kT$ and $H'=J'/kT$. In this notation we have

$$\begin{aligned} U &= -NJ(\partial\log\lambda/\partial H) - NJ'(\partial\log\lambda/\partial H') \\ &= -NkT(H(\partial\log\lambda/\partial H) \\ &\qquad + H'(\partial\log\lambda/\partial H')) \end{aligned} \tag{111a}$$

$$\begin{aligned} C = Nk(&H^2(\partial^2\log\lambda/\partial H^2) \\ &+ 2HH'(\partial^2\log\lambda/\partial H\partial H') \\ &+ H'^2(\partial^2\log\lambda/\partial H'^2)). \end{aligned} \tag{111b}$$

The two terms of (111a) are separately the mean energies of interaction in the two perpendicular directions in the crystal (remember the interpretation of temperature as a statistical parameter).

In differentiating the integral of (106) we consider H^* as a function of H which satisfies [cf. (17)]

$$dH^*/dH = -\sinh 2H^* = -1/\sinh 2H.$$

The following formulas, wherein γ, δ', and δ^* are considered as functions of H', H^*, and ω, are easily obtained by differentiation from the formulas (89); some of them are obvious by inspection of Fig. 4.

$$\begin{aligned} \partial\gamma/\partial H' &= 2\cos\delta^*, \\ \partial\gamma/\partial H^* &= 2\cos\delta', \\ \partial^2\gamma/\partial H'^2 &= 4\sin^2\delta^*\coth\gamma, \\ \partial^2\gamma/\partial H^{*2} &= 4\sin^2\delta'\coth\gamma, \\ \partial^2\gamma/\partial H'\partial H^* &= -4\sin\delta^*\sin\delta'/\sinh\gamma. \end{aligned} \tag{112}$$

Comparison with (106) yields for substitution in (111)

$$\begin{aligned} \partial\log\lambda/\partial H' &= \int_0^\pi \cos\delta^*\, d\omega/\pi, \\ \partial\log\lambda/\partial H &= \cosh 2H^* - \sinh 2H^*\int_0^\pi \cos\delta'\, d\omega/\pi \end{aligned} \tag{113a}$$

and

$$\partial^2\log\lambda/\partial H'^2 = 2\int_0^\pi \sin^2\delta^*\coth\gamma\, d\omega/\pi,$$

[18] Kramers and Wannier might well have inferred this much from the uniform sign of the terms, which locates the nearest singularity on the real axis.

$$\partial^2 \log \lambda/\partial H \partial H' = 2 \sinh 2H^* \times \int_0^\pi (\sin \delta^* \sin \delta'/\sinh \gamma) d\omega/\pi,$$

$$\partial^2 \log \lambda/\partial H^2 = 2 \sinh^2 2H^* \times \left(-1+\coth 2H^* \int_0^\pi \cos \delta' \, d\omega/\pi + \int_0^\pi \sin^2 \delta' \coth \gamma \, d\omega/\pi\right). \quad (113b)$$

The reduction of these integrals by means of an uniformizing elliptic substitution for the hyperbolic triangle of Fig. 4 is dealt with in the appendix. The qualitative behavior of the integrals is easily seen from Fig. 4: The integrals (113a) are continuous functions of H' and H (or H^*) for all values of these parameters, even for $H'=H^*$ (critical point). The three integrals (113b) are infinite at the critical point, otherwise finite. The singularity results from a conspiracy: In the case $H'=H^*$ we have $\gamma(0)=0$ and at the same time $\delta'(0)=\delta^*(0)=\frac{1}{2}\pi$, although at all other temperatures

$$\gamma(\omega) \geqq \gamma(0) = 2|H'-H^*| > 0,$$
$$\sin \delta'(0) = \sin \delta^*(0) = \sin 0 = \sin \pi = 0.$$

For the special case of quadratic symmetry $H'=H$ the computation of the thermodynamic functions can be simplified considerably. The most convenient starting point is the double integral of (109c), which is converted into a single integral with the aid of (107). Using the notation

$$k_1 = 4\kappa = 2 \sinh 2H/\cosh^2 2H, \quad k_1'' = \pm(1-k_1^2)^{\frac{1}{2}} = 2\tanh^2 2H - 1; \quad |k_1''| = k_1' \quad (114)$$

we obtain

$$\log(\lambda/2\cosh 2H) = \frac{1}{2\pi}\int_0^\pi \log(\tfrac{1}{2}(1+(1-k_1^2 \sin^2 \varphi)^{\frac{1}{2}}))d\varphi. \quad (115)$$

Differentiation under the integral sign yields for the energy U,

$$U = -NJ\frac{d \log \lambda}{dH} = -NJ \coth 2H\left(1+\frac{2}{\pi}k_1'' K_1\right) \quad (116)$$

and for the specific heat C,

$$C = Nk\frac{d^2 \log \lambda}{dH^2} = Nk(H \coth 2H)^2(2/\pi) \times (2K_1 - 2E_1 - (1-k_1'')(\tfrac{1}{2}\pi + k_1'' K_1)). \quad (117)$$

In these formulas K_1 and E_1 denote the complete elliptic integrals

$$K_1 = K(k_1) = \int_0^{\pi/2} (1-k_1^2 \sin^2 \varphi)^{-\frac{1}{2}} d\varphi,$$
$$E_1 = E(k_1) = \int_0^{\pi/2} (1-k_1^2 \sin^2 \varphi)^{\frac{1}{2}} d\varphi. \quad (118a)$$

The integral (115) cannot be expressed in closed form; but rapidly convergent series can be given. With the notation

$$K_1' = K(k_1'), \quad \log q_1 = \pi\tau_1 i = -\pi K_1'/K_1, \quad (118b)$$

$$G = 1^{-2} - 3^{-2} + 5^{-2} - 7^{-2} + \cdots = 0.915\,965\,594 \text{ (Catalan's constant)},$$

one or the other of the following expansions (derived in the appendix) will be found suitable for computation:

$$\log \lambda = \tfrac{1}{2}\log(2 \sinh 2H) - \tfrac{1}{4}\log q_1 + \sum_{n=1}^{\infty} (-)^n (2n-1) \log(1-q_1^{2n-1}), \quad (119a)$$

$$\log \lambda = \tfrac{1}{2}\log(2 \sinh 2H) + (2/\pi)G + \frac{1}{\pi}\sum_{n=0}^{\infty} (-)^n \times \frac{(1+(2n+1)(\pi i/\tau_1) - \exp[-(2n+1)\pi i/\tau_1])}{(2n+1)^2 \sinh^2((n+\frac{1}{2})\pi i/\tau_1)}. \quad (119b)$$

A singularity occurs for $H=H^*=\frac{1}{2}\log \cot \pi/8$, in which case $k_1=1$; $K_1=\infty$; $K_1'=\frac{1}{2}\pi$; $E_1=1$. The specific heat becomes infinite at this critical point; the energy is continuous because $k_1''=0$. The analytic nature of the singularity is evident from the approximate formulas

$$K_1 \sim \log(4/k_1') \sim \log(2^{\frac{1}{2}}/|H-H_c|), \quad C/Nk \sim (2/\pi)(\log \cot \pi/8)^2 (K_1 - 1 - \tfrac{1}{4}\pi). \quad (120)$$

The critical data are

$$H_c = J/kT_c = \tfrac{1}{2}\log\cot\pi/8 = 0.440\,686\,8,$$
$$-F_c/NkT_c = \log\lambda_c = \tfrac{1}{2}\log 2 + (2/\pi)G = 0.929\,695\,40, \quad (121)$$
$$-U_c/NJ = 2^{\frac{1}{2}} = 1.414\,213\,56,$$
$$S_c/Nk = \log\lambda_c - 2^{\frac{1}{2}}H_c = 0.306\,470 = \log 1.358\,621.$$

The critical temperature and energy were given already by Kramers and Wannier.[10] In addition, their estimate of "about 2.5335" for λ_c was very close to the exact value

$$\lambda_c = 2^{\frac{1}{2}}e^{2G/\pi} = 2.533\,737\,28.$$

The specific heat of a quadratic crystal is represented in Fig. 6 as a function of $1/H = (k/J)T$; the result of the best approximate computation in the literature[10] is indicated for comparison.

Figure 7 represents the specific heat curve of a highly anisotropic crystal ($J'/J = 1/100$), computed from Eq. (6.2) in the Appendix. The corresponding curves for the case of quadratic symmetry ($J'/J = 1$) and for the linear chain ($J'/J = 0$) are also shown. The abscissa is $2/(H+H') = 2kT/(J+J')$, so that the three curves have the same area.

SOME PROPERTIES OF FINITE CRYSTALS

The partition function of any *finite* crystal is an analytic function of the temperature. Perfect order and a sharp transition point occur only when the extent of the crystal is infinite in two directions. It is a matter of interest to study the approach to complete order and the sharpening of the transition point with increasing size (width) of the crystal.

Boundary Tension

First, let us compute the "boundary tension" between two regions of opposite order below the transition point. This we can do by a slight variation of the model. We simply chose a *negative* interaction energy between adjacent atoms in the same tier:

$$u = +J'\sum_1^n \mu_j\mu_{j+1}.$$

Now if n is *even*, the reversal of J' has the same trivial effect as a redefinition of the sign of every other μ_j. The interpretation of the result is a little different in that the type of order which occurs below the transition point is now a superlattice with the ideal structure indicated by Fig. 8. However, let us choose an *odd* value of n. Now a perfect alternation of signs around the polygon of n atoms is impossible; in one place at least the given superlattice must be adjacent to one of opposite order. As we build a long crystal on the odd polygonal base, we build it with one misfit "seam." The free energy difference due to this seam will equal that of a boundary between regions of opposite order.

The formula (93) is still valid, only now

$$J'/kT = -H' > H^* > 0$$

whence

$$\log\lambda_{\max} - \tfrac{1}{2}n\log(2\sinh 2H)$$
$$= \gamma_1+\gamma_3+\cdots+\gamma_{2m-1} - (|H'| - H^*)$$
$$= \gamma_1+\gamma_3+\cdots+\gamma_{2m-1}+\tfrac{1}{2}\gamma_{2m+1} - 2(|H'| - H^*)$$

where

$$\cosh\gamma_r = \cosh 2H'\cosh 2H^* - \sinh(-2H')\sinh 2H^*\cos(\pi-\omega_r).$$

The replacement of ω_r by $\pi-\omega_r$ has no appreciable effect on the sum; the modification of the partition function due to the seam is therefore practically equal to

$$-2|H'| + 2H^*.$$

This represents the effect of a lengthwise boundary for our original model as well, and we obtain

$$\sigma'/kT = -\log\lambda_b' = 2(H'-H^*), \qquad \sigma' = 2J' - kT\log\coth(J/kT) \quad (122a)$$

for the boundary tension σ' (per atom) of a longitudinal boundary. The transverse boundary tension σ is similarly given by

$$\sigma/kT = -\log\lambda_b = 2(H-H'^*). \quad (122b)$$

The boundary tensions both vanish at the critical point, as one should expect. The formulas

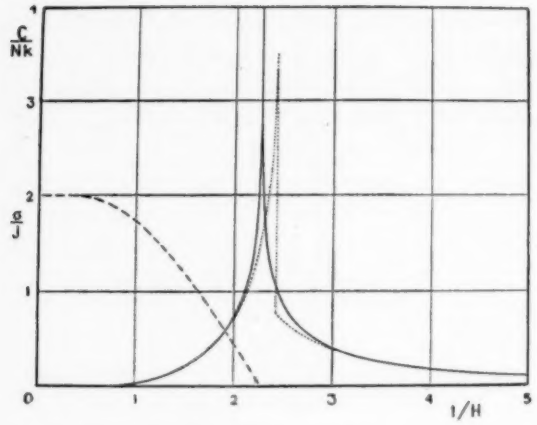

FIG. 6. Properties of quadratic crystal. — — — — — — Boundary tension σ between regions of opposite order. ———— Specific heat C. - - - - - - - - - - - - Approximate computation of C by Kramers and Wannier.

for the boundary entropies and energies follow

$$\begin{aligned} s_b' &= -d\sigma'/dT = 2k((H/\sinh 2H)+H^*), \\ s_b &= -d\sigma/dT = 2k((H'/\sinh 2H')+H'^*), \\ u_b' &= \sigma'+Ts_b' = (2/\sinh 2H)J+2J', \\ u_b &= \sigma+Ts_b = 2J+(2/\sinh 2H')J'. \end{aligned} \tag{123}$$

The variation of σ with the temperature for a quadratic crystal ($J=J'$) is represented graphically in Fig. 6.

Mean Ordered Length

In a crystal of moderate width n we may expect to find sections of rather well-defined order similar to that of an infinite crystal, with occasional transitions to opposite order. The result (122b) allows an estimate of the "mean ordered length" l_0 between such interruptions. By the general theory of fluctuations

$$\begin{aligned} l_0 = \lambda_b^{-n} &= \exp[2n(H-H'^*)] \\ &= (e^{2H}\tanh H')^n. \end{aligned} \tag{124}$$

Evidently, when n is large enough we have

$$l_0 \gg n.$$

The estimate (124) is significant when this condition is fulfilled.

The Specific Heat of a Finite Crystal

Since the partition function of a finite crystal is an analytic function of the temperature, its specific heat will be finite at all temperatures. However, a maximum will occur near the transition point of the infinite crystal; this maximum will be increased and sharpened with increasing size of the crystal.

Kramers and Wannier[10] computed the specific heats at the transition point successively for $n=1, 2, \cdots, 6$ (screw arrangement). From the results they inferred the asymptotic rule that the height of the maximum increases linearly with $\log n$. We shall verify this remarkable conjecture.

The maximum of (C/N) for a finite crystal does not occur exactly at the asymptotic critical point; but the differences in location and magnitude are only of the order $n^{-2}\log n$. This order of accuracy will suffice.

To compute the specific heat we substitute the exact partition function (95) of a finite crystal in (111b), whereby the relations (112) are useful. The specialization to the critical case

$$H'=H^*; \quad \mathrm{gd}\, 2H+\mathrm{gd}\, 2H'=\tfrac{1}{2}\pi; \quad \sinh 2H \sinh 2H'=1$$

simplifies the computation in several respects; the relations

$$\delta'=\delta^*=\delta, \quad \sinh \tfrac{1}{2}\gamma = \sinh 2H' \,|\sin \tfrac{1}{2}\omega|$$

are valid in this case. We write the result in the form

$$\begin{aligned} C/Nk = &-2H^2\sinh^2 2H'+(H'+H\sinh 2H')^2 \\ &\times\sinh 2H\times\frac{1}{n}\sum_{r=1}^{n}\mathrm{cosec}[(r-\tfrac{1}{2})\pi/n) \\ &+\frac{1}{n}\sum_{r=1}^{n}[(H'+H\sinh 2H')^2 \\ &\times(2\sin^2\delta_{2r-1}\coth\gamma_{2r-1}-\mathrm{cosech}\,\tfrac{1}{2}\gamma_{2r-1}) \\ &-4HH'\sinh 2H'\sin^2\delta_{2r-1}\tanh\tfrac{1}{2}\gamma_{2r-1} \\ &+H^2\sinh 4H'\cos\delta_{2r-1}]. \end{aligned} \tag{125}$$

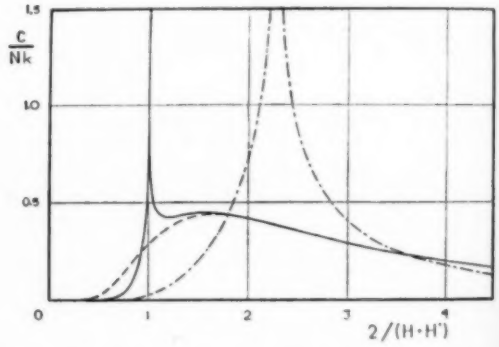

FIG. 7. Specific heats for varying degrees of anisotropy. ———— $J'/J=1/100$; — — — — — — $J'/J=1$ (quadratic crystal); - - - - - - $J'=0$ (linear chain).

The second summand, when considered as a periodic function of the variable $\omega_{2r-1}=(2r-1)\pi/2n$, has a differential quotient of bounded variation. Its sum may be replaced accordingly by the corresponding integral, with an error of the order n^{-2}.

We have purposely split off the first sum

$$S_1=\frac{1}{n}\sum_{r=1}^{n}\operatorname{cosec}((r-\tfrac{1}{2})\pi/n).$$

The corresponding integral diverges. For an asymptotic estimate of the sum we expand the cosecants in partial fractions; the result is easily arranged in the form

$$S_1=\frac{4}{\pi}\left(\frac{1}{1}+\frac{1}{3}+\cdots+\frac{1}{2n-1}-\frac{1}{2n+1}-\frac{1}{2n+3}-\cdots-\frac{1}{4n-1}+\frac{1}{4n+1}+\cdots\right)$$

$$=\frac{2}{\pi}\sum_{m=0}^{\infty}(-)^m(\psi((m+1)n+\tfrac{1}{2})-\psi(mn+\tfrac{1}{2}))$$

whereby

$$\psi(z)\equiv\Gamma'(z)/\Gamma(z)=\log(z-\tfrac{1}{2})+O(z^{-2}).$$

From the given asymptotic estimate of $\psi(z)$ together with

$$\psi(\tfrac{1}{2})=-2\log 2-C_E,$$

$$C_E=0.577\ 215\ 665,\quad\text{(Euler's constant)}$$

$$\log\left(\frac{2}{1}\cdot\frac{2}{3}\cdot\frac{4}{3}\cdot\frac{4}{5}\cdots\right)=\log\frac{\pi}{2},\quad\text{(Wallis' product)}$$

we obtain

$$S_1=(2/\pi)(\log(8n/\pi)+C_E)+O(n^{-2}).$$

Substitution of the given estimates in (125) yields the asymptotic formula for the specific heat maximum

$$C/Nk\sim(2/\pi)[\sinh 2H(H'+H\sinh 2H')^2\times(\log n+\log(8/\pi\cosh 2H')+C_E)+\sinh 2H(H'-H\sinh 2H')^2-2(H'\sinh 2H)^2\,\mathrm{gd}\,2H'-2(H\sinh 2H')^2\,\mathrm{gd}\,2H].\quad(126)$$

The result is not quite symmetrical with regard to H and H'; neither was such symmetry to be expected. Interchange of the two leads to the replacement

$$\log(n/\cosh 2H')\rightarrow\log(n/\cosh 2H).$$

For the case of quadratic symmetry

$$H=H'=\tfrac{1}{2}\log\cot\pi/8$$

the coefficient of $\log n$ attains a maximum. We find

$$C/Nk\sim(2/\pi)(\log\cot\pi/8)^2\times(\log n+\log(2^{5/2}/\pi)+C_E-\tfrac{1}{4}\pi)=0.4945\log n+0.1879.\quad(127)$$

The estimate indicated graphically by Kramers and Wannier[10] may be described by the equation

$$C/Nk=0.48\log n+0.21.$$

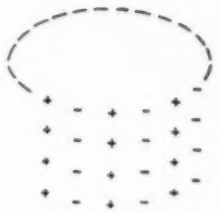

FIG. 8. Superlattice at low temperatures in crystal for which the interaction energy between neighbors of opposite spin is $J>0$ lengthwise and $-J'<0$ transversely.

APPENDIX

We shall deal here with the evaluation of various integrals which occur in the text. Most of these can be reduced in straightforward fashion to complete elliptic integrals; only the partition function itself is of a type one step higher than the theta functions, and involves a little analysis which is not found in textbooks.

1. General Notation

One of the main reasons for setting this material apart is that the notation must be specified because there are several systems in common use. We shall adopt the notation used by Whitaker and Watson.[19]

[19] E. T. Whitaker and G. N. Watson, *Modern Analysis* (Cambridge University Press, 1927), fourth edition, Chapters 20–22. Referred to in the following as WW.

Theta Functions

$$\vartheta_3(z|\tau)=\vartheta_3(z)=\vartheta_4(z+\tfrac{1}{2}\pi)$$
$$=\sum_{-\infty}^{\infty}\exp(n^2\pi i\tau)\cos 2nz,$$
$$\vartheta_2(z|\tau)=\vartheta_2(z)=\vartheta_1(z+\tfrac{1}{2}\pi)$$
$$=\sum_{-\infty}^{\infty}\exp[(n+\tfrac{1}{2})^2\pi i\tau]\cos(2n+1)z, \tag{1.1}$$
$$\vartheta_r=\vartheta_r(0);\quad \vartheta_r''=\vartheta_r''(0);\quad (r=2,3,4).$$

Periods, Modulus, Comodulus

$$2K=\vartheta_3^2\pi;\quad 2iK'=\vartheta_3^2\pi\tau,$$
$$k=\sin\theta=\vartheta_2^2/\vartheta_3^2,$$
$$k'=\cos\theta=\vartheta_4^2/\vartheta_3^2, \tag{1.2}$$
$$\log q=\pi i\tau=-\pi K'/K.$$

We shall only have to deal with "natural" cases in which $-i\tau$ is real (not negative); $0<k\leqq 1$; $0\leqq k'<1$. The ratio τ of the periods will be specified when necessary. Tables of $\log q$ are available.[20]

Jacobian Elliptic Functions

$$\operatorname{sn}(\vartheta_3^2 z)=(\vartheta_3/\vartheta_2)\vartheta_1(z)/\vartheta_4(z),$$
$$\operatorname{cn}(\vartheta_3^2 z)=(\vartheta_4/\vartheta_2)\vartheta_2(z)/\vartheta_4(z),$$
$$\operatorname{dn}(\vartheta_3^2 z)=(\vartheta_4/\vartheta_3)\vartheta_3(z)/\vartheta_4(z), \tag{1.3}$$
$$\operatorname{am} u=\sin^{-1}(\operatorname{sn} u)=\cos^{-1}(\operatorname{cn} u).$$

We shall use Glaisher's notation for the quotients of the Jacobian elliptic functions

$$\operatorname{sc} u=\operatorname{sn} u/\operatorname{cn} u;\quad \operatorname{nd} u=1/\operatorname{dn} u;\quad \text{etc.} \tag{1.4}$$

The Functional Relations

$$\operatorname{cn}^2 u+\operatorname{sn}^2 u=\operatorname{dn}^2 u+k^2\operatorname{sn}^2 u=1 \tag{1.5}$$

are important for the uniformization of certain algebraic functions.

Elliptic Integrals of the First Kind

$$d(\operatorname{sn} u)/du=\operatorname{cn} u\operatorname{dn} u;\quad \text{etc.}$$
$$u=F(k,\operatorname{am} u)=\int_0^{\operatorname{am} u}(1-k^2\sin^2\varphi)^{-\frac{1}{2}}d\varphi, \tag{1.6}$$
$$K(k)=F(k,\tfrac{1}{2}\pi);\quad K'(k)=K(k').$$

[20] Four place tables of $\log q$ by 5′ intervals of the modular angle are given by E. Jahnke and F. Emde, *Tables of Functions* (B. G. Teubner, Leipzig and Berlin, 1933), second edition, p. 122.

Elliptic Integrals of the Second Kind

These involve the following definitions and relations.

$$Z(u)=\vartheta_3^{-2}\vartheta_4'(\vartheta_3^{-2}u)/\vartheta_4(\vartheta_3^{-2}u),$$
$$E=\int_0^{\pi/2}(1-k^2\sin^2\varphi)^{\frac{1}{2}}d\varphi$$
$$=\int_0^K \operatorname{dn}^2 u\,du=(-\vartheta_2''/\vartheta_2\vartheta_3^2)\pi/2, \tag{1.7}$$
$$E(u)=Z(u)+(E/K)u=\int_0^u \operatorname{dn}^2 v\,dv.$$

Complete Elliptic Integral of the Third Kind

$$KZ(a)=\int_0^K k^2\operatorname{sn} a\operatorname{cn} a\operatorname{dn} a\operatorname{sn}^2 u$$
$$\times(1-k^2\operatorname{sn}^2 a\operatorname{sn}^2 u)^{-1}du. \tag{1.8}$$

2. Uniformizing Substitution

The trigonometric functions of the angles and sides of a spherical triangle with two fixed parts can always be expressed in terms of single-valued functions by a suitable elliptic substitution. The same is true for hyperbolic (and plane) triangles. In any case the determination of the modulus is suggested by the sine proportion.

For the triangle of Fig. 4, with two given sides $2H'$ and $2H^*$, the simplest uniformizing substitution depends on which side is longer. For temperatures below the critical point we choose the modulus k, the imaginary parameter ia, and the new variable u as follows

$$k=k_0=\sin\Theta_0=\sinh 2H^*/\sinh 2H'$$
$$=1/\sinh 2H\sinh 2H'<1,$$
$$\operatorname{am}(ia)=\operatorname{am}(2iK_0'y,k_0)=2iH', \tag{2.1a}$$
$$\operatorname{am} u=\delta'.$$

Then the trigonometric, *viz.*, hyperbolic functions of δ^*, δ', $2H^*$ and $2H'$ are given by the formulas

$$\sin\delta'=\operatorname{sn} u;\quad \sin\delta^*=k\operatorname{sn} u$$
$$\cos\delta'=\operatorname{cn} u;\quad \cos\delta^*=\operatorname{dn} u$$
$$\tan g'=\sinh 2H'=-i\operatorname{sn} ia \tag{2.2a}$$
$$\cot g=\sinh 2H^*=-ik\operatorname{sn} ia$$
$$\sec g'=\cosh 2H'=\operatorname{cn} ia$$
$$\operatorname{cosec} g=\cosh 2H^*=\operatorname{dn} ia.$$

We are using the abbreviation

$$g'=\text{gd}\,2H';\quad g=\text{gd}\,2H=\tfrac{1}{2}\pi-\text{gd}\,2H^* \tag{2.3}$$

for the gudermannian angles, which can often be employed to advantage in numerical computations.

For temperatures above the critical point the starred and the primed quantities exchange roles:

$$\begin{aligned} k=k_0&=\sin\Theta_0=\sinh 2H'/\sinh 2H^*\\ &=\sinh 2H'\sinh 2H=<1,\\ \text{am}(ia)&=\text{am}(2iK_0'y,k_0)=2iH^*,\\ \text{am}\,u&=\delta^* \end{aligned} \tag{2.1b}$$

and explicitly

$$\begin{aligned} \sin\delta'&=k\,\text{sn}\,u;\quad \sin\delta^*=\text{sn}\,u\\ \cos\delta'&=\text{dn}\,u;\quad \cos\delta^*=\text{cn}\,u\\ \tan g'&=\sinh 2H'=-ik\,\text{sn}\,ia\\ \cot g&=\sinh 2H^*=-i\,\text{sn}\,ia\\ \sec g'&=\cosh 2H'=\text{dn}\,ia\\ \text{cosec}\,g&=\cosh 2H^*=\text{cn}\,ia. \end{aligned} \tag{2.2b}$$

The formulas for ω and γ are the same in the two cases. The abbreviation

$$M=\text{dn}\,ia\,\text{dn}\,u-k\,\text{cn}\,ia\,\text{cn}\,u$$

will be convenient; then

$$\begin{aligned} \cosh\gamma&=(\text{cn}\,ia\,\text{dn}\,u-k\,\text{dn}\,ia\,\text{cn}\,u)/M\\ \sinh\gamma&=-ik'^2\,\text{sn}\,ia/M\\ -\cos\omega&=(\text{dn}\,ia\,\text{cn}\,u-k\,\text{cn}\,ia\,\text{dn}\,u)/M\\ \sin\omega&=k'^2\,\text{sn}\,u/M. \end{aligned} \tag{2.4}$$

Moreover, when ω and γ are considered as functions of u and a

$$\begin{aligned} -\partial\omega/\partial u=\partial\gamma/\partial a&=k'^2/M,\\ \partial\gamma/\partial u=\partial\omega/\partial a&=ik'^2k\,\text{sn}\,ia\,\text{sn}\,u/M. \end{aligned} \tag{2.5}$$

The conformal mapping indicated by (2.5) may be described by the functional relation

$$\cot\tfrac{1}{2}(\omega-i\gamma)=(1+k)\,\text{sc}\,\tfrac{1}{2}(u+ia)\,\text{nd}\,\tfrac{1}{2}(u+ia). \tag{2.6}$$

3. Alternative Substitution

While the substitution given above is preferred for most purposes, there are certain advantages to be gained by a Landen transformation to modulus and periods given by

$$\begin{aligned} k_1'&=\cos\Theta_1=\coth(H'+H^*)\tanh|H'-H^*|\\ &=|\cos(g+g')|/\cos(g-g')=(1-k_0)/(1+k_0),\\ k_1&=\sin\Theta_1=2(\sinh 2H\sinh 2H')^{\frac{1}{2}}/\\ &\qquad(1+\sinh 2H\sinh 2H'),\\ K_1&=(1+k_0)K_0,\\ K_1'&=\tfrac{1}{2}(1+k_0)K_0'=K_0'/(1+k_1'),\\ \tau_1&=iK_1'/K_1=\tfrac{1}{2}\tau_0=\tfrac{1}{2}\tau. \end{aligned} \tag{3.1}$$

The parameter

$$ia_1=2yiK_1'=\tfrac{1}{2}(1+k_0)ia_0 \tag{3.2}$$

and the variable u_1 are given by

$$\begin{aligned} \text{am}(ia_1,k_1)&=i(H'+H^*),\\ \text{am}(u_1,k_1)&=\tfrac{1}{2}(\delta'+\delta^*) \end{aligned} \tag{3.3}$$

and the following relations hold

$$\begin{aligned} \text{am}(K_1-ia_1)&=\tfrac{1}{2}\pi-i|H'-H^*|,\\ \text{am}(K_1-u_1)&=\tfrac{1}{2}\pi-\tfrac{1}{2}|\delta'-\delta^*|,\\ \text{am}(u_1\pm ia_1)&=\tfrac{1}{2}(\pi-\omega\pm i\gamma). \end{aligned} \tag{3.4}$$

Here the functions of the double parameter are of some interest

$$\begin{aligned} \text{sc}(2ia_1)&=\text{sc}(4iyK_1')=i\cos(g-g'),\\ \text{nc}(2ia_1)&=\text{nc}(4iyK_1')=\sin(g-g'),\\ \text{dc}(2ia_1)&=\text{dc}(4iyK_1')=\sin(g+g'). \end{aligned} \tag{3.5}$$

This substitution shows up the analytic nature of the parameter through the critical point, and (2.6) is replaced by a simpler equivalent in (3.4). Moreover, formulas valid for all temperatures can be constructed by furnishing a sign for the comodulus

$$\begin{aligned} k_1'&=|k_1''|;\\ k_1''&=\coth(H'+H^*)\tanh(H'-H^*). \end{aligned} \tag{3.6}$$

That advantage together with the previous usage of Kramers and Wannier[10] decided the choice of elliptic substitution in the text.

4. Discussion of the Parameter

The imaginary parameter ia given by (2.1) can be evaluated as a real elliptic integral of the first kind. For that purpose we use Jacobi's imaginary transformation, described by the

relations

$$i\,\mathrm{cs}(iu,k)\,\mathrm{sn}(u,k')=\mathrm{cn}(iu,k)\,\mathrm{cn}(u,k')$$
$$=\mathrm{dn}(iu,k)\,\mathrm{cd}(u,k')=1 \quad (4.1)$$

and the parameter can be determined by the formula

$$\mathrm{am}(a_0,k_0')=\mathrm{am}(2yK_0',k_0')=\mathrm{gd}\,2H'=g',$$
$$a_0=2yK_0'=F(\cos\Theta_0,g'). \quad (4.2)$$

In tables this elliptic integral is often denoted by $F(90°-\Theta_0,g')$. Alternative formulas can be obtained by Landon transformations, whereby the "elliptic angle" πy is invariant. From (3.4) and (3.5) we obtain, respectively,

$$\mathrm{am}(a_1,\cos\Theta_1)=\mathrm{am}(2yK_1',k_1')$$
$$=\mathrm{gd}(H'+H^*), \quad (4.3)$$
$$\mathrm{am}(2a_1,\cos\Theta_1)=\mathrm{am}(4yK_1',k_1')$$
$$=\tfrac{1}{2}\pi-g+g'. \quad (4.4)$$

Further Landen transformations are best described by the quotients of theta functions. The following are suitable for temperatures not too far removed from the critical point

$$\tan^2\tfrac{1}{2}\Theta_2=\sin\Theta_1$$
$$=(\tan 2g\tan 2g')^{\frac{1}{2}}/\cos(g-g'), \quad (4.5a)$$
$$(\cos\Theta_2)^{\frac{1}{2}}\,\mathrm{sn}(a_2,\cos\Theta_2)$$
$$=\frac{\vartheta_1(2\pi y|-4/\tau)}{\vartheta_4(2\pi y|-4/\tau)}=\frac{\sinh|H'-H^*|}{\cosh(H'+H^*)}$$
$$=|\tan\tfrac{1}{2}(g+g'-\tfrac{1}{2}\pi)|, \quad (4.5b)$$
$$(\cos\Theta_2)^{\frac{1}{2}}\,\mathrm{sn}(2a_2,\cos\Theta_2)=\frac{\vartheta_1(4\pi y|-4/\tau)}{\vartheta_4(4\pi y|-4/\tau)}$$
$$=\sin(g-g')\,|\cot(g+g')|. \quad (4.5c)$$

For temperatures not too close to the critical point we may take

$$k_{-1}=\sin\Theta_{-1}=\tan^2\tfrac{1}{2}\theta_0, \quad (4.6a)$$

and the theta series involved in the following formula (imaginary argument) will converge rapidly:

$$-ik_{-1}^{\frac{1}{2}}\,\mathrm{sn}(iyK_{-1}',k_{-1})=\frac{\vartheta_1(\pi\tau y|2\tau)}{i\vartheta_4(\pi\tau y|2\tau)}$$
$$=\begin{cases}e^{-2H}; & (H'>H^*)\\ \tanh H'; & (H'<H^*).\end{cases} \quad (4.6b)$$

One or the other of the two formulas (4.5) and (4.6) will yield at least 3 significant figures per term of the theta series. When a table of $\log q$ is available (a table of complete elliptic integrals will do), it is not necessary to evaluate θ_2 or Θ_{-1} explicitly.

As regards the variation of the parameter a with the temperature, we note first of all that

$$y=a_0/2K_0'=a_1/2K_1'$$

is analytic at the critical point. This is evident from (3.1) and (3.3); the elliptic integrals which determine a_1 and K_1' are analytic functions of $\cos^2\Theta_1$, which has no singularity there. In this sense the singularities of the various functions at the critical point are completely described by the degeneration of the period parallelogram

$$i/\tau=K/K'=\infty; \quad (H'=H^*).$$

For extreme temperatures, with

$$H=J/kT; \quad H'=J'/kT$$

the asymptotic estimates

$$\lim_{T=0}(2y)=H'/(H+H')=J'/(J+J'),$$
$$\lim_{T=\infty}(2y)=\tfrac{1}{2} \quad (4.7)$$

can be derived from (2.1).

The parameter is an unsymmetrical function of H and H'; the nature of the asymmetry is evident from either of the formulas (4.4) and (4.5c), which involve the double parameter: Interchanging the roles of H and H' replaces y by $\frac{1}{2}-y$, and the parameter ia_0 is replaced by its elliptic complement $i(K_0'-a_0)$. Thus (2.1a) and (2.1b) have the counterparts

$$\mathrm{am}(iK'-ia,k_0)=\mathrm{am}(iK_0'(1-2y),k_0)$$
$$=\begin{cases}2iH; & (H'>H^*)\\ 2iH'^*; & (H'<H^*).\end{cases} \quad (4.8)$$

It is evident that if $J'<J$, we shall have

$$y<\tfrac{1}{4}; \quad a<\tfrac{1}{2}K'; \quad (J'<J) \quad (4.9)$$

for all temperatures, and in the special case of quadratic symmetry

$$y=\tfrac{1}{4}; \quad a=\tfrac{1}{2}K'; \quad (J=J'). \quad (4.10)$$

This is the reason why the results for that case

can be expressed by the complete integrals $K(k)$ and $E(k)$ alone, as given in the text.

5. Reduction of Integrals

By the substitution (2.2), the integrals of (113) in the text are readily evaluated as complete elliptic integrals. For example,

$$\int_0^\tau \cos\delta' d\omega = \int_0^{2K} k'^2 \operatorname{cn} u(\operatorname{dn} ia \operatorname{dn} u - k \operatorname{cn} ia \operatorname{cn} u)^{-1} du; \quad (H' > H^*).$$

If we replace u by $2K-u$, the sign of $\operatorname{cn} u$ is changed; that of $\operatorname{dn} u$ is preserved. Accordingly, that part of the integrand which is odd with regard to $\operatorname{cn} u$ may be omitted, which yields

$$\frac{k \operatorname{cn} ia \operatorname{cn}^2 u}{1-k^2 \operatorname{sn}^2 ia \operatorname{sn}^2 u} = k \operatorname{cn} ia - \frac{k \operatorname{cn} ia \operatorname{dn}^2 ia \operatorname{sn}^2 u}{1-k^2 \operatorname{sn}^2 ia \operatorname{sn}^2 u}$$

whence

$$\int_0^\tau \cos\delta' d\omega = 2K(k \operatorname{cn} ia - k^{-1} \operatorname{ds} ia\, Z(ia)); \quad (H' > H^*).$$

The other integrals (113) are treated similarly. The results are

$$\begin{aligned}
\int_0^\tau \cos\delta^* d\omega &= -2iK(k \operatorname{sn} ia \coth 2H^* - Z(ia) \coth 2H'),\\
\int_0^\tau \cos\delta' d\omega &= -2iK(k \operatorname{sn} ia \coth 2H' - Z(ia) \coth 2H^*),\\
\int_0^\tau (\sin\delta^* \sin\delta'/\sinh\gamma) d\omega &= 2(K-E)(i/k \operatorname{sn} ia),\\
\sinh^2 2H' \int_0^\tau \sin^2\delta^* \coth\gamma\, d\omega &= \sinh^2 2H^* \int_0^\tau \sin^2\delta' \coth\gamma\, d\omega = -2iKZ(ia).
\end{aligned} \tag{5.1}$$

The mixed notation is designed to throw the distinction between the cases (2.2a) and (2.2b) entirely into the choice of modulus and parameter; so that the formulas (5.1) are equally valid for $H' < H^*$ and for $H' > H^*$.

The Z function of imaginary argument which enters into (5.1) can be expressed in terms of the tabulated functions of real argument $Z(a, k')$ as follows:

$$Z(iu, k) = \operatorname{dn}(iu, k) \operatorname{sc}(iu, k) - iZ(u, k') - i(\pi u/2KK'). \tag{5.2}$$

For substitution in (113) it is convenient to make use of the function

$$Z(iK'-ia) = -\operatorname{dn} ia \operatorname{cs} ia - i(\pi/2K) - Z(ia) \tag{5.3}$$

together with $Z(ia)$; this leads to more symmetrical formulas. The connection between the corresponding functions of real argument is

$$Z(a, k') + Z(K'-a, k') = k'^2(-i) \operatorname{sc} ia \operatorname{nd} ia. \tag{5.4}$$

6. Derived Thermodynamic Functions

In assembling the terms of the formula (113a) for the energy it is best to deal with the cases $H' > H^*$ and $H' < H^*$ separately. The results are

$$U = -NJ'(\partial \log\lambda/\partial H') - NJ(\partial \log\lambda/\partial H), \tag{6.1a}$$

$$\partial \log\lambda/\partial H' = \coth 2H'(2y + (2K/\pi)Z(2yK', k')), \quad (H' > H^*) \tag{6.1b}$$

$$\partial \log\lambda/\partial H = \coth 2H \times (1-2y+(2K/\pi)Z((1-2y)K', k'))$$

valid for temperatures below the critical point; above the critical point we have instead

$$\partial \log\lambda/\partial H' = \coth 2H' \times (2y-(2K/\pi)Z((1-2y)K', k')) \quad (H' < H^*). \tag{6.1c}$$

$$\partial \log\lambda/\partial H = \coth 2H \times (1-2y-(2K/\pi)Z(2yK', k'))$$

The energy is continuous at the critical point because, when u is real [cf. (5.4)]

$$0 \leqq Z(u, k') \leqq 1-k.$$

For the specific heat we obtain from (113b) and (5.1), in mixed notation valid for all temperatures

$$\frac{C}{Nk} = \frac{4}{\pi}\left(-iKZ(ia)\left(\frac{H'}{\sinh 2H'}\right)^2 - iKZ(iK'-ia)\left(\frac{H}{\sinh 2H}\right)^2 + 2(K-E)\left(\frac{\operatorname{sn} ia}{i \sinh 2H'}\right)HH'\right). \tag{6.2}$$

Every term is positive. The specific heat is infinite at the critical point, where $k=1$. This is caused by the factor K; the general case is substantially like the special case of quadratic symmetry treated in the text.

7. The Partition Function

To compute the partition function (106) in terms of τ and y we first differentiate under the integral sign

$$\frac{\partial}{\partial a}\int_0^\tau \gamma\, d\omega=\int_0^{2K}\left(-\frac{\partial\gamma}{\partial a}\frac{\partial\omega}{\partial u}-\gamma\frac{\partial^2\omega}{\partial a\partial u}\right)du.$$

Integration by parts yields with the aid of (2.5)

$$\int_0^{2K}\left(-\frac{\partial\gamma}{\partial a}\frac{\partial\omega}{\partial u}+\frac{\partial\gamma}{\partial u}\frac{\partial\omega}{\partial a}\right)du$$
$$=\int_0^{2K}\left(\left(\frac{\partial\gamma}{\partial a}\right)^2+\left(\frac{\partial\gamma}{\partial u}\right)^2\right)du$$
$$=\int_0^{2K}\left(\frac{\mathrm{dn}^2\, ia\ \mathrm{dn}^2\, u+k^2\,\mathrm{cn}^2\, ia\,\mathrm{cn}^2\, u}{1-k^2\,\mathrm{sn}^2\, ia\,\mathrm{sn}^2\, u}\right)du.$$

The integral is easily evaluated; then considering that

$$\gamma(0,u)=\cosh^{-1}(1)=0$$

for $a=0$, we have

$$\int_0^\tau \gamma\, d\omega=2K\int_0^u \Phi(iu)du, \tag{7.1}$$

$$\Phi(u)=2\,\mathrm{dn}^2\, u-k'^2-2\,\mathrm{dn}\, u\,\mathrm{cs}\, u\, Z(u).$$

The function $\Phi(u)$ is even and periodic with the period $2K$. Its singularities are poles at the points

$$u=2mK+niK';\quad (m, n \text{ integers};\ n\neq 0).$$

Jacobi's imaginary transformation (4.1), (5.2) yields

$$\Phi(iu)=-k'^2+\mathrm{dc}(u,k')\,\mathrm{ns}(u,k')$$
$$\times(2Z(u,k')+(\pi u/KK')). \tag{7.2}$$

Accordingly, the poles of $\Phi(u)$ are simple; the residues are

$$R(2mK+niK')=R(niK')=(-)^n n\pi i/K. \tag{7.3}$$

It is easily seen that $\Phi(u)$ satisfies the standard conditions for development in partial fractions *qua* function of $\cos(\pi u/K)$. The residues (7.3) together with the condition

$$\Phi(K)+\Phi(K+iK')=k'^2-k'^2=0$$

suffice to determine the expansion

$$\Phi(u)=\left(\frac{\pi}{2K}\right)^2\left(1-8\sum_{n=1}^{\infty}(-)^n n\right.$$
$$\left.\times\frac{(q^n\cos(\pi u/K)-q^{2n})}{(1-2q^n\cos(\pi u/K)+q^{2n})}\right). \tag{7.4}$$

The integration required by (7.1) is readily performed, and the formula (106) of the text becomes

$$-\frac{F}{NkT}=\log\lambda=\tfrac{1}{2}\log(2\sinh 2H)+\frac{1}{2\pi}\int_0^\tau \gamma\, d\omega$$
$$=\tfrac{1}{2}\log(2\sinh 2H)-\tfrac{1}{2}y\log q$$
$$-\sum_{n=1}^{\infty}(-)^n n\log\left(\frac{1-q^{n+2y}}{1-q^{n-2y}}\right). \tag{7.5}$$

Specialization to the case $y=\frac{1}{4}$ yields the formula (119a) of the text, where $q_1{}^2=q$.

The series of (7.5) converges rapidly except in the immediate neighborhood of the critical point. To obtain an expansion suitable for computation in that region we note from (7.2) that

$$\Phi(iu)-(\pi u/2KK')i\,\mathrm{cs}\, iu\,\mathrm{dn}\, iu$$
$$=2\mathrm{dc}(u,k')\,\mathrm{ns}(u,k')Z(u,k')-k'^2$$

is a periodic function of u with the real period $2K'$. Its Fourier series is easily derived with the aid of the identity

$$K(2\,\mathrm{dc}\, a\,\mathrm{ns}\, a\, Z(a)-k^2)$$
$$=\int_0^K k^2(\mathrm{sn}(u-a)\,\mathrm{sn}(u+a)-\mathrm{cn}(u-a)\,\mathrm{cn}(u+a))du$$

from those of the Jacobian elliptic functions.[21] The result is

$$\Phi(iu)-\frac{\pi u}{2KK'}i\,\mathrm{cs}\, iu\,\mathrm{dn}\, iu$$
$$=2\left(\frac{\pi}{K'}\right)^2\sum_{n=0}^{\infty}\frac{\cos((2n+1)\pi u/K')}{\sinh^2((2n+1)\pi K/K')}.$$

[21] WW, reference 19, 22.6.

Moreover,[22]

$$iu\,\mathrm{cs}\,iu\,\mathrm{dn}\,iu-\frac{d}{du}(u\log(-ik^{\frac{1}{2}}\,\mathrm{sn}\,iu))$$

$$=-\log(k^{\frac{1}{2}}\,\mathrm{sc}(u,k'))=\log\cot(\pi u/2K')$$

$$+\sum_{n=0}^{\infty}\frac{2e^{-(2n+1)\pi K/K'}\cos((2n+1)\pi u/K')}{(2n+1)\sinh((2n+1)\pi K/K')}.$$

Termwise integration of the Fourier series yields the alternative expansion for the partition function

$$-F/NkT=\log\lambda=\tfrac{1}{2}\log(2\sinh 2H)$$

$$+\frac{K}{\pi}\int_0^{\infty}\Phi(iu)du=y\log(2\sinh 2H')$$

$$+(\tfrac{1}{2}-y)\log(2\sinh 2H)+2\int_0^{y}\log\cot(\pi z)dz$$

$$+\frac{1}{\pi}\sum_{n=0}^{\infty}\frac{(1+(4n+2)(\pi i/\tau)-\exp[-(4n+2)\pi i/\tau])}{(2n+1)^2\sinh^2((2n+1)\pi i/\tau)}$$

$$\times\sin((4n+2)\pi y). \quad (7.6)$$

The formula (119b) of the text is obtained by specialization to the case $H'=H$; $y=\frac{1}{4}$, with $\tau=2\tau_1$, whereby

$$\int_0^{\pi/4}\log\cot x\,dx=1^{-2}-3^{-2}+5^{-2}-7^{-2}+\cdots=G.$$

[22] WW, reference 19, 22.5, example 3.

8. Critical Data

The transition temperature is given by the condition

$$\sinh 2H\sinh 2H'$$
$$=\sinh(2J/kT)\sinh(2J'/kT)=1;\quad (T=T_c). \quad (8.1)$$

Then

$$\tau=0;\quad K=\infty;\quad K'=\tfrac{1}{2}\pi$$
$$\pi y=a=\mathrm{gd}\,2H'=\tfrac{1}{2}\pi-\mathrm{gd}\,2H. \quad (8.2)$$

The formula (6.1) for the energy becomes

$$U_c=-(2/\pi)(NJ'\,\mathrm{gd}\,2H'\coth 2H'$$
$$+NJ\,\mathrm{gd}\,2H\coth 2H) \quad (8.3)$$

and the formula (7.6) for the partition function simplifies to

$$-F_c/NkT=\log\lambda_c=\tfrac{1}{2}\log 2+(\tfrac{1}{2}-2y)\log\cot\pi y$$
$$+2\int_0^{y}\log\cot\pi z\,dz. \quad (8.4)$$

The specific heat becomes infinite; the approximate formula

$$C/Nk\sim(4/\pi)(K(H+H'\sinh 2H)^2\sinh 2H'$$
$$-H^2\sinh^2 2H'\,\mathrm{gd}\,2H-2HH'$$
$$-H'^2\sinh^2 2H\,\mathrm{gd}\,2H') \quad (8.5)$$

where

$$K\sim\log(4/k')\sim\tfrac{1}{2}[\log(4T/|T-T_c|)$$
$$-\log(H\coth 2H+H'\coth 2H')]$$

is valid for temperatures near the critical point.

Letter to the Editor

PROMPT publication of brief reports of important discoveries in physics may be secured by addressing them to this department. The closing date for this department is the third of the month. Because of the late closing date for the section no proof can be shown to authors. The Board of Editors does not hold itself responsible for the opinions expressed by the correspondents. Communications should not in general exceed 600 words in length.

Continuous X-Ray Spectrum: Note to Experimenters

ROBERT WEINSTOCK
Department of Physics, Stanford University, Stanford University, California
January 20, 1944

THE theoretical dependence of the continuous x-ray intensity from thin targets—relativity and retardation of potential neglected—upon the angle of observation is given solely through the multiplicative factor

$$Q(\Theta)=(L_x^2\sin^2\Theta+L_z^2\cos^2\Theta+L_y^2),$$

where Θ is the angle between the direction of observation and that of the bombarding electrons; the quantities L_x^2, L_y^2, L_z^2 are calculable by means of complicated series expansions.[1] The x axis is taken along the direction of the electron beam, while the y direction is perpendicular both to this and to the direction of observation. Through symmetry, we have $L_y^2=L_z^2$.

Although the individual calculations of L_x^2, $L_y^2(=L_z^2)$ can generally be carried through without an unreasonable amount of effort, the sum $L^2=L_x^2+L_y^2+L_z^2=L_x^2+2L_y^2$ may be computed, usually, at the expense of appreciably less labor.[2] For this reason, comparison of experiment with theory may be facilitated somewhat if observation is made at an angle Θ for which the factor $Q(\Theta)$ is merely a multiple K of L^2, or

$$L_x^2\sin^2\Theta+L_y^2(1+\cos^2\Theta)=K(L_x^2+2L_y^2).$$

Equating coefficients we obtain

$$\sin^2\Theta=K,\quad 1+\cos^2\Theta=2K,$$

whence $K=2/3$; so that finally

$$\Theta=54°44'\text{ or }125°16'.$$

Hence it is suggested that—unless angular distribution is sought—future measurements upon the intensity of continuous x radiation from thin targets be made at an angle of 54°44′ with the (forward or reverse) direction of electron bombardment, provided the geometry of the experimental set-up is not rendered unwieldy as a result.

[1] R. Weinstock, Phys. Rev. **64**, 276 (1943).
[2] A. Sommerfeld and A. W. Maue, Ann. d. Physik **23**, 589 (1935).

Proceedings of the American Physical Society

MEETING AT PASADENA, CALIFORNIA, DECEMBER 27, 1943

THE 258th meeting of the American Physical Society was held at the California Institute of Technology, Pasadena, California, on Monday, December 27, 1943. Once again the meeting was very successful, in spite of the numerous handicaps resulting from war conditions. The attendance varied from 50 to 70, and 40 members of the society and guests had luncheon together at the Athenaeum. Those in attendance came almost exclusively from Southern California, but limitations of travel made this fact almost inevitable. Much of the success of the meeting, and presumably the unexpected size of the attendance, was due to the four invited papers, which had been arranged by the combined efforts of Dr. Darrow, Dr. Millikan, and the local secretary. All of the four papers were important and were much appreciated by the audience. The number of contributed papers—fifteen—was far greater than had been anticipated, and resulted in a program almost too long for a single day. The morning session opened at 9:30 A.M. and adjourned at 12:15 P.M. The afternoon session opened at 1:30 P.M. and adjourned at 4:45 P.M. During the morning session two invited papers were presented, *viz.*,

Specificity of Intermolecular Interaction. LINUS PAULING, *California Institute of Technology.*

The Morphology of Nebulae and Clusters of Nebulae. FRITZ ZWICKY, *California Institute of Technology.*

During the afternoon session the following two invited papers were presented:

The Problem of Rendering Sea Water Potable. ALEXANDER GOETZ (in collaboration with S. J. Broadwell and D. C. Warner), *California Institute of Technology.*

Physical Methods in Hydrocarbon Research. OTTO BEECK, *Shell Development Company, Emeryville, California.*

Abstracts of the fifteen contributed papers follow. None of these was read by title.

R. T. BIRGE,
Local Secretary for the Pacific Coast

ABSTRACTS OF CONTRIBUTED PAPERS

1. Analysis of a Multivibrator. S. C. SNOWDON, *California Institute of Technology (Introduced by W. H. Pickering).*—A theoretical analysis of the action of a fundamental multivibrator has been undertaken along the lines of Van der Pol's analysis.[1] A more exact approximation to the transfer characteristic has been used and an exact solution of the equation has been found in the case where the shunt capacities of the tubes can be neglected. In this approximation the period of oscillation has been calculated and checked experimentally. The limiting frequency of oscillation in which the wave form is sinusoidal can be calculated as in Van der Pol's case. The results agree with experiment within three percent.

[1] B. Van der Pol, Phil. Mag. 2, 978, 1926.

2. A Voltage Regulator for High Voltages. W. H. PICKERING AND S. C. SNOWDEN, *California Institute of Technology.*—The standard degenerative voltage regulator circuit usually becomes difficult to use at voltages above a few kilovolts. This is particularly true in applications where the positive terminal is grounded. The new circuit avoids the difficulties by using a radiofrequency signal modulated by the variations in output voltage to transmit these variations across the potential difference to a tube in series with the high potential bus. The voltage limitations are accordingly removed and furthermore, either terminal of the output may be at ground potential. The sensitivity of the regulator depends as usual upon the total effective amplification of the circuit. Long-time stability depends on the stability of the amplitude or frequency of the radiofrequency signal.

3. A Light Source for the Primary Standard of Wave-Length. CHAO-WANG HSUEH, *California Institute of Technology.*—Despite some objections,[1] the red Cd line, 6438.4696A, still remains the primary standard of wavelength for lack of a satisfactory substitute. In our laboratory a light source of the Michelson type has been constructed for this standard line. The interferometer spectrograms show that the line is as narrow as, or even narrower than, that emitted from the Osira Cd lamp (Adam Hilger), and is very intense. Our lamp produces a satisfactory spectrogram with only thirty minutes' exposure. Under the same conditions the Osira lamp gives a lighter spectrogram with six hours' exposure. Furthermore, the intensity of our lamp can be varied over a wide range by changing the primary voltage of the transformer. The effective light-emitting area is 50×2.5 mm^2 which, if necessary, can be enlarged by means of a magnifying lens. The Doppler effect should disappear because the light is observed in a direction perpendicular to that of the current. Owing to

the high intensity, simultaneous observation of the standard line and of lines from another source is possible either by using a half-reflecting mirror, or by placing the latter source in front of the spectrograph slit. These features eliminate the important objections against a light source for the standard Cd line.

[1] W. F. Meggers, Rev. Mod. Phys. **14**, 59 (1942).

4. On the Elastic Vibrations of Cylindric Shells. PAUL S. EPSTEIN, *California Institute of Technology.*—The problem of the characteristic oscillations of curved shells with the usual border conditions (clamped edges and free edges) has remained hitherto unsolved. A method of treating elastic shells given by the author[1] permits of obtaining the solution, which was worked out for shells having the shape of circular cylinders. The result is particularly simple in the case of very thin shells. The three types of border conditions, namely, clamped edges, free edges, and supported edges, lead to the same characteristic frequencies. But the character of the oscillations, as evidenced by the distribution of the nodal lines, is not the same for clamped as for free edges.

[1] Paul S. Epstein, J. Math. and Phys. **21**, 198 (1942).

5. Forbidden Lines of Ca II in a Stellar Spectrum. PAUL W. MERRILL, *Mount Wilson Observatory.*—A low dispersion spectrogram of the fourth-magnitude star υ Sagittarii, type cApe, obtained by H. F. Weaver at Mount Wilson in 1942, showed the $^2S-{}^2P$ triplet of Ca II, λλ8498, 8542, 8662 in emission. Spectrograms with higher dispersion (21A/mm), obtained by the writer in 1943, showed in addition the forbidden doublet $^2S-{}^2D$, λ7291.47, λ7323.88. No previous observations of these forbidden lines either in the laboratory or in astronomical sources seem to be on record. The star is a spectroscopic binary of period 138 days whose brighter component (the only one observed) has a range in radial velocity of 96 km/sec according to an orbit computed in 1914 by R. E. Wilson from the measured displacements of the dark lines. The bright lines of H and Ca II indicate little if any change in velocity. Hence they probably originate not in either component of the binary pair but in an enveloping gaseous cloud.

6. Further Studies on the Least Penetrating Component of the Incoming Cosmic Rays. R. A. MILLIKAN, H. V. NEHER, AND W. H. PICKERING, *California Institute of Technology.*—Although the war has prevented us from making such convincing tests on the existence of helium annihilation rays as we reported earlier[1] on silicon, oxygen, nitrogen, and carbon annihilation rays, we are able to present herewith heretofore-unpublished evidence obtained with the aid of high altitude electroscope measurements for the existence of approximately the energy to be computed from the helium annihilation hypothesis.

[1] Millikan, Neher, and Pickering, Phys. Rev. **63**, 234 (1943).

7. The Average Specific Ionization of the Mesotrons 100 Ft. Underground. WAYNE E. HAZEN, *University of California.*—Cloud-chamber photographs have been taken in a tunnel with 100 ft. of rock overhead. The chamber was operated in such a way that the ionization of cosmic-ray mesotrons could be obtained from the number of drops that condensed on positive ions. No magnetic field was used. A preliminary survey of the photographs has given a value of 60 ion pairs per cm in air at N.T.P. for ionization events in which less than 2500 ev of energy was lost by the cosmic ray per primary ionization (in other words: clusters of more than 80 drops were omitted). It was found that approximately 10 percent of the energy loss of a mesotron is attributable to collisions in which between 1200 and 2500 ev is lost to an electron. There have been two determinations of the specific ionization of cosmic rays at sea level in this laboratory: one resulted in a value of 56, the other in a value of 46 ion pairs per cm of air at N.T.P. One expects an increase in the average specific ionization with depth since the average energy increases with depth. A rough calculation indicates that one might expect a 10 percent increase in the average specific ionization at a depth of 100 ft.

8. Friction of Binary Alloys with Thin Film Lubrication. S. KYROPOULOS, *California Institute of Technology.*—An apparatus originally designed for investigation of lubricant characteristics[1] was converted to measure over-temperatures of alloys rubbing against steel. Equilibrium temperature is usually reached in one-half hour; accuracy ±0.3°C. As a basis of bearing alloys, first specimens were investigated covering the phase diagram Pb-Sb. Allowing for irregularities due to the crystallization process and solid solubility, the hardness of these alloys follows substantially a linear relationship. The overtemperature-composition curve is from 0–20 percent Sb almost its mirror image. From 20–100 percent Sb the curve goes through a minimum around 40 percent Sb, thus being substantially convex to the composition axis. This phenomenon may be interpreted as an effect of the differential thermal expansion of the duplex structure, resulting in a shift toward more fluid lubrication. Apparatus and procedure followed permit study of precipitation hardening effects on friction and some insight into basic contributing factors such as plasticity and shearing off of particles and their reaction on various lubricants.

[1] S. Kyropoulos, Refiner **18**, 273, 320, 399 (1939); **19**, 85 (1940).

9. Present Status of Spectroscopic Methods of Analysis. M. F. HASLER, *Applied Research Laboratories, Glendale, California.*—Today's versions of many instruments usually considered as tools of the physicist but now being used almost exclusively for the analysis of materials by the spectroscopic method, are described. The scope of the spectroscopic method is discussed as is its present day position. The future possibilities opened up by direct reading instruments, made practical by recent advances in vacuum-tube design, are considered.

10. Frequency-Band Character of Shock Vibrations. S. LEROY BROWN, *University of Texas.*—A so-called shock vibration is one with a fundamental frequency but the amplitude is zero for more than half the cycle. Analysis of specific wave forms shows that, though the intensity of the harmonics decreases with frequency, there are bands of relatively greater intensity. For example a square-top wave of height h for a quarter of a cycle (height zero for three-quarters of the cycle) gives $1.4h/\pi$, $2h/2\pi$, $1.4h/3\pi$, 0, $1.4h/5\pi$, $2h/6\pi$, $1.4h/7\pi$, 0, $1.4h/9\pi$, $2h/10\pi$, $1.4h/11\pi$, 0, $1.4h/13\pi$, $2h/14\pi$, etc., for the amplitudes of the harmonics. A vibration of 20 cycles per second, the wave form of which is half a sine curve for one-twentieth of the cycle (zero for nineteen-twentieths of the cycle), gives weak harmonics around 600 cycles per second, comparatively strong harmonics around 800 cycles per second, weak harmonics around 1000 cycles per second, etc. If the half-sine curve occupies a small fraction of a cycle, the amplitudes of the lower harmonics decrease very slightly with frequency.

11. A High Sensitivity String Galvanometer. ARTHUR E. LOCKENVITZ, *University of Texas.*—A string galvanometer is described having a sensitivity as high as 10^{-9} ampere per scale division and at this sensitivity a period of less than a tenth of a second. A new method of keeping the string under constant tension is used. A platinum wire 0.001 mm in diameter and about 7 cm long is fastened at the ends to rigid terminals but in such a way that the wire is very slack. Near one end of this platinum wire a second wire of the same diameter is tied so that it is at right angles to the first and its ends are fastened to fixed terminals like the first. This string assembly is in a magnetic field so that both wires are at right angles to the field. An auxiliary current of a few microamperes produces a force action in the second wire which causes the main string to be held under any desired constant tension. By means of a simple switching arrangement, the sensitivity and period can be varied over wide limits. The instrument is extremely stable and rigid.

12. The Explosion of Ether-Air Mixtures by Electrical Sparks. A. M. ZAREM, *California Institute of Technology (Introduced by R. A. Millikan).*—Sparks were passed between spherical and pointed electrodes immersed in a combustible ether-air mixture. It was found that the energy in a spark required to explode the mixture decreased as the sparking potential was increased. At 4000 volts, a non-oscillatory spark current as low as 400 microamperes (peak value) exploded the mixture. At 2000 volts the peak current required for explosion was of the order of amperes. The shape of the electrodes affected the minimum energy necessary for explosion. No explosions were obtained using a prolonged corona discharge from a Wimshurst machine with voltages ranging up to 35,000 volts. Explosions were obtained, however, when a spark was passed between either pointed or spherical electrodes at 4000 volts. In many cases the peak current in the spark which caused explosion at the lower voltage was not as great as the corona discharge current.

13. Excitation of Electromagnetic Waves in Wave-Guides and Cavities. JOHN MILES, *California Institute of Technology (Introduced by R. A. Millikan).*—The impedance of thin transverse wires in rectangular wave-guides and cavities has been evaluated by application of the vector potential. Both the resistive and the reactive components have been obtained, and one is thus enabled to place a driving or receiving element so as to match a given source or load for the maximum power transfer. The problem of short circuiting wires has also been calculated. The solution of the analogous problems in a circular wave-guide is indicated.

14. X-Ray Inspection of Spotwelds in Aluminum Alloys. R. C. MCMASTER, *California Institute of Technology (Introduced by R. A. Millikan).*—This paper presents preliminary results of a study whose purpose is to develop practical industrial methods for the non-destructive testing of spotwelds in aluminum alloys. Procedures for x-ray inspection using industrial equipment have been developed, and correlations have been obtained between radiographs of spotwelds and spotweld structure, quality and strength. The scope and limitations of the method are indicated through the presentation of results of tests on thousands of industrially-made spotwelds. The results of preliminary tests employing fluoroscopic and special x-ray equipment are outlined.

15. Sparking Potentials in Air in a Plane Parallel Gap at and below Atmospheric Pressure. LEON H. FISHER, *University of California.*—The streamer theory of the electric spark developed by Loeb and Meek[1] has indicated the importance of sparking potential studies in air at half an atmosphere pressure. Sparking potentials in a plane parallel gap in air have been measured as a function of plate distance and pressure. Below atmospheric pressure, the sparking potential curve as a function of distance at constant pressure shows a peculiar leveling off at large plate distances. This effect increases with decreasing pressure, and has been shown to be due to the effect of the metal walls of the large chamber used (50-cm diameter). Significant measurements at low pressures will require the use of larger chambers than have been used previously. The walls of the chamber do not influence the measurements at atmospheric pressure, and the sparking potential for a one-centimeter gap at atmospheric pressure at 22°C is 30.1 kv. The data at atmospheric pressure, when analyzed either by Townsend's sparking equation or by Meek's equation, are more self consistent than any other available data. Water vapor causes a small but definite scattering in the potentials at which sparks occur.

[1] L. B. Loeb and J. M. Meek, *The Mechanism of the Electric Spark* (Stanford University Press, 1941).